THE MOLECULAR CHARACTERIZATION OF SOUTH AFRICAN ISOLATES OF GRAPEVINE RUPESTRIS STEM PITTING-ASSOCIATED VIRUS (GRSPaV)
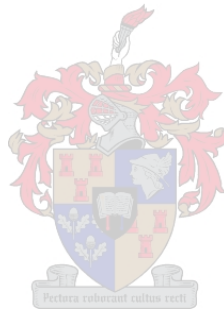
Liesl Christine Noach

Thesis presented in partial fulfillment of the requirements for the degree of Master of Science at the Department of Genetics, Stellenbosch University

Supervisor: Prof JT Burger

December 2010

Declaration

By submitting this thesis electronically, I declare that the entirety of the work contained therin is my own, original work, that I am the owner of the copyright thereof (unless to the extent explicitly otherwise stated) and that I have not previously in its entirety or in part submitted it for obtaining any qualification.

Signature: ....   Date: ....

Abstract

The first aim of this study was to reliably and rapidly detect *Grapevine rupestris stem pitting-associated virus* (GRSPaV) in grapevine. This was achieved by screening 94 grapevines using crude plant extracts in both quantitative and conventional reverse transcription polymerase chain reaction (RT-PCR). The second aim was to establish a technique capable of differentiating GRSPaV sequence variants. The application of this technique is for the large-scale screening of diseased vines to associate sequence variants of GRSPaV with disease symptoms. Nested quantitative polymerase chain reaction and high resolution melting assays (qPCR-HRM) were developed for three regions of the GRSPaV genome (coat protein, RNA-dependant RNA-polymerase and triple gene block movement protein). The qPCR-HRM technique using the high saturation dye, EvaGreen™, and the Rotor-Gene™ 6000 analyzer was validated with a panel of sixteen sequence-characterized viral isolates. Diluted RT-PCR products and cloned cDNA gave the most consistent amplification plots and dissociation profiles. RT-PCR products generated from total RNA extracts were used as template for qPCR-HRM assays and for direct sequencing of sixteen samples in the three aforementioned regions. The average amplification efficiency for qPCR was 1.52±0.04. Auto-calling of user-define genotypes was performed at a confidence interval of 70%. Phylogenetic analysis of the three regions of the GRSPaV genome was performed with published GenBank sequences to confirm the HRM data. The dominant sequence variants found in the South African sample set radiated with Group II, reference full-length variant GRSPaV-SG1. GRSPaV-infected samples can in future be subjected to qPCR-HRM assays developed during this study. This can be performed to establish similarity to known genotypes and therefore phylogenetic groups. Mixed infection of sequence variants and quasi-species were a common occurrence. The assay will be useful in establishing correlation of specific genotypes to different phenotypical expression of viral disease. This could provide insight into the etiology of diseases associated with GRSPaV.

Opsomming

Die eerste doel van hierdie studie was om die virus wat met Rupestris-stamverpitting (*Grapevine rupestris stem pitting-associated virus* of "GRSPaV") in wingerd verbind is, vinnig en betroubaar op te spoor. Dit is bereik deur 94 wingerdstokke vir die teenwoordigheid van die virus te toets met beide kwantitatiewe en konvensionele tru-transkripsie polimerase kettingreaksies (RT - PCR) vanaf ongesuiwerde plant-ekstraksies. Die tweede doel was die daarstelling van 'n tegniek om onderskeid te tref tussen variante van GRSPaV met verskillende nukleotiedvolgordes. Hierdie tegniek kan op groot skaal gebruik word om ge-affekteerde wingerdstokke te toets om sodoende siektesimptome met spesifieke variante van GRSPaV te verbind. Ge-neste kwantitatiewe polimerase-kettingreaksies (qPCR) en hoë-resolusie smelt-analises (HRM) is ontwikkel vir drie streke van die GRSPaV-genoom (mantelproteïen, RNS-afhanklike RNS-polimerase en trippelgeenblok bewegingsproteïen). Die tegniek van qPCR-HRM met die hoë-versadingingskleurstof EvaGreen™ en die Rotor-Gene™ 6000 ontleder se geldigheid is bevestig deur vergelyking met 'n paneel van sestien virus-isolate waarvan die volgorde reeds bepaal is. Verdunde RT-PCR-produkte en gekloneerde DNS het die mees konsekwente amplifikasie-uitstipping en dissosiasieprofiele opgelewer. RT-PCR-produkte wat vanuit totale RNS-ekstrakte verkry is, is as templaat vir qPCR-HRM-analises gebruik. Dieselfde produkte is ook gebruik, om die volgorde van sestien monsters in drie streke direk te bepaal. Die gemiddelde amplifikasiedoeltreffendheid van die qPCR was 1.52±0.04. Gebruiker-gedefinieerde genotipes is deur middel van outo-oproeping teen 'n vertroue-interval van 70% uitgevoer. Filogenetiese analises vir drie streke van die GRSPaV-genoom is uitgevoer met gepubliseerde GenBank-volgordes om die HRM-data te bevestig. Die dominante volgorde-variante in die stel Suid-Afrikaanse monsters het ooreengestem met Groep II, vollengte-verwysingsvariant GRSPaV-SG1. Monsters wat met GRSPaV besmet is kan in die toekoms onderwerp word aan die qPCR-HRM-analises wat in hierdie studie ontwikkel is. Dit kan uitgevoer word om ooreenkomste met bekende genotipes te bepaal, en dus ook met filogenetiese groepe. Die besmetting van plante met meer as een volgorde-variant het algemeen voorgekom. Die kwasi-spesies populasie-struktuur van die virus het ook gedurig na vore gekom. Die toets sal nuttig wees in die bepaling van korrelasies tussen spesifieke genotipes en verskillende fenotipiese voorkomste van virussiektes. Dit kan insig verleen in die etiologie van siektes wat met GRSPaV verbind word.

Acknowledgements

TABLE OF CONTENTS

LIST OF ABBREVIATIONS

ApLV	*Apricot latent virus*
ASPV	*Apple stem pitting virus*
ATP	Adenosine Triphosphate
BLAST	Basic Local Alignment and Search Tool
bp	Base pairs
CAF	Central Analytical Facility
CB	Corky bark
cDNA	Copy DNA
CP	Coat Protein
C_q-value	Quantitation cycle
CTAB	Cetyltrimethylammonium Bromide
DNA	Deoxyribonucleic acid
ds	Double-stranded
DTT	Dithiothreitol
EDTA	Ethylene diamine tetra acetate
ELISA	Enzyme-linked immunosorbent assay
EtBr	Ethidium Bromide
g	Gram
GLRaV-2	*Grapevine Leafroll-associated virus 2*
GRSPaV	*Grapevine rupestris stem pitting-associated virus*
GRSPaV-1	*Grapevine rupestris stem pitting-associated virus - 1*
GRSPaV-BS	*Grapevine rupestris stem pitting-associated virus – cv. Berte Seyve*
GRSPaV-PN	*Grapevine rupestris stem pitting-associated virus – cv. Pinot Noir*
GRSPaV-SG1	*Grapevine rupestris stem pitting-associated virus – cv. St. George*
GRSPaV-SY	*Grapevine rupestris stem pitting-associated virus – cv. Syrah*
GSyV-1	*Grapevine Syrah virus-1*
GVA	*Grapevine virus A*
GVB	*Grapevine virus B*
GVC	*Grapevine virus C*
GVD	*Grapevine virus D*
GVE	*Grapevine virus E*
HEX-SSCP	Heteroduplex single stranded conformation polymorphism
HRM	High resolution melt analysis
ISEM	Immunosorbent electron microscopy
kb	Kilobase pairs
kDa	Kilodalton
KSG	Kober stem grooving
ℓ	Litres

LDA	low density arrays
LNSG	LN33 stem grooving
mg	Milligram
ml	Milliliter
NCR	non-coding region
nts	nucleotides
ORF	Open Reading Frame
PCMV	*Peach chlorotic mottle virus*
PCR	Polymerase chain reaction
PEG	Poly Ethylene Glycol
PTGS	post-transcriptional gene silencing
PVM	*Potato virus M*
PVX	*Potato virus X*
PVP	polyvinylpyrrolidone
qRT-PCR	Quantitative Reverse Transcription Polymerase Chain Reaction
RFLP	Restriction Fragment Length Polymorphism
RNA	Ribonucleic acid
RSP	Rupestris Stem Pitting
RT-PCR	Reverse Transcription Polymerase Chain Reaction
RW	Rugose Wood
SDS	Sodium dodecylsulfate
SNP	Single Nucleotide Polymorphism
ss	Single-stranded
ßME	ß-mercapthoethanol
TGB	triple gene block movement protein
TM	melting temperatures
Triton X-100	Octylphenolpoly [ethyleneglycolether]n
Tween 20	Poly[oxyethylene]n sorbitan-monolaurate
UV	ultra-violet
VZV	*Varicella-zoster virus*

LIST OF FIGURES

LIST OF TABLES

1. General Introduction

Grapevines (*Vitis vinifera* L., family *Vitaceae*) have been cultivated by several countries throughout the world for approximately 5000 years (Reisch and Pratt, 1996). This crop is therefore one of the most ancient and widely cultivated fruits produced in the world. This important commodity is enjoyed by millions of people for its versatile usage as fresh fruit, raisins and for the making of wine and juice. Perhaps due to the prolonged history of cultivation, grapevine plays host to the largest number of pathogens such as bacteria, fungi, insects, nematodes, phytoplasmas and viruses. These pathogens can detrimentally affect lifespan, fruit quality and yield.

Thus far, sixty different grapevine-infecting viruses from diverse taxonomic groups have been identified (Martelli, 2009). More interestingly, grapevines also host mixed infections of different viruses as well as mixed infections of different sequence variants of the same virus. This may be expected due to two prolonged viticultural practices. Firstly, grapevines are grown for approximately 20 years and the accumulation of point mutations over time due to the error-prone replication mechanism of viral polymerases may result in diverse viral sequence variants. Secondly, grapevines are commonly grown on hardy rootstocks to lessen abiotic and biotic strains such as phylloxera, nematodes, drought and other soil irregularities (Reisch and Pratt, 1996). Virus particles are transmitted across the graft union between scion and rootstock. These practices may have helped to combine multiple viruses into single vines (Meng and Gonsalves, 2003).

Viruses that infect woody plants are difficult to study due to complicated isolation procedures. For this reason, diagnosis and distribution of grapevine viral diseases have in the past been studied and described much more thoroughly than the causal virus agents (Flaherty, 1992). Compared to viruses that infect herbaceous plants, our knowledge of grapevine viruses is limited in terms of the molecular biology, host-pathogen interaction and etiology. This situation is mainly due to the traditional difficulties in perennial plants for fulfilling Koch's postulates: four principles which stipulate that a microorganism needs to be established as the causal agent for a disease (Goheen, 1989). The problems experienced with experimenting with grapevine are listed as follows (Meng and Gonsalves, 2003). Firstly, grapevine is a woody plant which produces high levels of polyphenolics and polysaccharides. These

compounds generally interfere with experimental protocols (Demeke and Adams, 1992). Secondly, grapevine being a perennial plant, significantly delays detection practices such as biological indexing (two year incubation period) and also delays the elucidation of the effect of latent viruses. Thirdly, grapevines are often simultaneously afflicted with several viruses due to the practice of grafting and transmission by insect vectors. Fourthly, viruses often occur in low titers and the distribution of many viruses is limited to the phloem tissue. Together these aspects severely hinder the study of grapevine viruses (Meng and Gonsalves, 2003).

The various viral diseases that grapevine are prone to are damaging and cause considerable crop losses worldwide (Martelli and Boudon-Padieu, 2006). According to the South African Wine Industry Information & Systems (SAWIS), South Africa (SA) is one of world's major wine producing countries. Of the 1.5 million tons of grapes crushed in 2008, 412 million liters of wine were exported and 19.3 million liters were sold domestically (SAWIS, 2008). South Africa exported 53.9% of the natural (non-fortified) wine produced in 2008, of which the United Kingdom, Germany, Sweden and the Netherlands are the greatest importers (SAWIS).

The following statistics demonstrate that the wine industry has a significant impact on the SA economy. At present, 101 957 hectares of prime wine producing territory is under cultivation in SA. White varieties account for 56% of plantings for wine, whereas red varieties account for 44%. The most widely planted white varieties are cv. Chenin Blanc, Sauvignon Blanc and Chardonnay, while the popular red cultivars are Cabernet Sauvignon, Shiraz, Merlot and Pinotage (WOSA, 2009). Over 250 000 people are employed by the wine industry. This figure includes farm labourers as well as those involved in packaging, retailing and wine tourism. A study on the macroeconomic impact of the wine industry on the Western Cape, commissioned by SAWIS and published in 2004, concluded that approximately R16.3 billion (excluding tourism) is contributed to the annual gross domestic product (GDP) of SA, which translates to 1.5% of the SA GDP. The study estimated that about R11.4 billion would eventually remain in the Western Cape to the benefit of its residents. Consequently, the wine industry contributes 8.2% to the Western Cape's gross geographic product (GGP).

Winetech is an association of SA institutions and individuals working towards the common goal of improving the position of the SA wine industry. This organization has identified

certain viruses as the most devastating pathogens affecting local vineyards. The economically important virus and virus-like diseases are: Leafroll syndrome, Fanleaf degeneration, Fleck disorder, Shiraz Disorder, Shiraz decline, Rugose Wood Complex and Phytoplasma disease. It is therefore through co-operative research support and initiatives that effective techniques for the detection and molecular screening of these pathogens can be developed.

The diseases under analysis in this study are Rugose Wood and Shiraz decline. The field spread of RW disease has been noted in South Africa since the early 1970's (Engelbrecht and Nel, 1971). This disease complex consists of many secondary diseases associated with viruses within the *Foveavirus* and *Vitivirus* genera. One of these secondary diseases is Rupestris Stem Pitting disease (RSP) which has been found to be consistently associated with *Grapevine rupestris stem pitting-associated virus* (GRSPaV) (Meng *et al.*, 1999).

An emerging disease of unclear etiology affecting only *V. vinifera* cv. Shiraz (syn. Syrah) has been identified in France and California. In South Africa this disease, termed Shiraz decline, has been observed in a specific clone (Shiraz99) imported from France in 1982. Symptoms of this disease were similar to reports of French researchers (Renault-Spilmont *et al.*, 2003), and also similar to symptoms of Rugose wood diseases. In an attempt to clarify the association of flexiviruses with these diseases, an investigation was initiated (Goszczynski, 2007). Goszczynski (2007) reported the presence of a certain sequence variant of GRSPaV in Shiraz clone 99. This was the premise for the current study on GRSPaV.

Little is known about the prevalence and distribution of GRSPaV in SA. No appropriate and sensitive diagnostic protocol to study GRSPaV has been developed. Therefore, few large scale diagnostic assays have been performed. Control of the viral disease is hampered by the reality that there are no cures or treatments for infected grapevines. Furthermore, no natural resistance genes have been found that confer resistance to grapevine viruses (Goldbach *et al.*, 2003). In order to control virus infection and spread, uninfected propagation material must be used. It is therefore important that sensitive, reliable diagnostic tools be developed that can be applied to test a sizeable number of samples.

The aim of this study was to give an indication of GRSPaV infection in SA vineyards. This was done with the vision to ultimately confirm the association of various GRSPaV molecular variants with Shiraz decline. Efforts were focused firstly to develop a rapid, reliable means of

detection of GRSPaV and secondly to develop a tool for strain determination of SA isolates of GRSPaV. This was accomplished through the screening of field samples using Reverse Transcription Polymerase Chain Reaction (RT-PCR). Selected field samples were subsequently subjected to High Resolution Melt analysis (HRM) for strain differentiation and the parallel sequencing of PCR fragments. The sequence information obtained was primarily used to verify the HRM analysis. The sequences obtained were also subjected to phylogenetic analysis and correlated to those sequences available in the GenBank database. This was performed to establish the dominant variant within the field-collected sample set.

The main findings of this study were as follows: firstly, a successful and sensitive diagnostic tool capable of large-scale screening of vines was developed in this study. GRSPaV was present in the majority of vines tested. This was in agreement with other studies performed where GRSPaV prevalence was high. The problems caused by the molecular diversity of GRSPaV in diagnosis were overcome by examining more than one area of the GRSPaV genome. Secondly, the validation of qPCR-HRM as a technique for viral strain typing was achieved. Groups of similar sequence variants had similar melt profiles and bins could be assigned according to published sequence data. Thirdly, it was found that most of the molecular variants of GRSPaV present within this sample group radiated with a single molecular variant group of GRSPaV: Group II. This result was corroborated by a concurrent metagenomic sequence study performed on the same sample group (Coetzee *et al*., 2009).

2. Literature Review

2.1 Introduction

Interest in research on *Grapevine Rupestris Stem Pitting-associated Virus* (GRSPaV) originated from the graft transmissible disease Rupestris Stem Pitting (RSP) which forms part of the Rugose Wood (RW) disease complex. The role of this virus in Shiraz decline and Vein necrosis is also prominent. These diseases collectively constitute some of the most devastating viral diseases of the grapevine. Accumulated field surveys and biological indexing data suggest that RSP is the most widespread component of the RW disease complex (Martelli, 1993).

Rupestris stem pitting associated virus-1 (RSPaV-1) (Meng *et al*., 1998) and *Grapevine rupestris stem pitting-associated virus* (GRPSaV) (Zhang and Rowhani, 2000; Zhang *et al*., 1998) were cloned independently as the putative agent of RSP in 1999. Sequence analysis revealed that these viruses were almost identical. For the purpose of this work, the virus will be referred to as GRSPaV as classified in the genus *Foveavirus* (Martelli and Jelkmann, 1998)*,* suggested family *Betaflexiviridae* and order *Tymovirales* (Martelli, 2009; Saldarelli, 2009; Martelli *et al*., 2007). GRSPaV has been found to have a close association with RSP (Meng *et al*., 1999), Vein necrosis on *V. rupestris* x *V. berlandieri* 100 Richiter (Borgo *et al*., 2009; Bouyahia *et al*., 2005) and Syrah decline (Beuve *et al*., 2009). No direct causal correlation has been drawn to factors such as climate, soil type, or geographical distribution.

Since 1999, several studies have reported the molecular variability of this virus with great genetic diversity and a distinct population structure (Lima *et al*., 2006). Phylogenetic analyses reveal the presence of at least four divergent variant (lineage) groups and a full-length representative genome for each of these groups has been sequenced (Meng and Gonsalves, 2007b). It was also demonstrated that agricultural grape varieties were host to a wider array of sequence variants, whereas rootstock varieties were usually infected with a single variant (Meng *et al*., 2006). The sequence information of several sequence variants of GRSPaV is known which allows the development of effective diagnostic techniques and the progress of understanding GRSPaV functional genomics

Studies have been performed which lay the foundation for determining the molecular mechanisms that govern GRSPaV movement and replication. The subcellular localization of three of the proteins that the viral genome encodes for, has recently been visualized (Rebelo *et al.*, 2008). These proteins are considered to be responsible for systemic movement of GRSPaV. The expression of recombinant coat protein of GRSPaV has allowed significant progress in the arena of rapid molecular diagnosis of GRSPaV abroad (Petrovic, 2003). Techniques such as Reverse Transcription Polymerase Chain Reaction (RT-PCR), Immunosorbent electron microscopy (ISEM), Enzyme-linked immunosorbent assay (ELISA) and Western or Dot-immuno blotting are routinely used in laboratories. The knowledge on the genetic diversity of GRSPaV has allowed the design of universal primers that can be used for the diagnosis of RSP. Nolasco *et al.* (2000) undertook a study to evaluate the sensitivity, specificity and positive predictive value of various primer pairs used for diagnosis. In the current study, several of these primer pairs were evaluated, taking into consideration the natural variability of plant viruses and the feasibility of total RNA as RT-PCR template. A rapid, sensitive detection protocol was developed, that relies on quantitative reverse transcription PCR (qRT-PCR).

A population cloning approach has traditionally been used to characterize RT-PCR products and therefore establish genetic diversity. Recently however, simpler and faster mutation scanning techniques have been developed (Wittwer *et al.*, 2003). High resolution melt analysis (HRM) is an analytical technique which exploits the dissociation behaviour of DNA under the influence of a gradual temperature gradient ($0.1°C/s$) in the presence of a high saturation dye. In this way samples can be characterized based on sequence length, GC content and DNA sequence complementarities by generating specific melt profiles. The slope and midpoint of melt phase is characteristic of every DNA fragment.

Using this technique it is possible to differentiate between a range of sequence variants without the need for electrophoretic analysis of amplicons via Restriction Fragment Length Polymorphism (RFLP) or Heteroduplex Single Stranded Conformation Polymorphism (HEX-SSCP) patterns (Varga and James, 2006; Varga and James, 2005). This technique is validated by sequencing and phylogenetic analysis. The figure below illustrates the ability of HRM analysis to discriminate between single nucleotide polymorphisms in different molecular variants.
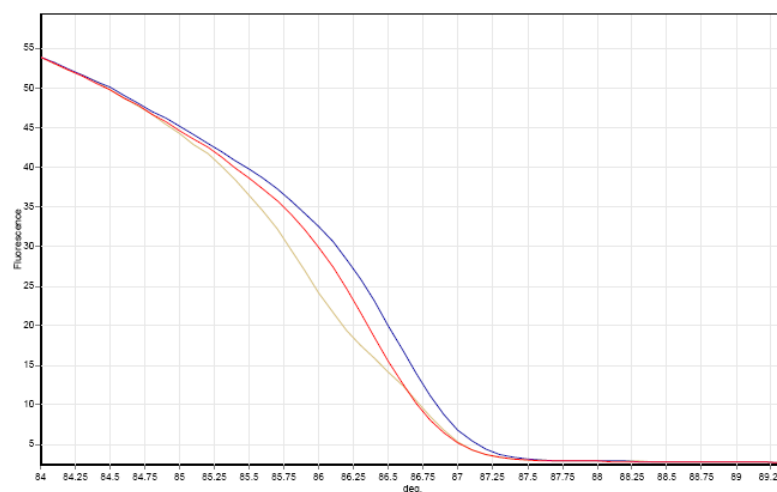
Figure 1: The melt profiles of variants of human monocarboxylate transporter alleles (A1470T) displaying a Class 4 Single Nucleotide Polymorphism (SNP) (Corbett, 2006)

2.2 Diseases with which GRSPaV is associated

There are several economically important diseases associated to GRSPaV. These diseases are discussed in the following paragraphs. The various methods that have been employed to control, prevent and confer resistance to viral diseases are also discussed.

2.2.1 Rugose Wood Disease

Rupestris Stem Pitting disease (RSP) forms part of a complex of graft transmissible diseases, termed Rugose Wood (RW) (Martelli and Boudon-Padieu, 2006). This complex of diseases was first described in 1961 in southern Italy (Graniti and Ciccarone, 1961), but has since been found to occur in most grapevine cultivating countries. It is characterized by reduced vigour, delayed bud opening and distortions of the woody cylinder, such as a spongy texture or unusual groove-like projections on the cambial face of the bark. Grafted vines often

7

display swollen bud unions and a marked difference in relative diameter of scion and rootstock. The severity of disease symptoms vary according to the rootstock and scion graft combinations and latency in infected vines are often observed. The RW complex causes graft incompatibility and thus a reduction in crop yield. Infected vines may decline considerably and die within a few years of planting (Meng *et al.*, 1999).

Biological indexing is the practice of grafting a candidate scion onto an indicator vine which will display symptoms. It is the traditional method for distinguishing disease. There are four disorders associated with Rugose Wood, which are detected by the grafting of three indexing plants (Savino *et al.*, 1989): Kober 5BB (*Vitis berlandieri* Planch. X *Vitis riparia* Michx.); LN 33 (Couderc 1613 x Thompson seedless) and *Vitis rupestris* St. George (Synonyms: Du Lot, *Vitis rupestris* Scheele) (Minafra *et al.*, 2000). The four disorders of Rugose Wood are: Kober stem grooving (KSG) indexed on Kober 5BB as having deep grooving in its woody trunk; Corky bark (CB) indexed on LN33 as severe stunting of this indicator plant accompanied by rolling and reddening of the leaves and internodal swelling or cracking; LN33 stem grooving (LNSG) indexed on LN 33 displaying similar grooving as with CB, but lacking the internodal swelling and foliar discoloration; and RSP indexed on *V. rupestris* St. George as distinct basipetal pitting downwards from the point of inoculation (Martelli, 1993).

In South Africa, a graft-transmissible stem-grooving disease has been observed in the vineyards of the Western Cape Province as early as 1971 (Engelbrecht and Nel, 1971). Further indexing studies revealed the presence of three types of wood disorders of the stem-grooving type, similar to what is now known as RSP, KSG and CB. Natural field spread of the KSG and CB was also observed, suggesting involvement of the vine mealybug *Planococcus ficus* (Engelbrecht *et al.*, 1991).

Putative agents consistently associated with the RW complex come from the family *Betaflexiviridae*, genus *Foveavirus* or *Vitivirus* (Martelli *et al.*, 2007). These viruses consist of flexuous, filamentous virions which are contained only in the phloem of the vines they infect. Vitiviruses are mechanically transmissible to herbaceous hosts, whereas foveaviruses lack this ability. Vitiviruses have been denoted *Grapevine virus A* to E (GVA, GVB, GVC, GVD and GVE), while *Grapevine rupestris stem pitting-associated virus* (GRSPaV) is a member of the genus *Foveavirus* and is the associated agent of RSP (Martelli and Jelkmann, 1998).

The etiology of RW disease has been extensively studied over a number of decades. In 1980 in Italy the first filamentous virus was recovered from a rugose wood-infected vine (Conti *et al*., 1980). Since then, advances made in immunology and molecular biology has contributed to a better understanding of this disease complex in terms of diagnostics and characterization. However, difficulties in fulfilling Koch's postulates prevent a well-defined causal relationship between virus or combinations of viruses and disease (Meng and Gonsalves, 2007a). The incidence of mixed infections further complicates the spectrum of RW viral disease (Prosser *et al*., 2007).

2.2.2   Rupestris Stem Pitting Disease (RSP)

In 1988, Goheen was the first plant pathologist to publish the description and widespread occurrence of Rupestris Stem Pitting (Goheen, 1988). RSP is defined as a disease that produces a strip of pits and grooves below the grafting point on the *V. rupestris* St. George indicator plants after graft inoculation. This graft transmissible disease causes a slow decline in the growth of *V. vinifera* cultivars. After several seasons, affected vines become much smaller than healthy vines, but no leaf reddening or yellowing is displayed. The disease causes a reduction in crop yield due to delayed ripening and low sugar content of the grapes. After several years vines may deteriorate fatally.

An indicator indexing survey undertaken in California in the late 1970's revealed that RSP was prevalent in a variety of imported grapevine selections: France – 66% of 70 vines, Germany – 42% of 53 vines and 67% of 33 selections from Australia (Goheen, 1989). The survey was performed on both symptomatic and asymptomatic plants. Other researchers confirmed the ubiquitous occurrence of this disease in South Africa (Engelbrecht and Nel, 1971), California (Hewitt and Neja, 1971), Mexico (Teliz *et al*., 1980), Australia (Fletcher, 1995), Italy (Conti *et al*., 1980) and China (Li *et al*., 1989).

As was mentioned previously, the best indicator for RSP infection is *V. rupestris* St. George. Chip bud grafting of a candidate onto this indicator is the best method of inoculation for indexing (Goheen, 1988). Biological indexing on woody indicators is labour-intensive and not suited for large scale assays. Another drawback is that virus induced disease symptoms are apparent only after the second or third growth season. As techniques for molecular diagnosis improved, this worldwide standard biological indicator was found to harbour

sequence variants of GRSPaV, which further complicated diagnosis. Using Reverse Transcription Polymerase Chain Reaction (RT-PCR), ELISA and Western Blot detection of GRSPaV, a sequence variant was detected from greenhouse and field grown St. George selections in New York and Canada (Meng *et al*., 2000; Petrovic *et al*., 2000). These findings were also confirmed by serological detection in the St. George selection from Italy (Minafra *et al*., 2000). The advantages of molecular detection over biological indexing are thus apparent, as previous biological surveys delivered false negative results. It was however experimentally demonstrated that infection by the sequence variant (designated GRSPaV-SG1) found in the St. George indicator is asymptomatic and that its presence should not have interfered with past indicator indexing for this disease (Meng *et al*., 2005).

2.2.3   Shiraz Decline

A relatively new disorder of the popular cultivar Shiraz (Syn. Syrah), termed Shiraz decline, has been reported to have a worldwide prevalence in vineyards (Zhang *et al*., 1998). The decline of this cultivar was observed in France (Renault-Spilmont *et al*., 2003) as well as California (Battany *et al*., 2004). Symptoms of this graft transmissible disorder include abnormal graft unions, premature leaf reddening and deep grooving of the stems of scions. Affected vines have reduced vigour due to graft failure, which normally leads to death in the grafted plant in approximately 3-6 years. The disorder does not affect the rootstock, but grafting of Shiraz to rootstocks becomes unfeasible. The yields of fruit and quality of wine produced by affected vines are reduced due to their decline in growth (Battany *et al*., 2004).

A consistent association of GRSPaV to Syrah decline has been observed in France (Beuve *et al*., 2009), Italy (Bianco *et al*., 2009), Australia (Habili *et al*., 2006) and California (Lima *et al*., 2006). The Shiraz clone 99B was imported to South Africa from France in 1982 and propagated on a large scale since 1997 (KWV, Vititech). This clone displayed similar symptoms as reported in other countries. A survey to examine the association of flexiviruses to Shiraz decline in South Africa was carried out (Goszczynski, 2007). This survey utilized a nested RT-PCR with degenerate primers developed by Dovas and Katis, (2003) to detect members of both the *Foveavirus* and *Vitivirus* genera. This investigation revealed that the Shiraz clone 99B (Vititec, KWV) was infected with viruses related to molecular strains of GRSPaV found in the USA as well as Australia. The presence of GRSPaV in SA vineyards therefore warrants further examination.

Many of the symptoms of Shiraz decline also occur upon infection with other grapevine-infecting viruses (Al Rwahnih *et al*., 2009). This complicates the explanation of Shiraz decline because an association to a virus or a complex of viruses becomes difficult. Recently, Al Rwahnih *et al*. (2009) applied a metagenomic sequencing strategy to a vine displaying decline symptoms. The transcriptome of this infected plant was sequenced and found to be contaminated with a wide array of viruses including GRSPaV and *Grapevine rupestris vein-feathering virus* (GRVFV). Mixed infection with GRSPaV sequence variants was predominantly found. The third-most prevalent virus in this vine extract was an unknown *Marafivirus* provisionally called *Grapevine Syrah virus-1* (GSyV-1). From this study, these researchers suggested that these three viruses are the predominant agents of Shiraz decline (Al Rwahnih *et al*., 2009).

2.2.4   Vein necrosis

Vein necrosis is a latent virus-like disease of grapevines that was first reported in 1973 (Legin and Vuittenez, 1973). It is a widespread disease, found in Europe, Australia, Brazil and the Unites States of America (predominantly in California) (Martelli and Boudon-Padieu, 2006). The disease is characterized by the appearance of necrosis on the lower side of leaf blades on the rootstock indicator 110 Richter (110R, *V. rupestris* X *V. berlandieri*) (Martelli and Boudon-Padieu, 2006). Growth of the vine is reduced as tendrils and shoots may also necrotize.

A close association between GRSPaV infection and Vein necrosis on 110R has been established with ELISA, RT-PCR, Western Blot and Biological indexing (Borgo *et al*., 2006; Bouyahia *et al*., 2005). Further comparative studies were carried out to determine the relationship between various molecular variants of GRSPaV and Vein necrosis on 110R. It was recently found that the expression of vein necrosis symptoms is restricted to infection with viral variant groups I and II of GRSPaV (Borgo *et al*., 2009; Bouyahia *et al*., 2009). The 110 Richter grapevine variety was not analyzed in this study

2.2.5   Viral eradication and disease control

Although, various methods have been used to control grapevine diseases caused by viruses, they still remain destructive to the industries. These methods employed include crop rotation, early detection and destruction of infected plants, resistance breeding, pesticide vector-

control and cross-protection (Goldbach *et al*., 2003). Diseased materials are primarily spread due to incorrect indexing or inadequate eradication of propagation materials. Therefore, ensuring the sanitary status of starting material requires the development of rapid, effective methods of detecting viral agents of disease. The availability of genome sequences of several GRSPaV isolates has enabled the expansion of a wide collection of molecular methods for rapid detection of GRSPaV (as will be discussed later). The consistent and accurate detection of RSP in potential grapevine rootstocks and scions will ensure that no infected vines are planted, thus restricting the spread and prevalence of this disease.

A number of sanitation techniques such as meristem or shoot tip culture, chemotherapy, thermotherapy and somatic embryogenesis have been applied to grapevine for GRSPaV eradication. Success however depends on grape cultivar, targeted virus and specific approach (Gambino *et al*., 2006). GRSPaV is reported to be a particularly recalcitrant virus to eliminate (Skiada *et al*., 2009; Minafra and Boscia, 2003) by meristem tip culture and thermotherapy. Recent efforts to eliminate GRSPaV from infected vines have however delivered promising results. A novel approach whereby *in vitro* established Agiorgitiko explants were cultured in the presence of the antiviral compounds Tiazofurin, Ribavirin or Mycophenolic Acid (Skiada *et al*., 2009). Up to 80% of explants which survived the anti-viral treatment with Tiazofurin at optimal concentration were found to be virus-free. To compare this approach to other sanitation techniques, this group also demonstrated up to 67% elimination rate of meristem cultures post thermotherapy of the same cultivar (Agiorgitiko). Further experimentation is still needed to evaluate the efficacy of other anti-viral compounds on other grapevine cultivars. Gribaudo *et al*. (2006) successfully applied somatic embryogenesis to the elimination of GRSPaV from all 97 lines of seven different Italian wine grape cultivars demonstrating a 100% elimination rate. Tissues used for starting cultures were from immature anthers and ovaries. The efficiency of *in vivo* thermotherapy for four of the 7 cultivars was examined simultaneously and indicated a much lower average elimination rate of 23.6% (Gribaudo *et al*., 2006).

A way to confer grapevines with viral disease resistance is to genetically transform the plants in either a stable or transient manner. Genetic transformation with sequences derived from the genome of GRSPaV would trigger RNA silencing in the plant host, which would lead to the degradation of incoming viral RNAs (Van Eeden, 2004). *Nicotiana benthamiana* plants

genetically engineered to express the Coat Protein (CP) of *Grapevine Leafroll-associated virus 2* (GLRaV-2) proved to be resistant to infection of GLRaV-2 upon mechanical inoculation (Ling *et al*., 2008). Low levels of RNA transcripts present in the inoculated transgenic plants of this above-mentioned study suggest evidence of post-transcriptional gene silencing (PTGS). Transgenic resistance in an herbaceous host provides a good prospect for the control of virus-induced disease in grapevine. Recently attempts were made to use the expression of pathogen-specific recombinant antibodies in plants to introduce viral resistance against grapevine-infecting ampeloviruses (Orecchia *et al*., 2008). Antibodies were transiently expressed in *N. benthamiana*, retaining antigenic capacity and were shown to bind specifically against four members of the family *Closteroviridae*. This candidate approach could also potentially be eligible for mediating broad-spectrum viral disease resistance in transgenic plants.

2.3 GRSPaV

The putatative agent of RSP as well as several other diseases, is classified taxonomically below. The genome organization and expression of the open reading frames (ORFs) of GRSPaV are discussed. The relationship of GRSPaV to members of other genera within the family *Flexiviridae* are also discussed. Finally, the transmission and economic importance of this virus is considered.

2.3.1   Morphology and Taxonomy

GRSPaV contains a monopartite positive sense, single-stranded RNA genome of approximately 8.7 kb. GRSPaV virions display flexuous, filamentous, non-enveloped characteristics of the original family *Flexiviridae.* To reflect the different lineages of the replication proteins (potex-like and carla-like) and the inclusion of fungal-infecting viruses, *Flexiviridae* has been reclassified and divided into three different families: *Alphaflexiviridae* (potex-like polymerases), *Betaflexiviridae* (carla-like polymerase) and *Gammaflexiviridae* (filamentous fungal-infecting viruses). The genus, *Foveavirus,* together with 5 other genera belongs to the family *Betaflexiviridae.* GRSPaV falls within the genus *Foveavirus* (Martelli and Jelkmann, 1998) as it has a helical symmetrical morphology of 723nm in length and 10-12nm in diameter (Figure 2) (Petrovic *et al*., 2003). Other members of the genus include: *Apple stem pitting virus* (ASPV), *Apricot latent virus* (ApLV) and *Peach chlorotic mottle virus* (PCMV).
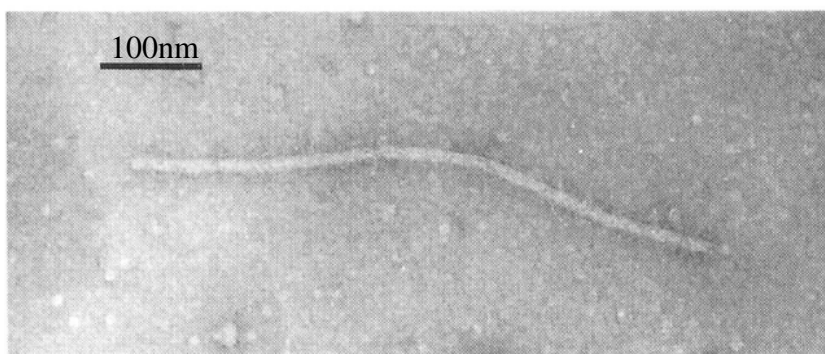
Figure 2: Negatively stained electron micrograph of GRSPaV displaying virion morphology. Bar represents 100nm (Petrovic *et al*., 2003).

2.3.2   Genome organization and Expression

The genome of GRSPaV consists of 8725 nucleotides (nt) and encodes five ORFs. The most terminal nt of the 5' non-coding region (NCR) is a guanosine and is presumed to be capped. The 5' NCR consists of 61 nt upstream of the start codon of ORF 1. The 3' terminal NCR is polyadenylated and consists of 176 nts.

Figure 3: Genome organization of GRSPaV (Meng and Gonsalves, 2007b). Conserved domains within ORF 1 are indicated by respective nucleotide positions: a methyl transferase (MTR), a highly variable region (HVR), a papain-like cysteine protease (PRO), an RNA helicase (HEL) and an RNA-dependant RNA polymerase (POL)

2.3.2.1   ORF 1

ORF 1 occupies the majority of the genome: 6486 base pairs (bp) corresponding to nt positions 61-6546 encoding a polyprotein precursor of 2161 amino acids (aa) with a calculated molecular weight of 244 kDa (Meng *et al*., 1998; Zhang *et al*., 1998). This translation product contains all of the domains that are conserved among the replicative proteins of the Alpha-virus-like superfamily of RNA viruses (Koonin and Dolja 1993, Strauss and Strauss 1994): a methyl transferase (MTR), an RNA helicase (HEL), a papain-like cysteine protease (PRO) and an RNA-dependant RNA polymerase (POL) (Figure 3) (Meng and Gonsalves, 2007b).

The presence of the PRO domain suggests the involvement of autocatalytic cleavage of the polypeptide encoded by ORF 1 to produce two or more fully functional proteins involved in replication of the virus. The 5' cap structure of both genomic and any sub-genomic RNA is attributed to the translation product of the MTR domain. The HEL domain is required for the unwinding of dsRNAs during genome replication. At nt position 451-750 there is a Highly Variable Region (HVR) of unknown function (Martelli *et al*., 2007).

2.3.2.2   ORFs 2-4

Downstream of ORF 1 lies a unit of three partially overlapping ORFs designated the 'triple gene block' movement protein (TGB) which is responsible for intra-cellular and cell-to-cell movement of emerging virions and ribonucleo-protein complexes through the infected plant (Morozov and Solovyev, 2003). Foveaviruses share this sequence feature with members of the genus *Carlavirus*, *Potexvirus, Mandarivirus* and *Allexivirus.* ORF 2 potentially encodes a 24.4 kDa polypeptide of 221 aa, and contains the conserved domains for ATPase, RNA-binding and helicase activities. ORF 3 yields a putative 12.8 kDa polypeptide of 117 aa and ORF 4 encodes a putative 8.4 kDa protein of 80 aa (Meng *et al.*, 1998; Zhang *et al.*, 1998).

The three proteins encoded by the ORFs 2-4 or the TGB are tentatively named TGBp1, TGBp2 and TGBp3 respectively. It was demonstrated recently that TGBp1 had both a cytosolic and nuclear localization (Rebelo *et al.*, 2008). TGBp1 is involved in the translocation of itself and newly synthesized viral complexes across plasmodesmata, a process most likely to require ATP (Meng and Gonsalves, 2007b). The mechanism of translocation however is unknown. In addition it has been revealed that TGBp1 functions as a suppressor of host RNA silencing, which is a requirement for sufficient systemic movement (Bayne *et al.*, 2005). Sequence prediction analysis of ORF 3 and ORF 4 indicates two and one conserved transmembrane domains respectively. Through a series of truncation and fusion mutants, TGBp2 and TGBp3 were found to be localized to the endoplasmic reticulum network (Rebelo *et al.*, 2008) via fluorescence microscopy.

2.3.2.3   ORF 5

ORF 5 corresponding to nt positions 7771-8550 encodes the coat protein (CP) of 28 kDa. This ORF was identified due to the presence of the conserved amino acid motif "RR/QX-XFDF" involved in salt bridge formation, which is characteristic of filamentous viruses with positive-strand RNA genomes (Meng *et al.*, 1998). Furthermore, polyclonal antibodies have been raised against a recombinant CP of GRSPaV which clearly coated particles of the virus (Figure 4) (Petrovic *et al.*, 2003). The 28 kDa protein was also consistently detected in GRSPaV-infected grapevines via Western Blot using the polyclonal antibodies (Meng *et al.*, 2000; Minafra *et al.*, 2000).

2.3.2.4   ORF 6

An additional 6th ORF was described at the 3' proximal portion of the GRSPaV genome which corresponds to nucleotide positions 8228-8586 and a 14 kDa protein (Zhang *et al.*, 1998). Nolasco *et al.* (2006) however debate the existence of this ORF due to a lack of selection pressure and note that further experimental data is required.

Figure 4: A single viron of GRSPaV visualized with immunosorbent electron microscopy (ISEM) (Petrovic *et al.*, 2003). Antisera generated against GRSPaV was used to generate theelectron micrograph. Bar represents 100nm.

2.3.3   Phylogenetic relationship to other genera of *Flexiviridae*

Based on sequence similarity and resemblance in genomic structure, GRSPaV is considered to be more closely related to carlaviruses such as *Potato virus M*, than to potexviruses (Meng and Gonsalves, 2007a, Martelli *et al.*, 2007). The size and organization of the 3' NCR and the translation products of ORF 1 and ORF 2 of GRSPaV are more similar to carlaviruses than to potexviruses. However, when a number of carlaviruses and potexviruses were phylogenetically compared to GRSPaV and ASPV in the CP region, these foveaviruses radiated with potexviruses at a bootstrap value of 71 (Zhang *et al.*, 1998). These lines of evidence may indicate that portions of the GRSPaV genome originated from separate sources (such as a carlavirus or potexvirus) due to an ancient recombination event (Meng and Gonsalves, 2003; Zhang *et al.*, 1998). However, the inter-species phylogenetic analysis of replicase sequences may be a better gauge for evolutionary relationship, since viral replicases are most conserved among messenger-sense RNA viruses (Martelli *et al.*, 2007). Figure 5 depicts the similarities in genomic size and composition as well as the functional domains of ORF 1 of the genera within the family *Flexiviridae*.

Figure 5: Schematic representing the genomic organization of type members of each of the genera within the family *Flexiviridae*. Functional domains: M – methyltransferase, A – AlkB, O – OTu-like peptidase, P – papain-like protease, H – RNA helicase, R – RNA-dependant RNA polymerase (Martelli *et al*., 2007)
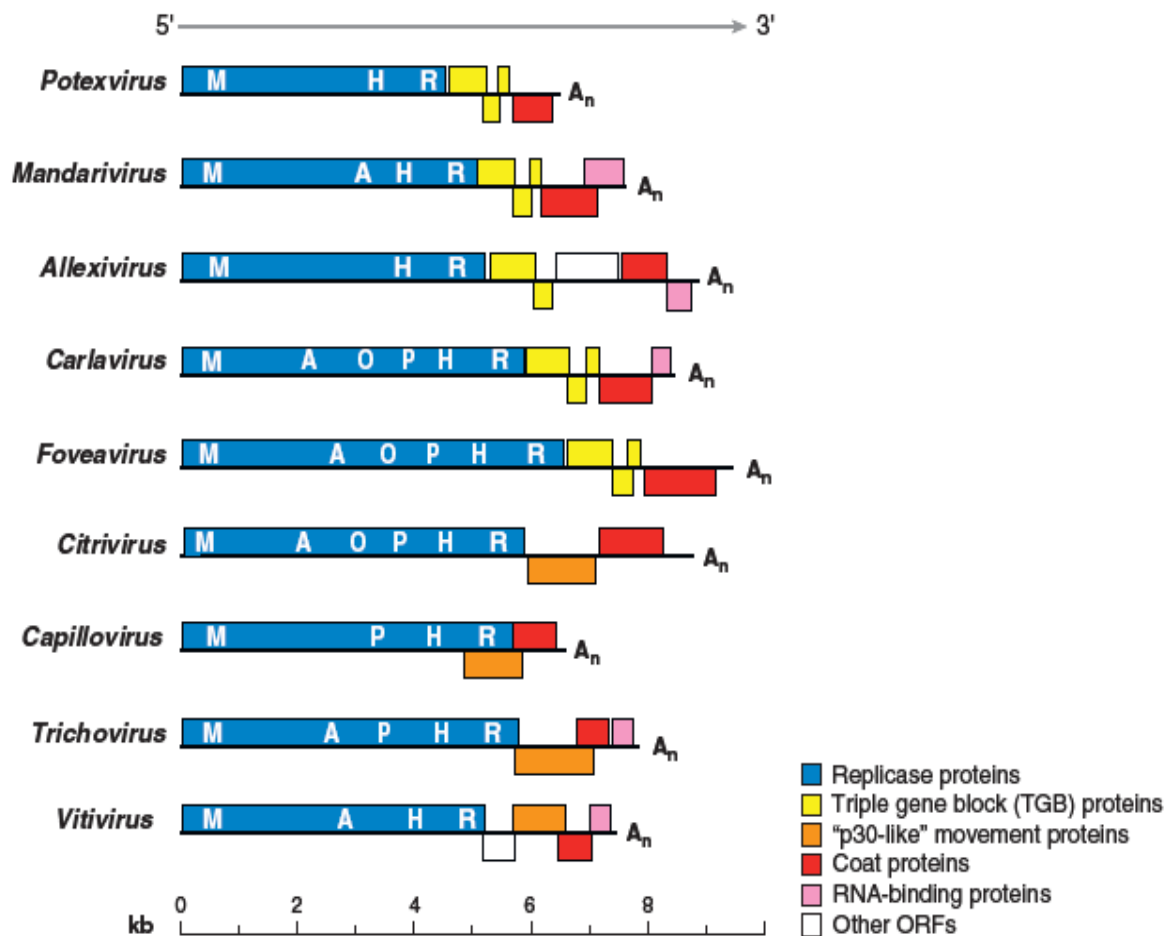
2.3.4   Transmission

No insect vector is known to transmit the putative causal agent of RSP (Zhang *et al*., 1998). The dissemination of GRSPaV is maintained largely by the efforts of humans: the international exchange of infected propagation material and the practice of grafting between diverse varieties of scion and rootstock cultivars. These phenomena are also responsible for the mixed infections that are known to occur within scion varieties (Meng *et al*., 2006).

Investigations into the possibility that GRSPaV is transmissible through pollen or seed have been promising. Rowhani *et al*. (2000) showed that GRSPaV was detected from pollen grains that were treated with 1% SDS, which suggests that the virus is carried internally. It was also shown that all the seeds collected from seven GRSPaV-infected *V. vinifera* varieties tested positive for GRSPaV, even after bleach treatment (Stewart and Nassuth, 2001). In 2006, it was experimentally demonstrated that GRSPaV is transmitted by seed from GRSPaV-infected mother plants to their progeny (Lima *et al*., 2006), but no inquiry into the distribution of virus within the seed was made. Invasion of the embryo by plant viruses is believed to be necessary for true seed transmission (Wang and Maule, 1994). Recent reports made it evident that GRSPaV was present in both embryonic and non-embryonic sections of seeds of three GRSPaV-infected grapevine varieties (Habili *et al*., 2009). This finding has implications for plant breeders and plant certification schemes.

2.3.5   Economic Importance

Without unequivocal evidence that GRSPaV is the causal agent for RSP, the economic importance of RSP remains to be determined (Meng and Gonsalves, 2007b). The presence of multiple sequence variants of GRSPaV hampers this process because differential pathogenicity of sequence variants exists. It is well established that divergent sequence variants may induce different symptoms, or that combinations of infections may cause a more severe form of a disease (Credi and Babini, 1997). It is also possible that GRSPaV infection may induce different types of symptoms on different genotypes of grapevines. The impact of GRSPaV infection on different grapevine species and cultivars is poorly understood as research in these areas is limited. Further investigation into the biology, host-pathogen relationship, genetic variability and virus-interaction of GRSPaV needs to be carried out.

2.4 Genetic Diversity of GRSPaV

The genomic diversity of GRSPaV has been widely reported (Nolasco *et al*., 2006; Santos *et al*., 2003; Rowhani *et al*., 2000; Soares *et al*., 2000; Meng *et al*., 1999). It is evident that GRSPaV exhibits a large amount of genetic variation, encompassing a broad range of sequence variants. The full length genomic sequences of GRSPaV are compared below as well as their differences in pathogenicity. The distinct population structure of GRSPaV isolates is also reviewed.

2.4.1 Comparison of Full-length genome sequences

To date, six fully sequenced genomes of GRSPaV originating from different grapevine isolates are available in GenBank. The sequence of the first isolate was obtained from pooled dsRNA preparations extracted from several French-American hybrid varieties. A cDNA library was created, radioactively hybridized and overlapping cDNA clones were selected, sequenced and assembled. This assembly yielded the first sequence of a high molecular mass dsRNA to be closely associated to RSP, namely RSPaV-1 (AF057136) (Meng *et al*., 1998). A second full-length genomic sequence for GRSPaV, based on dsRNA isolated from a single variety of *V. vinifera,* Cabernet Sauvignon, was independently reported in the same year (AF026278) (Zhang *et al*., 1998). These two isolates have since been found to share 98% nt identity and have been designated GRSPaV-1.

The genomes of two more isolates were sequenced: GRSPaV-SG1 (AY881626), the dominant variant infecting *V. rupestris* cv. 'St. George' and GRSPaV-BS (AY881627), a variant isolated from *V. vinifera* cv. 'Bertille Seyve 5563'(Meng *et al*., 2005). As mentioned previously, GRSPaV-SG1 was isolated from the woody indicator that has for many years served in biological indexing trials for RSP as well as Grapevine Fanleaf and Grapevine Fleck diseases (Martelli, 1993). St George is also frequently used as a rootstock for growing grapevine. Meng *et al*. (2005) demonstrated experimentally that GRSPaV-SG1 was asymptomatic, thus infection with this sequence variant should not hinder biological indexing. GRSPaV-SG1 and GRSPaV-BS share overall nt identities of 87.3% and 84.3% to GRSPaV-1 respectively (Table 1). These two sequence variants share 83.9% overall nt identity with each other (Meng *et al*., 2005).

In 2006, the genomic sequence of a fifth GRSPaV sequence variant originating from a Californian field selection of *V. vinifera* cv. Syrah which was exhibiting decline symptoms such as weak growth, red canopy and an enlarged graft union (Lima *et al*., 2006) became available. Although several other virus assays were performed, only GRSPaV was identified in this selection hence the classification, GRSPaV-SY (AY368590). This sequence variant showed a much lower nt identity to previously sequenced genomes, although the variation displayed was still lower than the species demarcation threshold of 28% nt dissimilarity (Adams *et al*., 2004).

Very recently, a sixth sequence variant of GRSPaV, designated GRSPaV-PN (AY368172), was isolated from declining *V. vinifera* cv. Pinot noir (clone 23) growing on Couderc 3309 rootstocks (Lima *et al*., 2009). These vines displayed acute stunting, leaf reddening, poor shoot and fruit development. Necrotic symptoms and distortions of the woody cylinder of the rootstocks were also observed. This sequence variant displayed as little as 76% nt identity with previously identified variants.

Table 1: Comparative analysis of nt sequences of the five full-length GRSPaV sequences and *Peach Chlorotic Mosaic Virus* (PCMV, GenBank Acc no EF693898.1), an outgroup foveavirus. PCMV is included in comparison to illustrate nucleotide dissimilarity between a virus from the same genus as the full-length variants of GRSPaV.

		NUCLEOTIDE IDENTITY (%)					
		GRSPaV-1	GRSPaV-SG1	GRSPaV-BS	GRSPaV-SY	GRSPaV-PN	PCMV
NUCLEOTIDE DISSIMILARITY	GRSPaV-1	-	87.3	84.3	77.1	76.0	51.4
	GRSPaV-SG1	12.7	-	83.9	77.3	78.0	52.0
	GRSPaV-BS	15.7	16.1	-	77.6	77.0	51.5
	GRSPaV-SY	22.9	22.7	22.4	-	77.0	51.8
	GRSPaV-PN	24.0	22.0	23.0	23.0	-	52.4
	PCMV	48.6	48.0	48.5	48.2	47.6	-

The four strains have identical genome structures despite variations at nucleotide level. GRSPaV-SY and GRSPaV-PN are most divergent when compared to the other 3 strains. The 5' UTR is the most conserved non-coding region (90-98.3% nt identity), while the CP is the most conserved among the coding regions (81-90.6% nt identity) (Meng and Gonsalves, 2007b). ORF 4 is the least conserved of the open reading frames.

2.4.2 Genetic Diversity and Variability

A high degree of sequence diversity was documented when the first GRSPaV isolates were being fully sequenced. The cDNA clones produced through reverse transcription using dsRNA templates from different grapevine varieties yielded nt identities of 82-99% relative to GRSPaV-1 (Zhang *et al.*, 1998). Similarly, Meng *et al.* (1999) found GRSPaV to consist of a heterogenous population of sequence variants sharing between 75-99% identities, but having identical genome structures. It was also found that this heterogeneous population separated into distinct groups of viral variants and that the incidence of mixed infection of a single vine with different viral variants of GRSPaV is high. By looking at several sources of *V. vinifera*, it was discovered that the presence of sequence variants is independent of genotype or geographic origin of the host plant, which raised further questions in terms of transmission and dissemination of this ubiquitous virus.

The findings outlined above stimulated further investigation into the genetic variability of GRSPaV from researchers around the globe. Using primers designed to the CP of GRSPaV, several research groups identified the existence of three distinct groups of viral variants obtained from different geographic regions, based on coat protein sequences alone (Casati *et al.*, 2003; Terlizzi and Credi, 2003; Rowhani *et al.*, 2000). Phylogenetic analysis of the CP sequences of 17 isolates from California and Italy was performed and a variation of up to 21% sequence dissimilarity was found (Rowhani *et al.*, 2000). Terlizzi *et al.* (2003) and Casati *et al.* (2003) examined 28 and 33 Italian isolates respectively in the same CP regions and both groups revealed high heterogeneity of up to 23% and 25% respectively.

More recent and extensive analysis of GRSPaV genetic variation revealed the presence of four groups of sequence variants (Nolasco *et al.*, 2006; Santos *et al.*, 2003). Nolasco *et al.* (2006) observed genetic variability of up to 19% between isolates from 46 Portuguese *V. vinifera* varieties, 2 Slovenian *V. vinifera* varieties and some wild *V. sylvestris* species. Sequence analysis placed these sequence variants into four phylogenetic groups, designated 1, 2a, 2b and 3, which co-incidentally clustered with each of the 4 isolates for which the genomes had been fully sequenced (Figure 6).
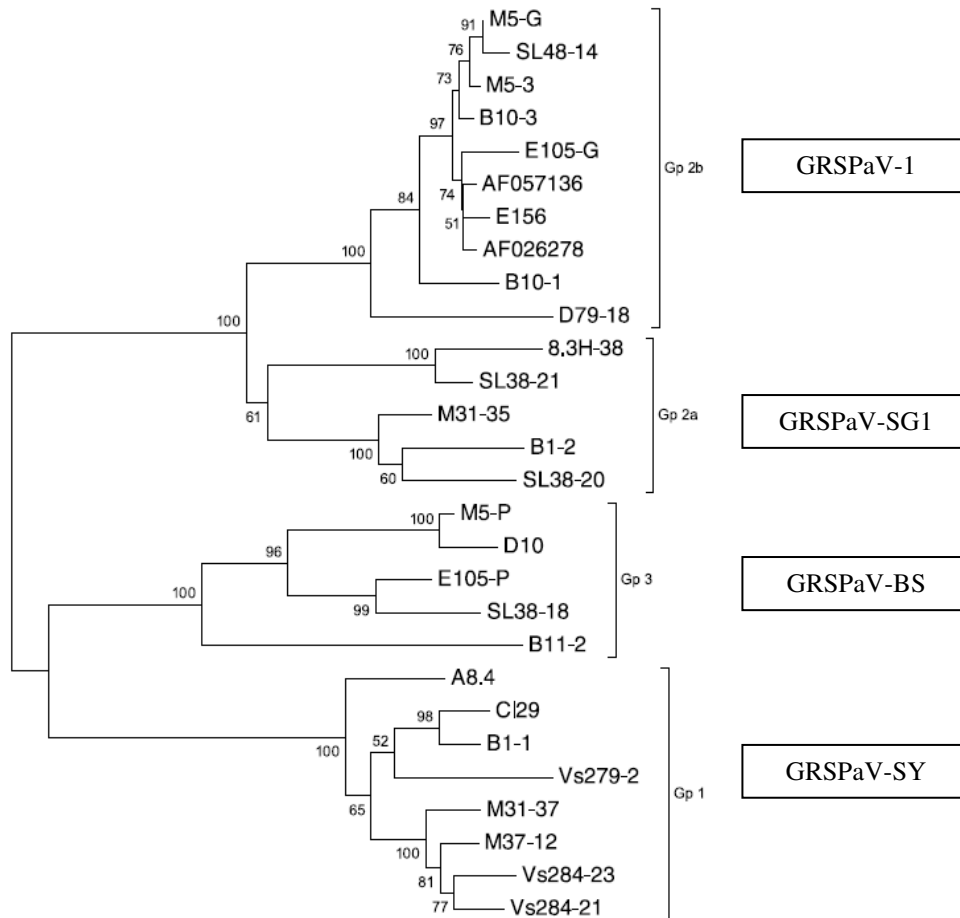
Figure 6: A neighbor-joining tree of Portuguese, Slovenian and wild *V. sylvestris* varieties displaying four variant groups. Genbank accession numbers for full length genomes are: AF026278 & AF057136 – GRSPaV-1, AY881626 – GRSPaV-SG1, AY881627 – GRSPaV-BS. (Nolasco *et al.*, 2006)

The discrepancy in the number of distinct viral variant groups surfaced due to the unearthing of a novel viral variant group (Group 1). From performing a phylogenetic analysis with published sequences, these authors concluded that variants obtained from groups 2a, 2b and 3 are common in different countries, whereas Group 1 variants are more rare (Nolasco *et al.*, 2006). Therefore the existence of only 3 groups proposed by other authors could be accounted for by unreported Group 1 variants, or the combination of Group 2a and 2b into one category because of a narrower relatedness among them. Furthermore, variants of the novel Group 1 were isolated from *V. sylvestris* as well as some of the cultivated varieties of *V. vinifera* in Portugal. The association of this viral variant group to disease symptoms remains unexplored. However, when the genome of the fifth GRSPaV variant became available, GRSPaV-SY, it was found to cluster with this variant group (Meng and Gonsalves, 2007b).

23

Notably in 2008, these findings were confirmed in a survey carried out on Japanese table grapes cv. Pione and cv. Kyoho. These varieties are hybrids between *V. vinifera* and *V. labrusca* which had been grafted on cv. Kober 5BB. Vines displaying symptoms of Rugose wood as well as asymptomatic plants were tested. The study revealed that GRSPaV isolates from Japan were divergent and were distributed across all four sequence variant groups with more than 70% bootstrap values (Figure 7) (Nakaune *et al*., 2008). Remarkably, the majority of isolates from Japan clustered in Group 1 which, as outlined above, is considered an uncommon viral variant group in other countries.
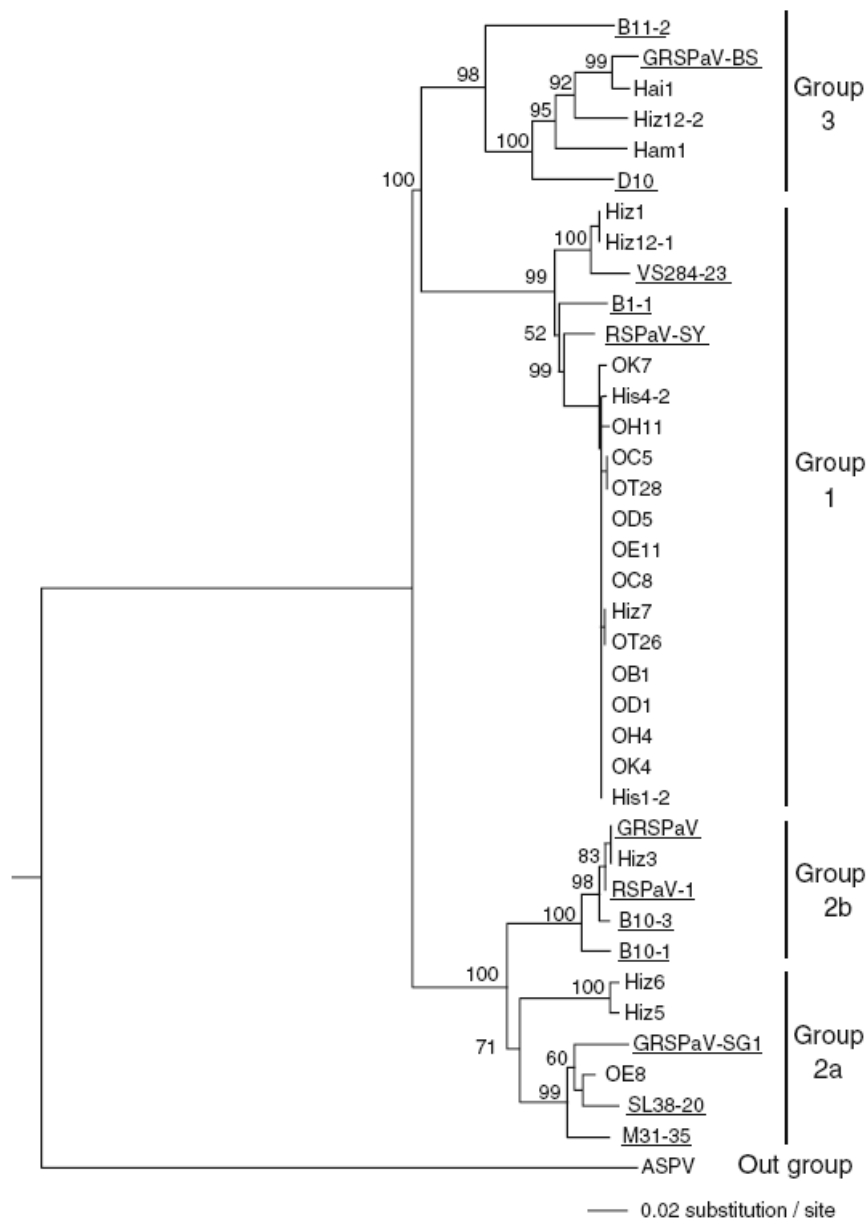
Figure 7: Phylogenetic analysis within the CP region of 24 Japanese GRSPaV isolates compared to an outgroup foveavirus (ASPV), five full-length GRSPaV sequences and selected Genbank sequences, submitted by Nolasco *et al*. 2006, which are representative of each phylogenetic group (D10 – AY927672, B11-2 - AY927679, B1-1 - AY927682, VS284-23 - AY927686, B10-1 - AY927680, B10-3 - AY927681, M31-35 - AY927673 and SL38-20 - AY927687)

24

In the studies summarized above, all sequence analyses were done using regions within the CP of GRSPaV. To compare the usefulness of examining different areas of the GRSPaV genome for strain typing and to validate the phylogenetic relationships observed previously, Meng *et al*. (2006) compared the helicase domain of ORF 1 (Primer set RSP13 & RSP14) with the mid-region of the CP (Primer set RSP21 & RSP22). Twenty four isolates from scion, rootstock and hybrid varieties of *V. vinifera, V. riparia* and *V. berlandieri* were assayed. Firstly, it was concluded that these two primer pairs were both effective in detecting the four groups of sequence variants, designated I, II, III and IV, as phylogenetic trees drawn from different genomic regions had similar structures (Figure 9 and Figure 8). This result confirms the existence of four distinct phylogenetic groups, regardless of genomic area or geographic zone being examined. Secondly, different population structures for GRSPaV variants were observed in scion vs. rootstock varieties. The scion varieties assessed were typically infected with mixtures of genomic variants from different viral variant groups, whereas the rootstocks were infected with a homogenous population of nearly identical sequence variants from a single viral variant group. Thirdly, these authors were able to show specific associations between two of the viral variant groups to two of the North American *Vitis* species, as well as their hybrid descendants. The viral variant group harbouring GRSPaV-1 was shown to be associated with *V. riparia* and the group holding GRSPaV-SG1 to be associated to *V. rupestris* (Meng *et al*., 2006).
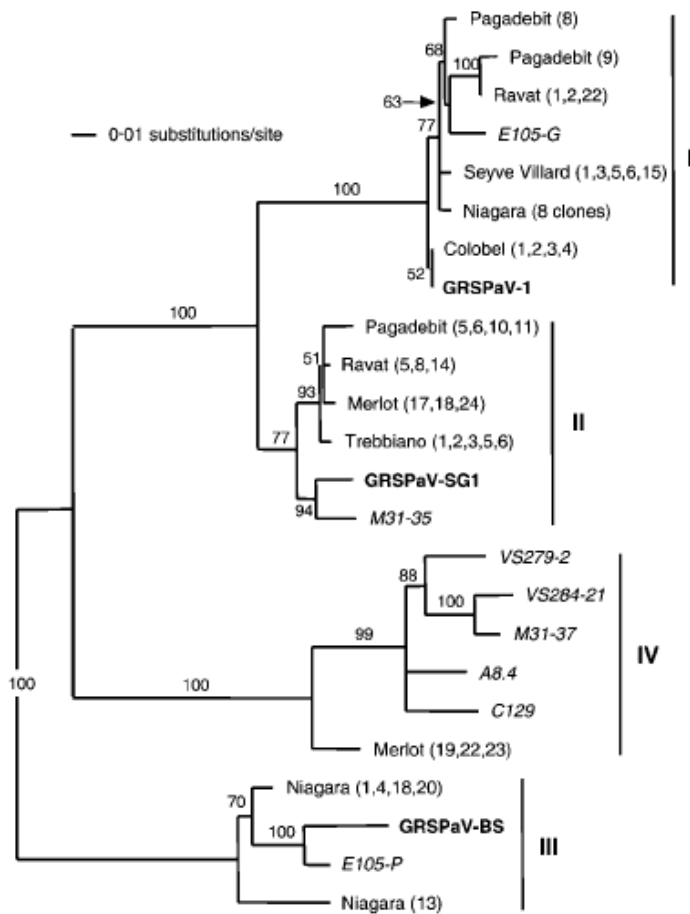
Figure 9: Unrooted phylogenetic tree analysis within the CP region (corresponding to nt 7917-8357) of 13 cDNA clones derived from North American varieties as well as 8 Portuguese *Vitis* isolates representative of four groups identified by Nolasco *et al*. (2006). Portuguese isolates are italicized and full-length genomes are shown in bold.
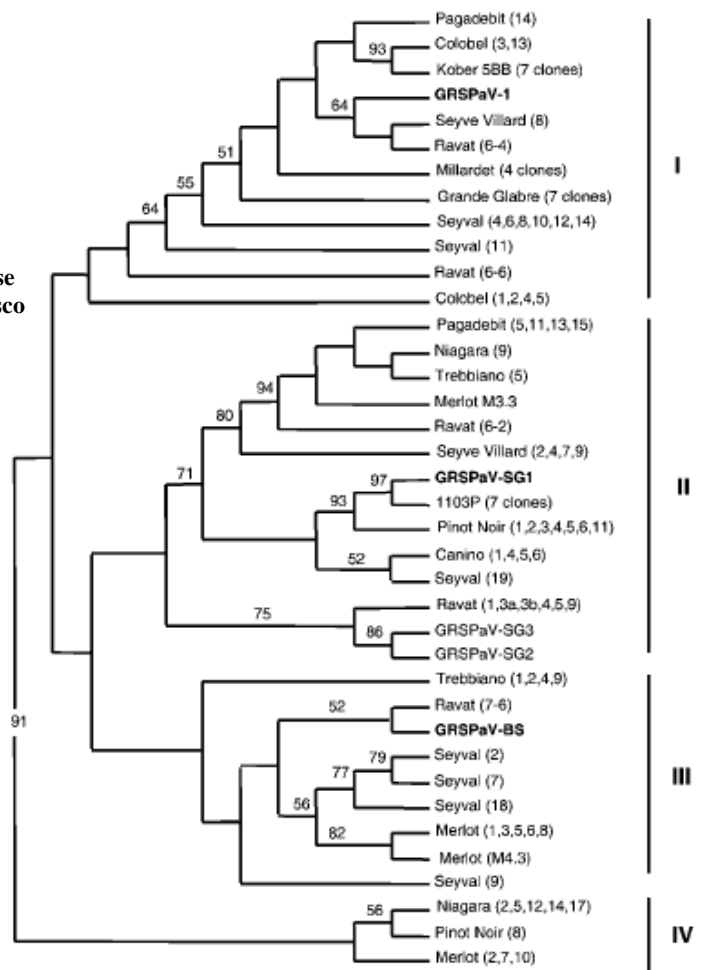
Figure 8: Unrooted phylogenetic tree analysis within the helicase domain of ORF 1 (corresponding to nt 4373-4711) of 24 GRSPaV isolates from three *Vitis* species of scions and rootstocks (Meng *et al*., 2006). Full-length sequences represented in bold. cDNA clones were derived from grapevines via RT-PCR and subsequent cloning and named after respective varieties.

26

For the remainder of this thesis, the designation Group I, II, III and IV will be used. To circumvent any misinterpretation of nomenclature the different categorizations are tabulated below (Table 2).

Table 2: Nomenclature of different GRSPaV viral variant groups by different authors, representative whole-genome sequences and respective GenBank accession numbers, authors responsible for publication of full-length genome and _Vitis_ species associated with viral variant group.

	Viral Variant Group			
	I	**II**	**III**	**IV**
Nolasco _et al_. 2006	2b	2a	3	1
Meng _et al_. 2006	GRSPaV-1	GRSPaV-SG1	GRSPaV-BS	GRPSaV-VS
Full-length representative genome	GRSPaV-1	GRSPaV-SG1	GRSPaV-BS	GRPSaV-SY
GenBank Accession number	AF026278 & AF057136	AY881626	AY881627	AY368590
Citation for full-length sequence	Zhang _et al_. 1998 & Meng _et al_. 1998	Meng _et al_. 2005	Meng _et al_. 2005	Lima _et al_. 2009
Vitis "lineage" associated	_V. riparia_	_V. rupestris_	_V. vinifera_	_V. sylvestris_

2.4.3   Differences in Pathogenicity

GRSPaV-SG1 has been demonstrated experimentally to be asymptomatic while GRSPaV-1 induces mild symptoms (Nakaune _et al_., 2008; Meng _et al_., 2005). Recent research on the correlation between biological and molecular testing of RSP has revealed a very strong association between GRSPaV and Vein Necrosis (Borgo _et al_., 2009; Bouyahia _et al_., 2005). Vein necrosis is a widespread disease of _V. vinifera_ grapevines characterized by necrotic veins on the underside of the leaves of graft inoculated vines. A growing amount of evidence has been gathered that GRSPaV-SY and similar viral variants are responsible for the decline and graft-incompatibility problems which include swelling of the bud union and pitting of the wood (Habili _et al_., 2006). It remains to be elucidated whether GRSPaV-BS and similar variants elicit these disease symptoms. GRSPaV-PN was isolated from a particular declining Pinot noir clone, but the causal nature of this viral sequence variant has not been established (Lima _et al_., 2009).

2.5 Molecular Diagnosis

As mentioned previously, the diagnosis of RSP has in the past relied wholly on bioassays. This method of diagnosis is impractical for screening large numbers of samples as symptom development can take two to three years from the time of inoculation. Grafted indicators also have to be maintained in the field for this time period which is costly and labour-intensive. Once a grapevine is infected, it cannot be cured and thus far no natural viral resistance genes have been found (Goldbach *et al*., 2003). Control of viral diseases in grapevines thus depends on detecting infection in nursery, propagation and imported materials. Factors such as seasonal fluctuations in virus titer as well as the uneven distribution of virus within the plants have to be considered when designing a sampling approach for diagnosis of GRSPaV (Stewart and Nassuth, 2001). The development of fast, sensitive and efficient diagnosis of grapevines became possible when the genomic sequences of several GRSPaV sequence variants became available. The methods that are discussed below can be used to simultaneously diagnose large samples of vines and include nucleic acid-based techniques as well as protein-based serological methods (Meng and Gonsalves, 2003).

2.5.1   RT-PCR: Reverse Transcription-Polymerase Chain Reaction

The sensitivity of RT-PCR detection seems to be correlated to the primer pair used for detection, when sensitivity is judged by the level of correlation to biological indexing. Zhang *et al*. (1998) reported a 58% correlation to positively indexed vines when a primer pair that covers the 3' terminal section of ORF 3 and the 5' segment of ORF 5 was used. When a second primer set derived from ORF 1 was used, the ability to detect samples which were truly positive increased to 90% (Zhang *et al*., 1998).

In an independent study, analogous findings were noted. Sensitivity of a certain primer pair spanning ORF 1 and 2 (RSP9 and RSP10) was found to be 85%. A second universal primer set (RSP13 and RSP14) within the helicase domain of ORF 1 was designed to detect several sequence variants (Meng *et al*., 1999). Nolasco *et al*. (2000) evaluated the ability of four pairs of primers from various regions of the GRSPaV genome to identify samples as truly positive or negative in a large scale assay. It was concluded that the combination of the above 2 primer pairs had the highest sensitivity (Nolasco *et al*., 2000). The discrepancy between results from biological indexing and those from RT-PCR, may be due to the inability of a

certain primer pair to detect certain sequence variants of GRSPaV. It is thus prudent to use more than one primer pair, from assorted areas of the genome to arrive at accurate diagnosis of vines, for applications such as grapevine source certification.

Protocols for the isolation of viral RNAs from various grapevine tissues as adequate templates for RT-PCR detection has improved recently. The isolation of dsRNA, the replicative intermediate of the viral RNA genome, from phloem-tissue has traditionally been the method of choice for RT-PCR detection, despite its labour-intensive nature and use of noxious compounds such as phenol and chloroform (Prosser *et al*., 2007). The commercial availability of total RNA isolation kits has allowed for a safer, cleaner and simpler procedure for viral RNA isolation. Stewart and Nassuth (2001) confirmed the validity of an RNA isolation kit for generating adequate RT-PCR template from various grapevine tissues despite seasonal variations in titer.

The detection of GRSPaV with other grapevine viruses in multiplex RT-PCR reactions have been widely reported (Gambino and Gribaudo, 2006; Nakaune and Nakano, 2006; Dovas and Katis, 2003; Nassuth *et al*., 2000; Zhang and Rowhani, 2000). Several strategies have been explored to attain high specificity and sensitivity in detection including the use of random or degenerate priming of reverse transcription followed by more specific amplification. The influence of the nucleic acid extraction procedure on RT-PCR results have also been examined and optimized by methods such as the addition of polyphenolic inhibitors (Dovas and Katis, 2003), the use of specialized tissue lysis equipment (Nakaune and Nakano, 2006) or specific nucleic acid extraction techniques (Tzanetakis and Martin, 2008).

2.5.2   Quantitative RT-PCR

The detection of plant viruses via Real-Time or quantitative RT-PCR (qRT-PCR) have gained wide acceptability for diagnosis due to its sensitivity, high throughput and lower risk of cross-contamination (Mackay *et al*., 2002). Detection using qRT-PCR has among others, been used for *Sugarcane leaf virus* (Korimbocus *et al*., 2002), *Leek yellow stripe virus* and *Onion yellow dwarf virus* (Lunello *et al*., 2004), *Potato yellow vein virus* (López *et al*., 2006) and *Citrus tristeza virus* (Saponari *et al*., 2008).

The high levels of phenolic compounds and polysaccharides present within woody plants are notorious for inhibiting the enzymes of PCR (Demeke and Adams, 1992). Despite this, the

successful use of qRT-PCR for detection of viruses in woody plants such as grapevine has been reported (Malan *et al*., 2009; Hren *et al*., 2007; Osman *et al*., 2007; Osman and Rowhani, 2006). Recently, fluorescent TaqMan® RT-PCR assays were developed for the detection of viruses associated with the RW disease complex: GVA, GVB, GVD and GRSPaV (Osman and Rowhani, 2008). When comparisons were drawn to conventional RT-PCR techniques using serial dilutions of RNA extract and plant sap, TaqMan® RT-PCR assays demonstrated higher sensitivity (Osman and Rowhani, 2008). These assays could detect viruses at higher dilutions of purified RNA and plant sap.

An extension of the TaqMan® RT-PCR assay is its application to low density arrays (LDA) which uses 384 well microplates. Osman *et al*. (2009) were able to utilize this technique to simultaneously detect 13 grapevine viruses including GRSPaV with higher sensitivity and higher throughput than other methods.

2.5.3   Serological Techniques

The unavailability of antisera for GRSPaV hindered the initial diagnosis of GRSPaV using serological techniques such as Western Blots, Enzyme-linked immunosorbent assays (ELISA) and dot immuno-blotting. After the genomic sequence of GRSPaV-1 was published, antiserum to a recombinant CP of GRSPaV was presented by two autonomous research groups (Petrovic *et al*., 2003; Minafra *et al*., 2000). The production of polyclonal antibodies requires the expression of the viral protein in a bacterial system and the subsequent immunization of the expressed product in a mammalian organism.

Western Blots were found to be the most effective serological detection method using various types of GRSPaV-infected tissue such as leaves, petioles and phloem (Meng *et al*., 2003). Results of Western Blots were comparable to those of RT-PCR and biological indexing. Seasonal changes in antigen levels were however observed from both research groups. GRSPaV was more readily detected during summer months when vineyards experience a high growth rate when compared to winter months (Petrovic *et al*., 2003; Minafra *et al*., 2000). However, GRSPaV can be detected from cambium material throughout the year. Geographical and climate influences on antigen production within vines caused only slight variations in the window of detection. This technique is currently used for routine and high throughput detection assays.

Although aggregations of flexous particles were observed in the phloem tissue of positively RSP-indexed vines as early as 1993 (Tzeng *et al.*, 1993), the absence of antisera at this stage failed to satisfy a relationship between these virions and RSP. The visualization of GRSPaV particles within grapevine tissues through Immunosorbent electron microscopy (ISEM) was enabled by the availability of polyclonal antibodies to the CP of GRSPaV (Petrovic *et al.*, 2003). The use of expensive equipment and highly skilled labour however, precludes this valuable technique for routine diagnosis.

Unfortunately attempts at indirect ELISA have been unsuccessful for diagnosis of GRSPaV due to high levels of background signal observed in healthy plants (Meng *et al.*, 2003; Minafra *et al.*, 2000). ELISA was only effective in tissues containing high antigen concentration such as tissues harvested in spring or summer. A similar technique, dot immuno-blotting, has been tested for large-scale diagnosis of GRSPaV (Minafra *et al.*, 2000). However, similar problems were encountered as with ELISA.

In summary, the most cost-effective means of detection remains RT-PCR and Western Blots, or a combination of these two methods.

2.6 Molecular Diversity Analysis

All RNA viruses have the potential to diverge quite significantly due to the high error rate of the replication mechanism of RNA-dependent polymerases (Drake and Holland, 1999). These enzymes lack the proof-reading ability present in the polymerases of other organisms. Therefore, the population structure of a virus species can be considered as a collection of quasi-species. Viral quasi-species refer to those closely related genomes of a particular viral species that is continuously subjected to selection and competition (Hull, 2001). This intrinsic variation is often helpful to adapt to new hosts or their defense mechanisms.

This adaptability often hampers the separation of sequence variants into distinct phylogenetic groups. For most viruses, as with GRSPaV, a distribution of sequence variants exist which is centered on a few 'master' sequences. It is important to thus analyze other biological properties of the virus which include antigenic indices, predicted amino acid sequence and host-pathogen interaction. The incidence of mixed infection of significantly divergent strains in a single plant is unlikely to be due to the accumulation of point mutations over time. It is

more likely due to the introduction of distinct sequence variants into the same plants through the practice of grafting (Meng *et al*., 2006).

Several methods are employed to investigate molecular diversity. The genetic variation is ultimately characterized by establishing the DNA sequence of every viral isolate. This process can however be costly and time-consuming. A procedure for the large scale screening of grapevine populations for diverse viral sequence variants can thus be useful. The development of tools based on PCR proved popular because the high sensitivity allows the amplification of specific product from a high background. Previously, PCR coupled to the differential gel electrophoretic mobility of sequence variants have been exploited for strain typing of viral variants in GVA (Goszczynski and Jooste, 2002) and GRSPaV (Santos *et al*., 2003) (Figure 10).
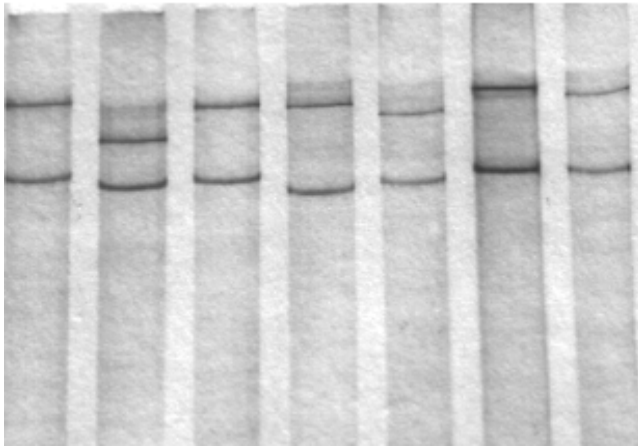
Figure 10: SSCP analysis of cDNA clones produced through RT-PCR of a single viral isolate indicate the presence of several genomic variants (Santos *et al*., 2003).

Several other strain typing techniques have been reported for *Plum pox virus* (PPV), genus *Potyvirus*, family *Potyviridae* (Varga and James, 2005). These include ELISA with strain-specific monoclonal antibodies (Myrta *et al*., 2000) and RT-PCR with RFLP analysis (Wetzel *et al*., 1991). Although effective, these methods of strain typing are complicated and lengthy. High resolution melt analysis of amplicons is a simpler, faster and consistent procedure for detection and strain discrimination.

A technique using high resolution genotyping by amplicon melting analysis was developed for SNP genotyping (Wittwer *et al*., 2003). This technique was initially used to characterize

PCR product samples according to their dissociation behaviour as they are slowly melted (0.1°C/s) from dsDNA to ssDNA in the presence of a high saturation dye and without the use of fluorescent probes. Varga *et al*. (2006) described a multiplex qRT-PCR and melt curve analysis for strain identification of two major sequence variants of PPV, a positive-sense, single-stranded RNA genome infecting plants. The different strains are identified by their distinctive melting temperatures (T_M), which is a function of their sequence length, GC-content and DNA sequence complimentarity. The T_M of every non-identical DNA fragment is thus unique for that fragment (Figure 11).

This cost and time effective technique is an effective way to genotype samples without the use of a probe. Another advantage is the elimination of electrophoretic analysis of amplicons using toxic compounds such as Ethidium bromide and polyacrylamide. In addition, cross contamination of samples is prevented as a closed-tube assay is utilized without the need for post PCR processing.
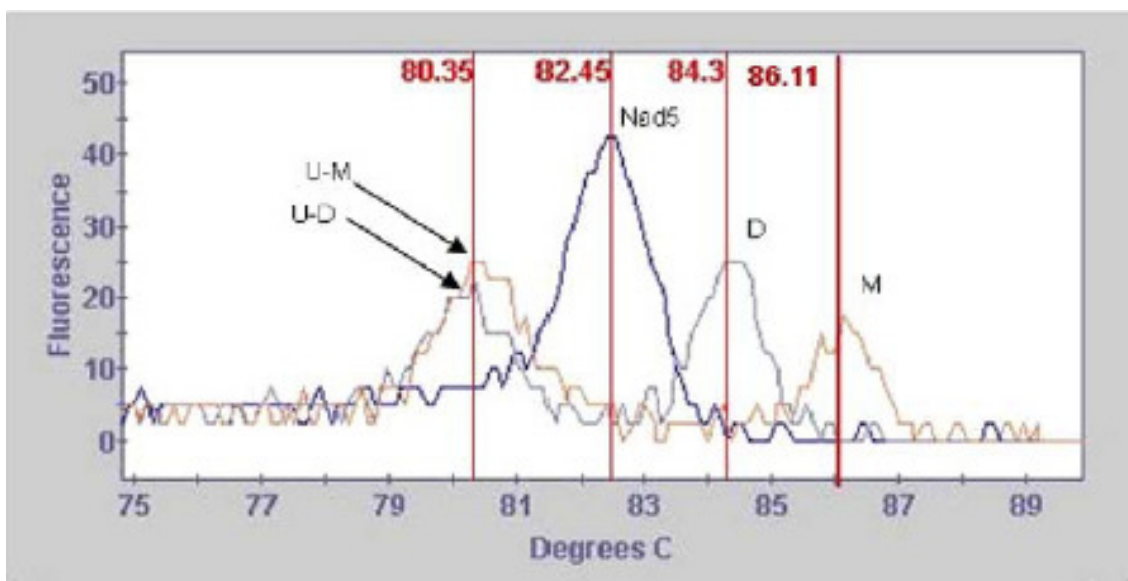
Figure 11: Strain differentiation of PPV by multiplex qRT-PCR. Nad5 = Plant RNA internal control; D – Amplification product of PPV strain D specific primer pair; M – Amplification product of Strain M specific primer pair. U-M & U-D – amplification products of universal PPV primer pair (Varga and James, 2004).

More recently, high-resolution melt analysis was performed on different strains of varicella-zoster virus (VZV), a member of the subfamily *Herpesviridae,* and the causal agent of chickenpox in children (Toi and Dwyer, 2008). The melt profile of amplicons of the live attenuated VZV vaccine (V-Oka) was compared to those of wild-type strains of VZV. SNPs within five different regions of the VZV genome were examined for 78 patients. Genotype C indicates a strain of VZV that is prevalent in Europe and is similar to the reference isolate VZV-S (Figure 12).
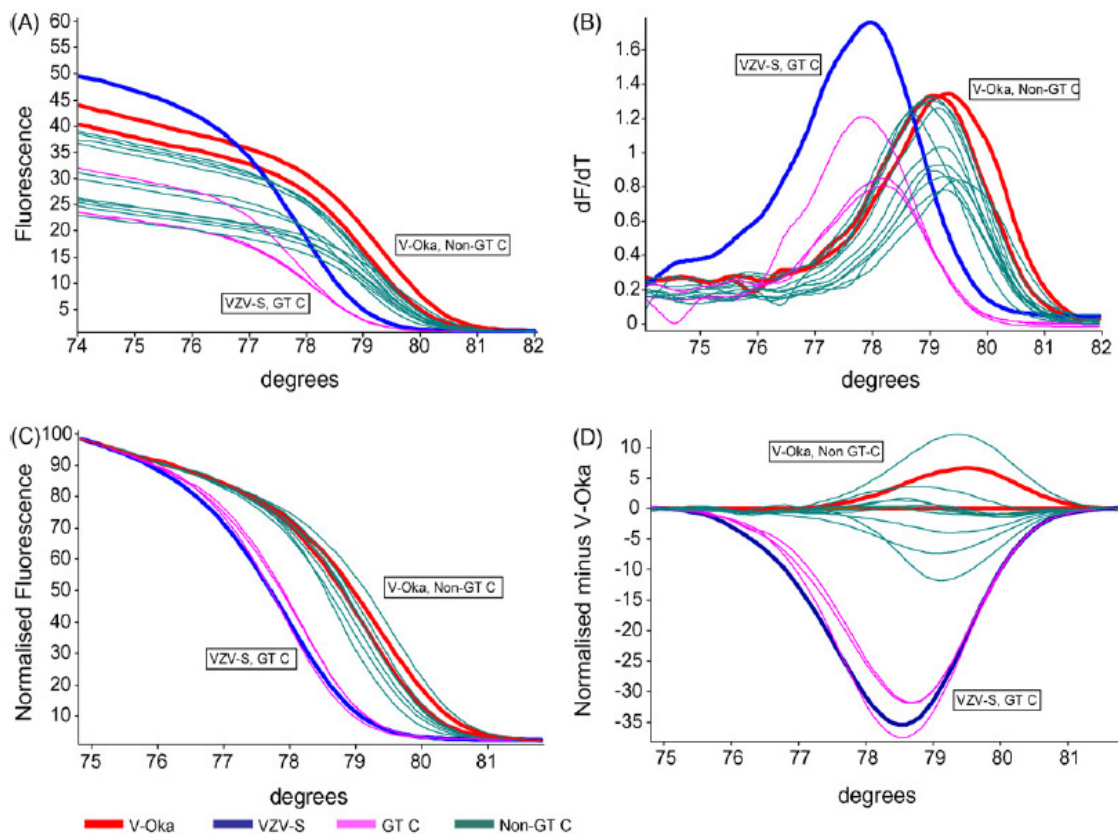
Figure 12: A – raw data of dissociation of an amplicon encompassing a class 1 SNP (C>T) within ORF 21 of VZV; B - The derivative of the fluorescence displays distinct melt peaks for the vaccine strain (V-Oka), internal control (VZV-S), European strain Genotype C (GT-C) and wild type spread; C – Normalized HRM melt profiles; D – HRM Difference graphs plotted relative to an average plot of the vaccine strain (Toi and Dwyer, 2008).

It must be noted that the above strategies to analyze genetic variation relies on the reverse transcription and amplification of viral RNA. The fidelity of two enzymes involved, i.e. Reverse transcriptase and DNA polymerase, is crucial for accuracy and validity of research methodology. Errors introduced by these synthetic enzymes, could result in an overestimation of molecular diversity. Generally, RT-PR produces less than 0.5% errors (Teycheney *et al*., 2005). Such low error rates, cannot account for the high genetic variation displayed by GRSPaV viral isolates (Meng *et al*., 2006).

Analysis of the molecular diversity and functional genomics of GRSPaV is possible because of the wide array of sequence information available for the different sequence variants. Universal primers have been designed to different areas of the GRSPaV genome to detect this virus. In this work, a rapid, sensitive detection protocol was developed, that makes use of these primers and qRT-PCR. When these primers are used in sequencing, they can simultaneously be used to clarify phylogenetic relationships between sequence variants (Meng, 2005). For this reason, these primers (Table 4) were used in the development of a tool for strain differentiation of GRSPaV. High resolution melt analysis has previously showed potential for strain typing. It is also possible to detect lower amounts of variance, as a single nucleotide polymorphism can be distinguished. The technique, however, must initially be confirmed with sequencing and phylogenetic analysis. This technique could be useful to elucidate GRSPaV genotypes and ultimately associate certain phylogenetic groups with disease symptomatology.

3. Materials and Methods

3.1   Overview of Experimental Design

Plant material was sampled from various farms located within the winelands area of the Western Cape. The optimization of the protocols for the cold storage and processing of plant material followed.

Infection status of plant material was established and the optimization of different diagnostic protocols for detection of GRSPaV was performed. Published universal primers were used in the RT-PCR detection of a range of different molecular variants. The isolation of RNA from field collected samples was required. Subsequent reverse transcription necessitated RNA template of good quality and integrity.

Nested quantitative polymerase chain reaction with High Resolution Melting analysis (qPCR-HRM) was performed to differentiate between viral variants. Primers for nested qPCR-HRM were designed using published sequences in order to compare HRM analysis with existing phylogenies for GRSPaV. Fragments generated by diagnostic RT-PCR were used for qPCR-HRM and were sequenced. HRM data and sequencing results was thus combined and correlated to validate the qPCR-HRM technique

Phylogenetic and other analysis of obtained nucleotide sequences were carried out. Comparisons to published sequences were made to establish phylogenetic relationship to molecular variant groups.

3.2 Plant Material

3.2.1 Plant Material

Canes, leaf petioles and leaves from naturally infected *V. vinifera* plants were harvested throughout the growing season from four different farms in the Western Cape, South Africa. In total, 94 randomly selected grapevines were analyzed. Uninfected control plants were cultivated *in vitro* and propagated by callus culture on a modified MS medium in a sterile environment (Murashige and Skoog, 1962).

Table 3: Summary of plant material analyzed. KK – Kanonkop Wine estate, GV – Grondves, KWV, NVB – Nietvoorbij experimental farm, BD – Tradouw Wine estate.

	Cultivar	Farm	Region	No of Samples	Harvest
KK	Merlot	Kanonkop	Stellenbosch	32	Nov 2008, Feb 2009
GV	Shiraz, clone 99B	Grondves	Stellenbosch	22	Nov 2008, May 2009
NVB	(rootstock)	Nietvoorbij	Stellenbosch	34	Jun 2009
BD	Shiraz	Tradouw	Barrydale	2	July 2009
Virus-free	*V. sultana*	*In vitro* plantlet	-	-	-

3.2.2 Sample Storage and Processing

Young, virus-free *in vitro* plantlets were maintained in greenhouse conditions: 16:8 light-dark cycles and at temperatures of 20-25°C. All grinding equipment and glassware was baked at 165°C for a minimum of four hours. The stems and leaves of virus-free plantlets were macerated in liquid nitrogen using a sterile pestle and mortar.

Canes were kept dormant at 4°C. The bark was removed to expose the phloem tissue as the presence of GRSPaV is restricted to the phloem (Martelli, 1993). Phloem was scraped from at least two canes per plant analyzed. Integrity of RNA was preserved by processing samples as rapidly as possible and stored at -80°C. Phloem scrapings, leaf veins and leaf petioles were homogenized in liquid nitrogen using the POLYTRON® PT2100 dispersing aggregate (Kinematica AG) at 11 000 – 26 000 rpm. This homogenizer was sterilized by exposure to UV light for 30 min prior to each use.

3.3 Nucleic Acid Extraction

3.3.1 RNA – CTAB extraction

Total RNA extractions were performed according to White *et al*. (2008).

Briefly, two hundred mg of macerated grapevine tissue was combined with 1.2 ml of preheated (65°C) extraction buffer [2% CTAB (Cetyltrimethylammonium Bromide), 2% PVP (polyvinylpyrrolidone), 100 mM Tris-HCl pH 8.0, 25 mM EDTA (ethylene diamine tetra acetate) pH 8.0, 2 M NaCl, 0.5 g/ℓ Spermidine]. ß-mercapthoethanol (ßME) was added to a final concentration of 3% v/v. Samples were immediately vortexed (30 sec) and incubated at 65°C for 30 min. After centrifugation at 13 200 rpm for 10 min, the supernatant was retained and subjected to two consecutive chloroform: iso-amyl alcohol (24:1) (C:I) extractions as follows. Equal volumes of C:I and extract supernatant were mixed thoroughly for 1 min and centrifuged at 13 200 rpm for 10 min. Following the last centrifugation step, the upper aqueous phase was collected and precipitated in a final concentration of 2 M LiCl at 4°C for a minimum of 16 hours. RNA was recovered by centrifugation (4°C) at 13 200 rpm for one hour. The resultant RNA pellets were washed by centrifugation (4°C) at 13 200 rpm for 5 min in 70% RNase-free EtOH. Wash solution was removed from RNA pellets by aspiration and pellets were dissolved in 50 µl of Milli-Q® water (White *et al*., 2008).

3.3.1.1 DNase I treatment of RNA preparations

DNase treatment of purified RNA was performed in a final volume of 200 µl and involved the addition of 1 U RFD (RNase-free DNase I, Fermentas) and 20 µl 10X DNase Buffer [100 mM Tris-HCl pH 7.5, 25 mM $MgCl_2$, 1 mM $CaCl_2$] to RNA samples. Samples were subsequently incubated at room temperature for 30 min. RNA was subjected to a phenol chloroform extraction to remove RFD enzyme and buffer components. An equal volume of phenol pH 4.3 was added, vortexed (30 sec), centrifuged (4°C) at 13 200 rpm for 5 min and the upper phase was retained. This was followed by the same extraction procedure with an equal volume of chloroform. RNA was precipitated by adding 3 M NaOAc pH 5.2 (one tenth of the volume of collected supernatant) and 2.5X the volume of absolute EtOH. Precipitation occurred at -20°C for 20-30 min. RNA was harvested by centrifugation (4°C) at 13 200 rpm for 30 min and washed with70% EtOH by centrifugation (4°C) at 13 200 rpm for 5 min. Measures to ensure the lack of EtOH contamination of purified RNA included removal of the

remainder of wash solution by aspiration and the short incubation of pellets at 65°C (1 min) and 37°C (5 min). RNA pellets were dissolved in 50 µl of Milli-Q® water and stored in 10 µl aliquots at -80°C.

3.3.1.2 Evaluation of purity, concentration and quality of RNA

The purity and concentration of RNA were determined using the spectrophotometric absorbance of samples at 230, 260 and 280 nm as measured by the NanoDrop™ 1000 spectrophotometer (Thermo Fisher Scientific Inc). Manufacturer's instructions (V3.6.0 © Thermo Fisher Scientific) indicate that the A_{260}/A_{280} ratio of absorbance assesses the purity of RNA (recommended: 1.8-2.2), while the A_{260}/A_{230} ratio of absorbance specify the likelihood of the presence of co-purified contaminants (recommended: <2). The sample concentration was deduced from the absorbance at 260 nm and according to the Beer-Lambert equation (Paynter, 1981). The quality of RNA was evaluated by 1% agarose gel electrophoresis. Gel apparatus, combs, trays and tanks were submerged in 10% SDS (Sodium dodecylsulfate) and rinsed in DEPC-treated dH_2O (diethylpyrocarbonate used at 0.002%). RNase-free loading buffer and 1x TAE were used.

RT-PCR amplification was performed with RNA which was stored for longer than a period of two months. This amplification served as an internal control to ensure suitability of isolated RNA as RT-PCR template. The grapevine gene targeted for amplification was ß-Tubulin using primers Vv-tubulin 479 F (TGGTGACCTGAACCACTTGA) & Vv-tubulin 479 R (TCACCCTCCTGAACATCTCC). This primer set amplified a product of 479bp. The amplification procedure is described in Section 3.4.3.

3.3.2 dsRNA – Affinity chromatography

Double stranded RNA, the replicative form of the RNA viral genome, was extracted from phloem scrapings and petiole material according to a modified version of the method published by Hu *et al*. (1990).

Ten grams of homogenized grapevine tissue was suspended in 45 ml of 2X STE buffer [1x STE consists of 100 mM NaCl, 50 mM Tris-HCl pH 8.0, 1 mM EDTA pH 8.0], 15 ml 10% SDS, 50ml 1:1 phenol:chloroform, 1.2 ml 40 mg/ml bentonite, 1 ml ßME was added to this extract. The mixture was stirred at room temperature for 30 min and then centrifuged (4°C) at 10 000 rpm for 15 min. The aqueous supernatant was transferred to a measuring cylinder and

adjusted to 80 ml volume with 1X STE. The mixture was gently agitated with 16 ml of absolute EtOH (99.6%) and 0.5 g of CF11 cellulose (Whatman) for 30 min to one hour at room temperature. The cellulose-slurry was loaded onto a chromatography column (Promega) and allowed to run through. The column was washed with 100 ml 16% EtOH-1X STE buffered solution and the flow through was discarded. The dsRNA was eluted sequentially with three 3 ml aliquots of 1X STE in a sterile container and precipitated at -20°C overnight in 2X the total volume (9ml) absolute EtOH and 0.9 ml 3 M NaOAc, pH 5.0 (Hu *et al.*, 1990). Half of this precipitation solution was used to retrieve dsRNA by centrifugation (4°C) at 13 200 rpm for one hour. The resulting pellets were washed with 0.5 ml of 70% EtOH and dried in a Captair™bio (Erlab) sterile environment on ice for 30 min. Dried pellets were resuspended in 20µl Milli-Q® (Millipore) water and stored at -20°C. Purified dsRNA was electrophoresed on 1% agarose for 30 min at 100 mV and visualized with EtBr under ultra-violet (UV) light.

3.3.3   Virus extract – GES-method

A third sample preparation procedure was explored and modified (Malan *et al.*, 2009) in this study as a means for an inexpensive, rapid diagnosis of vines. It was originally developed and compared to other procedures by Osman *et al.* (2007).

Three hundred mg of phloem material was ground to a fine powder in liquid nitrogen using a sterile pestle and mortar. Samples were further homogenized in a grinding buffer pH 8.2 [60.5 g/l Tris-HCl pH 8.2, 8 g/l NaCl, 20 g/l PVP, 10 g/l PEG (Poly Ethylene Glycol), 2 g/l $MgCl_2.6H_2O$, 50 ml HCl Tween 20 (Poly[oxyethylene]$_n$ sorbitan-monolaurate)]. Four µl of the slurry was added to 50 µl of GES denaturing buffer [0.1 M glycine, 0.05 M NaCl and 1 mM EDTA]. Mixtures were denatured by placing tubes in ice water immediately after a 10 min incubation step at 95°C. 1-2 µl of this denatured product can then be used directly in PCR application. Osman *et al.* (2007) noted that this procedure incorporates more PCR inhibiting agents than purified RNA preparations, but is still effective for detection in real-time TaqMan® PCR (Section 3.4.3).

3.4 Polymerase Chain Reaction

3.4.1 Primers

3.4.1.1 Diagnostic Primers

Diagnostic PCR primers used in this study are listed in Table 4. A number of primers were designed by Meng *et al*. (1999, 2003) to detect a wide array of sequence variants (Table 4). Efficiency of these primers was also evaluated in a large-scale assay by Nolasco *et al*. (2000). The primer pair StempitCP-F and StempitCP-R was received courtesy of Ms M. Engelbrecht (affiliation) and is used for routine diagnosis of GRSPaV in SA.

Table 4: Primers used in RT-PCR to detect genomic variants of GRSPaV from grapevines. All diagnostic primers have an annealing temperature of 58°C.

Primer Name	Primer Sequence: 5'-3'	Citation	Amplicon Length	%GC
RSP9	GGC CAA GGT TCA GTT TG	(Meng *et al*., 1999)	498 bp	52.9
RSP10	ACA CCT GCT GTG AAA GC	(Meng *et al*., 1999)	498 bp	52.9
RSP13	GAT GAG GTC CAG TTG TTT CC	(Meng *et al*., 1999)	339 bp	50.0
RSP14	ATC CAA AGG ACC TTT TGA CC	(Meng *et al*., 1999)	339 bp	45.0
RSP21	GAG GAT TAT AGA GAA TGC AC	(Meng *et al*., 2003)	440 bp	40.0
RSP22	GCA CTC TCA TCT GTG ACT CC	(Meng *et al*., 2003)	440 bp	55.0
StempitCP-F	ACT TTC AAA GAC GGT GGA CAT GAG	Ms M. Engelbrecht	523 bp	45.8
StempitCP-R	AGC CAT AGC TTG TCT GAG CAC TTG	Ms M. Engelbrecht	523 bp	50.0
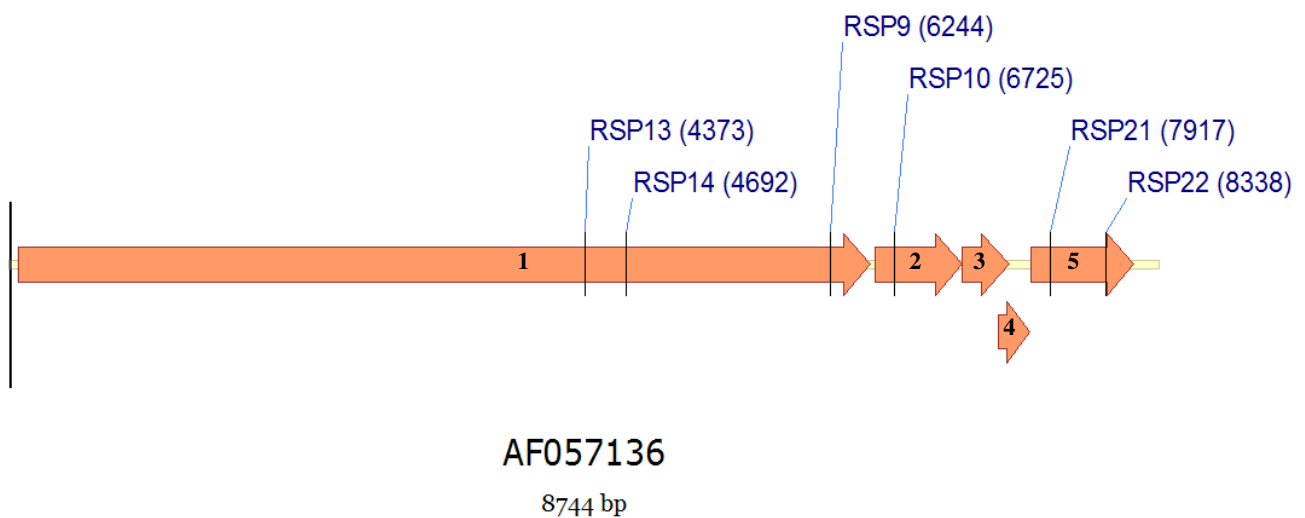
Figure 13: Diagnostic primer starting positions indicated in brackets on GRSPaV-1 (Acc no AF057136). Block arrows represent Open Reading Frames 1-5. StempitCP-F and StempitCP-R are excluded from figure as this primer set was not used for downstream applications (Section 4.4)

41

RSP13 & RSP14 were designed based on the consensus of multiple sequence variants within the conserved replicase domain of ORF 1. Sequence analysis of GRSPaV with ASPV and PVM revealed that the terminal end of ORF 1 and the 5' end of ORF 2 were conserved in nucleotide sequence. RSP9 & RSP10 lies within this region. A combination of these primer pairs was found to have the highest sensitivity and negative predictive value (Meng and Gonsalves, 2007a; Nolasco *et al.*, 2000). A third set of broad-spectrum primers, RSP21 and RSP22, were later designed within the CP region of GRSPaV (Meng *et al.*, 2003) as indicated in Figure 13. This primer set functioned as efficiently as RSP13 & RSP14.

3.4.1.2   Primers for use in qPCR-HRM

PCR primers were designed from a multiple alignment of the five full-length sequences of GRSPaV together with 212 GRSPaV sequences that are available from GenBank. Primes are given in Table 5. The accession numbers, genomic region, sequence length, geographic origin, submitting author and year of submission is available in Appendix A. Design of primers was achieved using the 'Alignment PCR' function of VectorNTI Advance® v10.3.0 (Invitrogen Life Technologies).

Parameters necessary for qPCR-HRM, included the use of small amplicons (80-200bp) to avoid the formation of secondary structures and multiple melt domains during the melt phase. The use of small amplicons thus allowed for better resolution of fragments. The folding characteristics of the amplicons and primers were determined using the DINAMelt Server, a secondary structure profiling software package, available at http://www.bioinfo.rpi.edu/applications/hybrid/twostate-fold.php from the Rensselaer Polytechnic Institute. A salt concentration of 50mM and Mg^{2+} concentration of 1.5mM at a folding (annealing) temperature of 50°C was used to predict secondary structures. Delta-G values above -1 were optimal, as very low delta-G values produce more secondary structures. Each of the amplicons designed for the HRM assay was also subjected to an *in silico* screen for specificity using BLASTn (Altschul *et al.*, 1990). The theoretical melting temperature and thermal denaturation profile for each amplicon was predicted using the implemented program available at: http://www.biophys.uni-duesseldorf.de/local/POLAND/poland.html (Steger, 1994).

Primers for qPCR-HRM were designed to fall nested within the diagnostic regions stipulated in 3.4.1.1 (Figure 14). The purpose of this experimental design was to correlate phylogenetic

analysis of sequence data with HRM data. Primers were designed to anneal within these diagnostic regions at the temperature range: 50°C - 60°C and to have approximately 50% G/C content. The optimization of primer design was restricted to adjusting primer length according to the position of the 3' GC-clamp as it was required to amplify small amplicons. Primer melting temperatures (Tm) were calculated, based on nearest neighbor parameters, using the Oligonucleotide Analyzer tool (Kuulasma, 2002) found on the website http://www.uku.fi/~kuulasma/OligoSoftware. Melting temperatures of primers were engineered to be within 2-3°C of each other. Primers were synthesized by Inqaba Biotech (Pretoria, South Africa) and IDT (Integrated DNA Technologies; California, USA).

Table 5: Primers used in qPCR-HRM assays to examine variance in South African populations of GRSPaV. All nested primers have an annealing temperature of 50°C.

Primer Name	Primer Sequence	Amplicon Length	%GC
RSP_910_HRM_3F	CCC ACA TTC TGT GGA TGG T	140 bp	52.6
RSP_910_HRM_4R	GCA TAG GAC ACC TCT ATC G	140 bp	52.6
RSP_1314_HRM_5R	ATG TGC TCT GAC ATG GAT CAC C	103 bp	50.0
RSP_2122_HRM_6F	TGA GCT GAT TCG TGC ATT TGG	195 bp	47.6
RSP_2122_HRM_7R	AAT CTG CGC AAT GTG GTC AC	195 bp	50.0
RSP_CP_HRM_1F	AAT ACC ACC AGC TAA TTG G	130 bp	42.1
RSP_CP_HRM_2R	TGT TGG AGC TCT TTT AAT TC	130 bp	35.0
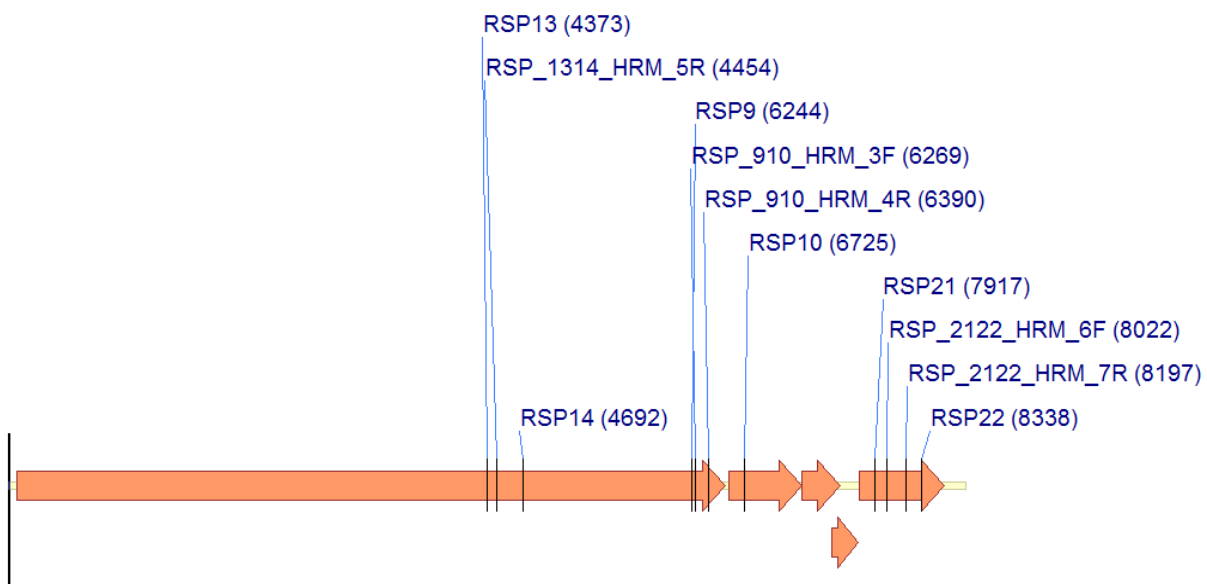
Figure 14: Nested qPCR-HRM primer starting positions indicated in brackets on GRSPaV-1 (Acc no AF057136). HRM amplicons fall within diagnostic regions.

3.4.2   Reverse Transcription Polymerase Chain Reaction

3.4.2.1   Primer Annealing

The first step of RT-PCR involves the denaturation of the RNA template and the annealing of one or more reverse primers when working with ssRNA (viral genome is positive sense). When dealing with dsRNA, both forward and reverse primers were annealed. For non-specific cDNA synthesis, reverse transcription was primed with 0.2 µg of random hexamers (Fermentas Life Sciences). RNA (500 ng to 2µg) was incubated at 70°C for 5 min with 0.25 µM of each primer and 8.55 µl Milli-Q® water. The primer annealing mixture was then flash cooled in ice slurry.

3.4.2.2   cDNA synthesis

First strand synthesis was performed using AMV Reverse Transcriptase (Fermentas Life Sciences) according to the manufacturer's instructions. In a final volume of 20 µl, 4 U of AMV, 1 mM DTT (dithiothreitol), 1X AMV RT Buffer [50 mM Tris-HCl pH 8.5, 8 mM MgCl$_2$, 30 mM KCl, 1 mM DTT], 20 U Ribolock™ RNase Inhibitor (Fermentas) and 1mM dNTPs (each) was added to the denatured RNA. The RT-mixture was subsequently incubated at 48°C for one hour and thereafter used in PCR or stored at -20°C. The cDNA synthesis protocol for non-specific transcription using random hexamers differed. It involved the following incubation steps: 25°C for 10 min, 42°C for 60 min and 70°C for 10 min.

3.4.2.3   PCR Amplification

The final step of RT-PCR entailed the amplification of cDNA derived from RNA. All conventional PCR reactions were performed in a GeneAmp® PCR System 9700 (Applied Biosystems) with enzymes and buffers supplied by Kapa Biosystems. Gradient PCR reactions were performed using a Mastercycler® Gradient (Eppendorf).

Final volumes of PCR reactions were adjusted as required. The following PCR conditions for cDNA derived from RNA were used: 2 µl template, 1X High Yield Reaction Buffer A, 1.5 mM MgCl$_2$, 1X cresol/sucrose loading dye [20% w/v sucrose, 1 mM Cresol Red], 0.2 mM dNTPs (each), 0.25 µM forward primer, 0.25 µM reverse primer and 1 U KapaTaq DNA polymerase. These PCR conditions also applied as a universal reaction for amplifications such as colony PCR, primer optimization in gradient or touchdown PCR, nested PCR, internal RNA control PCR or detection of DNA contamination in purified RNA.

Cycling conditions were adjusted slightly according to the primer pair used, however common PCR cycling conditions are tabulated below:

Table 6: General PCR cycling conditions.

Step	Temperature	Time Period	Cycles
Denaturation	94°C	5 min	
Denaturation	95°C	30 sec	
Primer Annealing	37°C	30 sec	Optional 5 cycles
Extension	72°C	40 sec	
Denaturation	95°C	30 sec	
Primer Annealing	50-65°C	30 sec	35 cycles
Extension	72°C	40 sec	
Final extension	72°C	7 min	
Hold	10°C	∞	

3.4.3   Single tube RT-PCR

This method was used for the rapid diagnosis of grapevines using crude viral extract (Section 0) or denatured RNA (Section 3.4.2.1) as template. The following components were added to 2 µl RT-PCR template to a final volume of 25 µl: 1X Kapa Buffer A , 1X cresol/sucrose loading dye, 1 mM DTT, 0.25 µM forward primer, 0.25 µM reverse primer, 0.2 mM dNTPS (each), 4U AMV and 1U KapaTaq™ polymerase.

Cycling conditions are tabularized below:

Table 7: PCR cycling conditions for single-tube RT-PCR.

Step	Temperature	Time Period	Cycles
Reverse Transcription	42°C	50 min	
Denaturation	94°C	5 min	
Denaturation	95°C	30 sec	
Primer Annealing	37°C	30 sec	Optional 5 cycles
Extension	72°C	30 sec	
Denaturation	95°C	30 sec	
Primer Annealing	50-65°C	30 sec	35 cycles
Extension	72°C	40 sec	
Final extension	72°C	7 min	
Hold	10°C	∞	

3.4.4　Single tube qRT-PCR

This method was also used for the rapid diagnosis of grapevines using crude viral extract (Section 0) or denatured RNA (Section 3.4.2.1) as template. Components used for qRT-PCR were part of the SensiMix™ One-Step Kit (Quantace). Diagnostic assays were performed as per manufacturer's instructions. Final reaction volumes for single tube qRT-PCR reactions were 25 µl and were manually made up of: 1X SensiMix™ One-Step Buffer, 1X SYBR® Green I Fluorescent Dye (Molecular Probes Inc), 0.24 µM forward primer, 0.24 µM reverse primer, 5 U RNase Inhibitor, 3 mM MgCl$_2$ and 2 µl RT-PCR template (crude viral extract or denatured RNA).

All quantitative amplifications were performed on the Rotor-Gene™ 6000 (Corbett Life Science). Transparent 0.2 ml single tubes were used in a 36-Well Rotor. The polymerase contained in the kit is undisclosed, however it is inactive at temperatures lower than 50°C and required heat activation after reverse transcription. Cycling conditions are given below:

Table 8: Single tube qRT-PCR cycling conditions acquiring to Green channel.

Step	Temperature	Time Period	Cycles
Reverse Transcription	42°C	45 min	
Enzyme Activation	95°C	10 min	
Denaturation	95°C	20 sec	
Primer Annealing	50-65°C	20 sec	45 cycles
Extension	72°C	50 sec	
Specificity Melt	72°C to 95°C	5 sec per 1°C	
Hold	10°C	∞	

3.5　Analysis of PCR Products

3.5.1　Analytical gel electrophoresis

Gel electrophoresis was performed to separate nucleic acid molecules by size and to evaluate quality and integrity of extracted nucleic acids (Sambrook *et al.*, 1989).

Agarose gel electrophoresis was achieved using 1-2% w/v agarose D1 LE (Hispanagar) gels in 1X TAE (Tris/acetate/EDTA) Buffer prepared from a 50X TAE stock solution (2 M Tris-HCl, 5.71% v/v Glacial acetic acid and 0.05 M EDTA pH 8.0). Electrophoresis was carried

out for 30-45 min at 80-120 mV. EtBr was used at 0.5 µg/ml in all agarose/TAE gels to facilitate DNA band visualization under ultra-violet (UV) light. Visualization of nucleic acids up to 10kb in size was achieved using 1% w/v agarose. Smaller nucleic acids required higher percentage agarose (2% w/v agarose) to achieve separation. Images of gels were captured under UV light by the MultiGenius™ Bio Imaging system (Syngene).

Two different loading dyes were used to facilitate loading of nucleic acid samples into wells of gels:

- 5X cresol/sucrose loading dye [20% w/v sucrose, 1 mM Cresol Red]

- 6X Orange Loading Dye Solution [10 mM Tris-HCl pH 7.6, 0.15% orange G, 0.03% xylene cyanol FF, 60% glycerol and 60 mM EDTA] (Fermentas Life Sciences)

Two molecular markers were used in this study to approximate sizes of DNA fragments. Both markers are available from Fermentas Life Sciences.

- GeneRuler™ 1kb DNA Ladder: 250 – 10 000bp (Figure 15)

- ZipRuler™ Express DNA Ladder Set: 100 – 10 000bp (Figure 16)
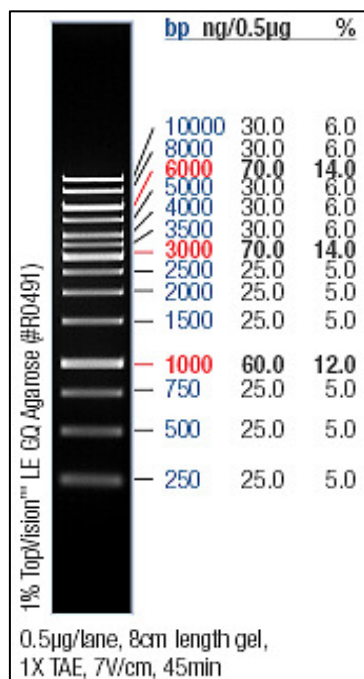
Figure 15: GeneRuler™ 1kb DNA Ladder (C ertificate of Analysis © Fermentas Life Sciences)
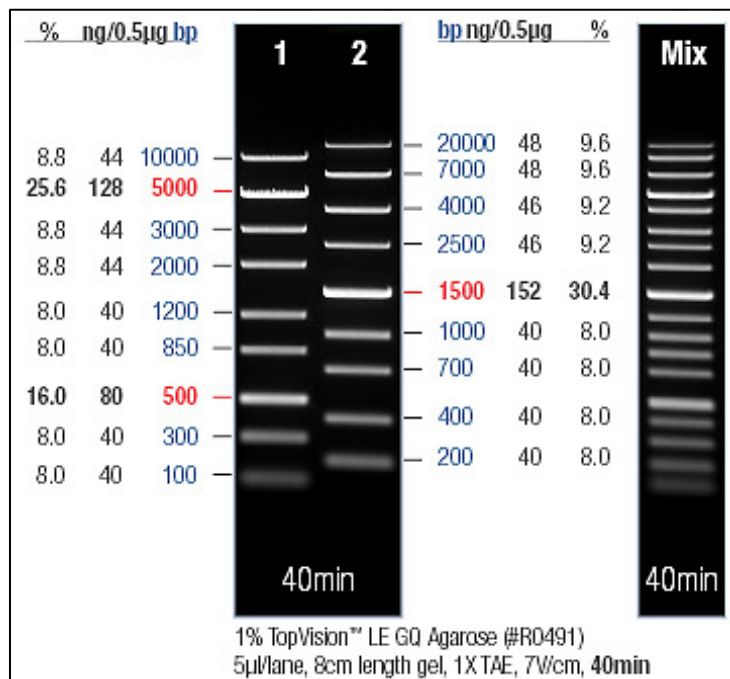
Figure 16: ZipRuler™ Express DNA Ladder Set (Certificate of Analysis © Fermentas Life Sciences)

3.5.2   qPCR HRM

3.5.2.1   Reaction conditions

Primary PCR products amplified from the diagnostic RT-PCR reactions were used as templates for nested qPCR-HRM reactions. This method was also recently described (Hofinger *et al.*, 2009). The SensiMix HRM™ Kit (Quantace) containing a Hotstart DNA Polymerase was used for this purpose. Amplification was carried out in the presence of the high-saturation fluorescent dye EvaGreen™ (Biotum). The subsequent products were subjected to a gradual increase in temperature to allow the gradual dissociation of DNA. The decrease in fluorescent signal was measured per 0.1°C temperature increment as the DNA dissociated and released the fluorescent dye.

The HRM Assay was designed according to the guidelines stipulated by the manufacturer and complying with recommended parameters (Corbett, 2006). The relative concentrations of primary PCR products were assessed with agarose gel electrophoresis and diluted accordingly. These primary PCR products formed the template for nested amplicons in HRM analysis and consisted of 1 µl of PCR products diluted 1:500 in Milli-Q® water. Reaction conditions in a final volume of 25 µl were as follows: 1X SensiMix HRM™ Buffer, 3 mM $MgCl_2$, 0.5 µl EvaGreen™ Dye, 0.25 µM forward primer and 0.25 µM reverse primer. Cycling conditions optimized for the Rotor-Gene™ 6000 (Corbett Life Sciences) are shown:

Table 9: qPCR-HRM cycling conditions acquiring to Green channel.

Step	Temperature	Time Period	Cycles
Enzyme Activation	95°C	10 min	
Denaturation	95°C	5 sec	
Primer Annealing	50°C	15 sec	45 cycles
Extension	72°C	20 sec	
High Resolution Melt	70°C to 95°C	1 sec per 0.1°C	
Hold	10°C	∞	

A cross-platform analysis of HRM applications revealed that PCR optimization plays a critical role in successful HRM analysis (White and Potts, 2006). Reaction conditions were systematically optimized with the following measures to deliver the reaction conditions described above:

Table 10: Summary of steps taken to optimize qPCR-HRM assay.

Optimization Step	Reason	Parameters tested
Magnesium Titration	Determine optimal co-factor concentration	1.0mM -4.0mM
Gradient PCR	Determine optimal annealing temperature	50-65°C
Primer concentration	Determine optimal primer concentration	0.1 µM- 0.35 µM
Template	Quality and quantity of nucleic acid analyzed	Genomic RNA, plasmid DNA, RT-PCR product

3.6 Analysis of qPCR-HRM data

3.6.1 Data analysis

All data analysis was achieved with the Rotor-Gene 6000 Series Software version 1.7, using several analysis modules embedded within the software.

The specificity of primers to target regions and the formation of primer dimers or other non-specific amplification, were analysed with the Melt analysis module. The plot of the first derivative of the fluorescence during the melt phase allowed secondary melt domains to be clearly distinguished.

Outliers of amplification were defined by the Comparative Quantitation analysis module. The amplification efficiency for each sample was calculated using the second derivative of the amplification plot (Fluorescence vs. Cycle). A 100% efficient reaction would indicate an amplification efficiency value of 2. This signifies a doubling of an amplicon after every cycle had taken place. The threshold for poor amplifiers was set at 1.4. An amplification efficiency of below the threshold of 1.4 thus denoted all outliers which were omitted from further analysis. The average amplification efficiency for a particular run was also calculated. A

great variation in amplification efficiency between samples was indicated by a large confidence interval. Confidence intervals below 0.09 were considered adequate for further analysis.

The main data output for the melt phase was a dissociation/melt profile of the decrease in fluorescence plotted against increasing temperature. Each melt profile is characteristic for every DNA fragment. Differences in initial fluorescence are common due to varying template concentrations or optics of the instrument (Wittwer *et al*., 2003). Melt profiles were normalized by equalizing the initial and final fluorescence of each sample to the average of the initial and final fluorescence values of all the samples within a single run. Normalization was achieved with the HRM analysis module with user-defined baseline data for pre- and post-melt periods. Normalized melt profiles provided a basic, visual representation of genotypes present in a run based on the temperature-shift and shape-shift of melt profiles. Automatic calculation of genotypes was achieved by the Auto-calling module of the software with user-defined genotypes. A confidence level was provided by r-values for automatically calculated genotypes. A threshold confidence percentage was defined at 70%, above which auto-calls could be computed.

Different genotypes were more easily visualized by plotting the difference in fluorescence (ΔF) between normalized melting profiles to a user-defined genotype. A genotype with known sequence was selected by the user as a reference genotype. The differences in fluorescence between the reference genotype and all other dissociation profiles were plotted against the increase in temperature. The reference sample (subtracted from itself) was thus zero across all temperatures. Samples of similar genotypes would cluster together in a visually distinct pattern. It is important to note that this visualization technique only indicates the level of sequence variation between samples in a particular run. According to manufacturer's directions, a difference curve peak with a ΔF-value of 5 or more was considered significantly different to the reference genotype.

3.6.2   Primary data output

3.6.2.1   Amplification

The raw data acquired during the nested amplification of RT-PCR products was depicted as an amplification plot of fluorescence versus the number of cycles of amplification. An increase in fluorescence reflected the accumulation of amplification product as the dye intercalates with dsDNA. The fractional cycle at which amplification overcomes a clear threshold of detection which can be distinguished from background noise is defined as the C_q-value (quantification cycle) (Bustin *et al*., 2009). High C_q values indicate poor amplification due to poor quality template, reaction inhibitors or sub-optimal conditions. The amplification efficiency of each reaction is automatically calculated from a graph of the second derivative of the fluorescence during amplification. A 100% efficient reaction has a calculated amplification efficiency value of 2.

3.6.2.2   Melt phase

The raw data acquired during the HRM phase was available to the user as a graph of the decrease in fluorescence as the time was increased in small increments. This graph is referred to as the melting profile. The melting profile was semi-automatically processed by the software in two ways and presented as two separate visual aids. The first output graph, henceforth referred to as the normalized melting profile, plotted the temperature-normalized fluorescence against the temperature. Two regions defining 100% and 0% fluorescence baselines on either side of the melt transition were manually defined by the user. These pre- and post-melt stages were used to normalize melt profiles and could influence the calculated confidence percentages (r-values) of the software auto-calling module. The second output graph, henceforth referred to as the difference graph, plotted the ΔF (the subtractive difference of the fluorescence of normalized melt profile to a reference genotype) against the temperature. Difference graphs were computed by selecting a reference genotype as a baseline and subtracting the normalized fluorescence of each test sample from this baseline.

A secondary analysis of the melt phase is the first derivative of the fluorescence during this gradual decrease in temperature. The graphs produced during this analysis is not suitable for genotype discrimination; however, it can be used as an indication of specificity of primer pairs to the target sequence. It can also give an indication of multiple melt domains or non-specific amplification, which required further optimization of reactions.

3.7 Cloning of PCR Products

3.7.1 Purification of PCR Products

3.7.1.1 Zymoclean

The Zymoclean Gel DNA Recovery Kit™ (Zymo Research Corporation) was used to purify DNA fragments from agarose gels according to manufacturer's instructions. PCR products required for ligation were excised from agarose/TAE gels with a scalpel and transferred to a microcentrifuge tube. Gel slices were incubated in a water bath (37-55°C) for 5-10 min with Agarose Dissolving Buffer (ADB) Buffer™ in the ratio: 30 µl of ADB™ per 10 mg of agarose gel. The following centrifugation steps occurred at 13 000 rpm for 30-60 sec. Once dissolved, the agarose solution was centrifuged in a Zymo-Spin I™ Column to bind the DNA to the column matrix (placed in a collection tube). The flow-through was discarded and 200 µl of Wash Buffer was added to the column before centrifugation. The wash step was repeated before transferring the column to a sterile microcentrifuge tube. The column was incubated with 6-10 µl of Milli-Q® at room temperature for 1 min before a final centrifugation step to elute DNA. The purified DNA was quantified using the NanoDrop™ 1000 Spectrophotometer according to the manufacturer's instructions.

3.7.1.2 SureClean

The SureClean (Bioline) Kit was used to directly purify DNA from PCR products according to manufacturer's instructions. An equal volume of SureClean was added to the nucleic acid solution, mixed thoroughly and incubated at room temperature for 10 min. DNA was pelleted by centrifugation at 13 200 rpm for 10 min and the supernatant was removed by aspiration. The DNA pellets were washed in 2X the original sample volume of 70% EtOH by vortexing (10 sec). Centrifugation at 13 200 rpm for 10 min followed to harvest DNA. Pellets were air dried and dissolved in 10 µl Milli-Q® water. Purified PCR product could then be used for applications such as cloning or sequencing.

3.7.2 Ligation

PCR Amplification fragments were TA-cloned into pDRIVE Cloning Vector (Figure 17) using the QIAGEN® PCR Cloning Kit according to the QIAGEN® PCR Cloning Handbook.

The amount of purified PCR product used for ligation depended on the insert:vector molar ratio used and was calculated using the following formula:

$$\frac{ng\ of\ vector \times kb\ size\ of\ insert}{kb\ size\ of\ vector} \times \frac{insert}{vector} molar\ ratio = ng\ of\ insert$$

A molar ratio of 3:1 was used for most ligations e.g.

$$\frac{50\ ng\ pDRIVE \times 0.5\ kb\ insert}{3.85\ kb} \times \frac{3}{1} molar\ ratio = 19.48\ ng\ of\ insert\ required$$

Ligation of purified PCR products to pDRIVE was performed in 10 µl volumes at 4°C overnight. Ligation conditions: 25-50 ng pDRIVE Cloning Vector, 1-4 µl purified PCR product and 1X Ligation Master Mix.
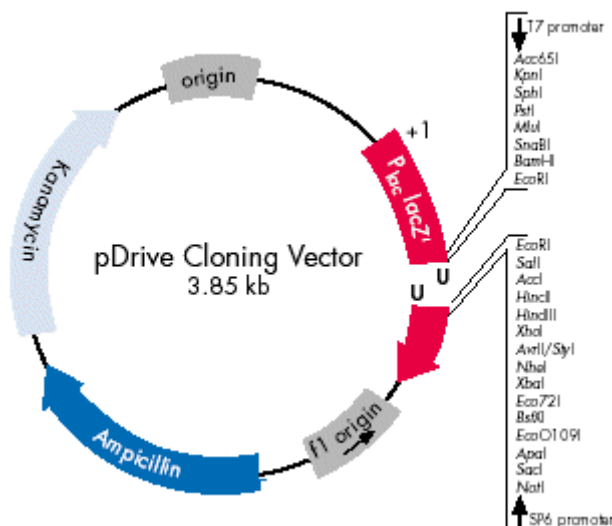
Figure 17: pDRIVE Cloning Vector displaying multiple cloning site (QIAGEN)

3.7.3   Transformation of Competent cells

3.7.3.1   Chemically competent cells

E. coli bacterial strains DH5α (Takara Bio Inc) and BL21 (Amersham Biosciences) were plated on LB/Agar plates without selection and incubated at 37°C overnight. A single colony of bacteria was inoculated into 5 ml of LB medium and incubated with vigorous shaking (250 rpm, 37°C, 16 hrs). This starter culture was inoculated in 500 ml LB media in a 5000 ml

Erlenmeyer flask. Growth of culture at 37°C and 225 rpm was monitored by measuring the absorption value (A_{600}) at regular intervals. After approximately 2-3 hrs, an optimal optical density (OD_{600}) of 0.5-0.6 was reached and the cells were incubated on ice for 10 min. The bacterial cells were harvested by centrifugation (4°C) at 5000 rpm for 10 min and the resulting pellets were resuspended in 100 ml of an ice-cold 0.1 M $MgCl_2$ solution by gently swirling the cell suspension on ice. All instruments, solutions and cell suspensions used in this procedure were chilled and handled carefully as competent cells are highly sensitive to temperature fluctuations. The cell suspension was incubated on ice for 20 min and subsequently centrifuged (4°C) at 4000 rpm for 10 min. The supernatant was discarded and pellets were gently resuspended in 10 ml of a 0.1 M $CaCl_2$/15% (v/v) glycerol solution on ice. Aliquots (100 µl) were dispensed into pre-chilled, sterile microcentrifuge tubes and flash frozen in ice cold ethanol. Chemically competent cells were thus prepared for transformation and were stored at -80°C.

3.7.3.2   Transformation protocol

Approximately 5 µl of the ligation reaction and ligation controls were gently mixed with 50-100 µl aliquots of thawed competent *E.coli* cells. Transformation was performed as described by Sambrook *et al*., (1989). The bacteria were incubated with DNA for 15-20 min on ice. The bacteria were heat shocked by incubation in a water bath at 42°C for 45 sec and immediate cooling on ice for 2 min. Transformed bacteria were then mixed with 900 µl SOC medium [20 g Bacto-Tryptone, 5 g Bacto-Yeast extract, 0.5 g NaCl, 2.5 ml 1 M KCl, 10 ml $MgCl_2$, 20 ml 1 M glucose, btv 1ℓ pH 7.0 with NaOH] and were incubated at 37°C for 90 min with gentle agitation (150 rpm). Bacterial suspensions (100 µl) were plated onto LB/agar/X-gal plates with Ampicillin selection at 100 µg/ml and incubated at 37°C overnight. The remainder of the transformation reaction was concentrated with centrifugation at13 000 rpm, for 10 sec and also plated.

3.7.3.3   Screening of recombinants by Colony PCR and blue white selection

Blue-white selection provided a visual indication of successful ligation and transformation in vectors containing the β-galactosidase coding sequence. Colony PCR was performed on 10 colonies per plate using vector-specific primers (T7 and SP6) to screen for the presence of insert. Positive colonies were inoculated in 5ml LB medium and were grown overnight at 37°C at 250 rpm. Overnight cultures were used for plasmid extraction and freezer cultures.

3.7.4   Plasmid DNA purification and Confirmation

Plasmid purification was achieved using the GeneJET™ Plasmid Miniprep Kit (Fermentas) according to manufacturer's instructions. Overnight bacterial culture (1.5-3ml) was harvested by centrifugation at 8000 rpm for 2 min. All subsequent centrifugations took place at 13 200 rpm. Pelleted cells were completely resuspended in 250 µl of Resuspension solution by vortexing. Bacteria were mixed with 250 µl of Lysis solution by inversion until the solution became slightly viscous and transparent. Addition of 300 µl of Neutralization solution required immediate mixing by inversion and led to the formation of a white precipitate. The suspension was centrifuged for 5 min. The supernatant was transferred to a GeneJET™ spin column and was centrifuged for 1 min, discarding the flow-through. Two identical wash steps followed where 500 µl of Wash solution was added to the spin column and centrifuged for 1 min. Residual wash solution was removed by a centrifugation step of 1 min. The spin column was transferred to a sterile microcentrifuge tube, incubated with 50 µl sterile water and centrifuged to elute plasmid DNA. DNA was quantified and stored at -20°C.

*Eco*RI digestion was performed for the confirmation of the presence of insert in plasmid DNA isolations. Digestion conditions: 1µg of template plasmid DNA, 1x Buffer EcoRI (50 mM Tris-HCl pH 7.5, 10 mM $MgCl_2$, 100 mM NaCl, 0.02% Triton X-100, 0.1 mg/ml BSA), 5 U of *Eco*RI per 20 µl reaction. Confirmed plasmid DNA was sequenced and used for other downstream applications described later. Freezer cultures of positive colonies of bacteria, confirmed by colony PCR and plasmid DNA restriction enzyme digestion, were made by adding 500 µl of 80% (v/v) glycerol to 500 µl of overnight *E. coli* culture. These cultures were stored at -80°C for a maximum period of 2 years.

3.8   Sequencing

3.8.1   Direct/plasmid sequencing

Bi-directional sequencing was performed on all constructs by the Central Analytical Facility (CAF), Stellenbosch University using the Applied Biosystems ABI PRISM BigDye™ Terminator v3.0 Ready Reaction Cycle Sequencing Kit following the ½ reaction protocol according to the manufacturer's instructions. Plasmid DNA (400 ng) or purified PCR product was used as template for all sequencing reactions. Primers specific to the vectors (plasmid

DNA) or primers used in diagnosis of vines (PCR products) were used for sequencing. PCR products were purified by ultrafiltration by CAF using the MACHEREY-NAGEL NucleoFast 96 PCR Kit according to manufacturer's instructions.

3.8.2   Nucleotide Sequence analysis and Alignment

Resulting electropherograms were initially inspected and evaluated with ABI Sequence Scanner v1.0 (Applied Biosystems). The generated GRSPaV nucleotide sequences were compared to sequences downloaded from GenBank (Appendix A) utilizing the software package Vector NTI Advance® v10.3.0 (Invitrogen Life Technologies). ContigExpress is an advanced function of the software which was used to further inspect chromatograms, to assemble sequenced fragments to form a single contiguous sequence and to view these assemblies graphically. AlignX function within Vector NTI as well as Clustal W embedded within BioEdit Sequence Alignment Editor v 7.09 (Hall, 1999) were used to create alignments of sequences. Finer alignment was performed by eye.

3.9   Phylogenetic analysis

Phylogenetic analysis of the aligned sequences was done using PAUP (4.0b10) (Swofford, 2003). A total of 48 sequences (16 within each of the 3 regions examined, Figure 13) and selected GenBank sequences (Appendix A) were used in the final phylogenetic analysis. GenBank sequences were selected to be representative of each of the four molecular variant groups that have been established previously (Meng and Gonsalves, 2007b). The outgroup used in this analysis was *Peach chlorotic mottle virus* (PCMV), a member of the genus *Foveavirus*. The aligned matrix was trimmed at the 5' and 3' ends so as to exclude missing characters. A heuristic search (1 000 replicates) using TBR branch swapping was used with all 1173 (cumulative) characters weighted equally to establish the shortest possible trees from the data matrix. A bootstrap analysis (1 000 replicates) using TBR branch swapping was performed to establish clade support. Branches with bootstrap values $\geq 75\%$ were considered as well supported whilst values between 75% and 50% were considered as moderately supported. Values below 50% were considered weakly supported and in line with traditional phylogenetic analysis are not indicated on phylograms.

4. Results

4.1 Nucleic acid extraction

Several problems were encountered when extracting viral nucleic acid that was suitable as RT-PCR template. This is a common difficulty in grapevine research as these woody plants are notorious for high levels of polyphenolics and polysaccharides which inhibit RT-PCR. Furthermore, viruses may have an irregular distribution or low titer within the plant during the growth season which further encumbers RNA isolation. These setbacks necessitate an efficient sampling strategy and extraction procedure.

4.1.1   RNA isolation

Concentrations and purity of RNA were quantified by the NanoDrop™ 1000 spectrophotometer (Thermo Fisher Scientific Inc). Yields of 200-1500 ng/μl were obtained from 200 mg ground phloem or petiole material. The A_{260}/A_{280} ratio of absorbance varied between 1.90 and 2.18 and the A_{260}/A_{230} ratio of absorbance was below 2.00. These two ratios indicate that samples did not contain contaminants which absorb strongly at 280 nm or 230 nm, such as protein or phenolic compounds.

The level of degradation of RNA was determined by agarose gel electrophoresis using buffer components containing DEPC and equipment treated with 10% SDS. These measures were taken to minimize RNase-contamination of gels. Two strong bands where the DNA marker migrates at approximately 1100bp and 700bp represent the ribosomal RNA 28S and 18S subunits respectively (Figure 18). Smearing or the lack of bands indicated degradation of isolated RNA. Genomic DNA contamination was visible as a large band upwards of 10kb.
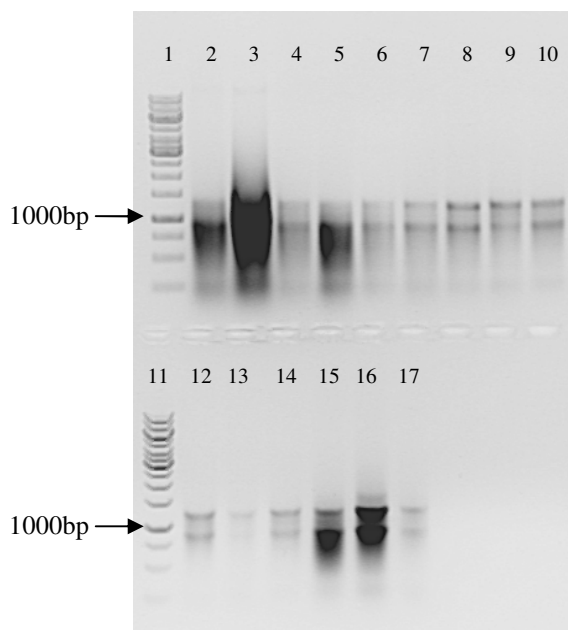
Figure 18: Variation in concentration and degradation of RNA as estimated by agarose gel electrophoresis of a random selection of samples. Lane 1 and 11 - GeneRuler™ 1kb DNA Ladder. Lanes 2 and 3 - genomic DNA contamination visible. Lanes 2, 3, 4 and 5 – varying levels of degradation. Lanes 6-10 and 12-17 – variation in concentration of RNA

The integrity of RNA stored for a period of time was confirmed with agarose gel electrophoresis (Figure 18) and amplification of the *V. vinifera* genome as an internal control (Figure 19). The products in Figure 19 were amplified with the selection of RNA samples represented in Figure 18. These two figures show that the integrity of RNA is related to the quality of amplification product observed by intensity of bands on an agarose gel. Degraded or low yields of RNA (e.g. Lanes 13 and 17) produced poor amplification (low intensity bands are visible).
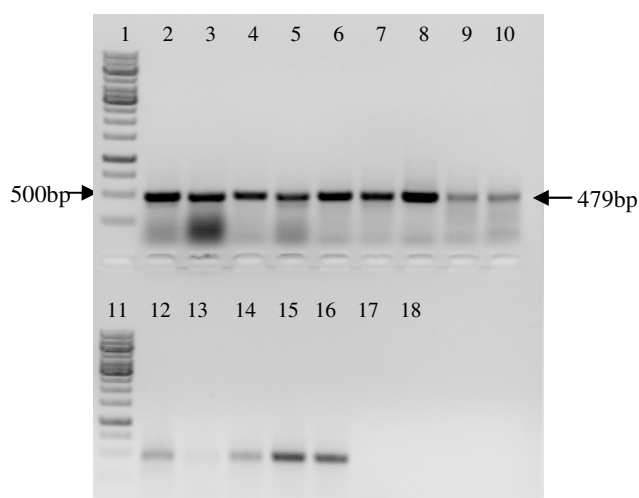
Figure 19: Amplification products of a portion of the ß-Tubulin gene of *V. vinifera* amplified as an internal control (479bp expected product size) to confirm validity of the same random selection of RNA samples as in Figure 18. Lane 1 and 11 - GeneRuler™ 1kb DNA Ladder. Lanes 2-10 and 12-17 – concentration of RNA reflects the intensity of amplification product. Lane 18 – Negative PCR control (water).

58

4.1.2   Double stranded RNA isolation

Various modifications to dsRNA isolation protocols were attempted to isolate the replicative form of GRSPaV from grapevines, with minimal success (optimization data not shown). Contamination of other nucleic acids was common. Various cultivars of *V. vinifera* with diverse viral infections were subjected to dsRNA isolation. Virally infected (*Potato Virus X -* PVX) *Nicotiana benthamiana* was used as a control for the dsRNA extraction technique. Successful dsRNA extractions were consistently performed with this material (Figure 20).
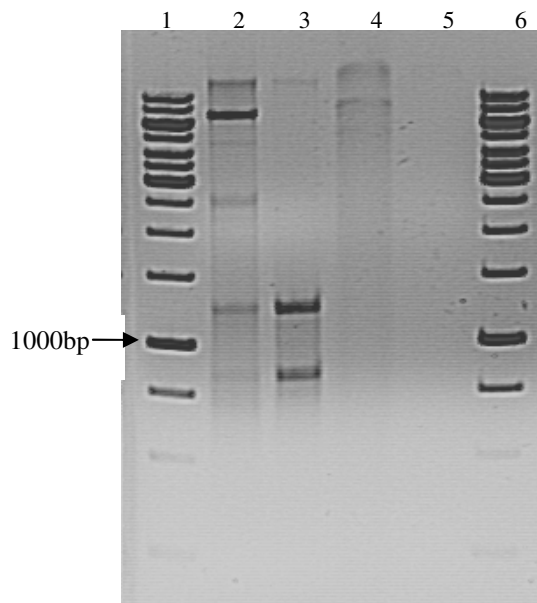
Figure 20: dsRNA extraction of PVX-infected *N. benthamiana* vs. GRSPaV-infected *V. vinifera* material showed genomic DNA and single-stranded RNA contamination. dsRNA extractions were treated with RNase A to remove RNA contamination. Lanes 1 and 6 - GeneRuler™ 1kb DNA Ladder. Lane 2 - dsRNA extraction of PVX-infected *N. benthamiana*. Lane 3 - dsRNA extraction of GRSPaV-infected *V. vinifera* material. Lane 4 – Genomic DNA and dsRNA visible in *N. benthamiana* extract treated with RNase A. Lane 5 – No nucleic acids visible in *V. vinifera* extract treated with RNase A.

The amount of starting material (10-30g) homogenized for extraction from grapevines did not affect the quality of dsRNA extracted. The use of reduced amounts of organic compounds such as chloroform and phenol had no effect on dsRNA yield as measured by intensity of bands on an agarose gel. Chloroform-only or Phenol-only extractions were performed with negligible differences in result. The cellulose-binding step was increased to 2 hours at room temperature. This time-consuming modification did not improve dsRNA yield. The concentration of EtOH (15-17% EtOH) and quantity of cellulose (0.3-9g) was also varied. This did not influence the dsRNA yield. Washing of the chromatography column was

omitted. This resulted in co-isolation of other nucleic acids and compounds. Elution apparatus was modified: a chromatography column delivered better results than a syringe plugged with sterile cotton wool. The single elution of dsRNA from the affinity chromatography column was increased to five elutions. DsRNA was eluted in smaller fractions and compared with agarose gel electrophoresis. The initial eluates contained larger quantities of dsRNA. Double elutions were also performed with additional cellulose binding steps. This reduced the yield of dsRNA. Additional precipitation steps were performed to improve the quality of dsRNA extracted. Better results were observed with additional precipitation steps, however yield of dsRNA did not improve. Diagnosis of GRSPaV, GVA and GLRaV-3 was achieved with low yields of dsRNA.

4.2   Detection of GRSPaV

4.2.1   Crude virus extraction – GES method

Diagnosis of GRSPaV infected vines was achieved with a rapid direct one-tube RT-PCR. This method of diagnosis was efficient for establishing the viral infection status of all the field collected samples analyzed in this study. Crude viral extracts were used with conventional end-point PCR amplification as well as quantitative PCR amplification successfully.

PCR amplification of crude viral extracts was compared to that of purified RNA in the coat protein region. This comparison was performed with both quantitative (Figure 21) and conventional (Figure 22) PCR amplification. The comparative results of two samples which were harvested, processed and extracted concurrently (A and B) are illustrated below. Equal amounts of material from plant A and plant B were used for RNA extraction and crude extract preparation. C_q-values for a threshold of detection which was set at 0.03551 were as follows: sample A: RNA = 19.18 and crude extract = 25.46; sample B: RNA = 18.79 and crude extract = 24.50. Lower C_q-values were observed when using purified RNA in qPCR. This indicates a larger amount of viral nucleic acid present in the purified RNA. Lower C_q-values may also indicate a smaller amount of PCR inhibitors present in the purified RNA. Stronger band intensities were observed with purified RNA in conventional PCR which indicates a larger amount of PCR end product (Figure 22).
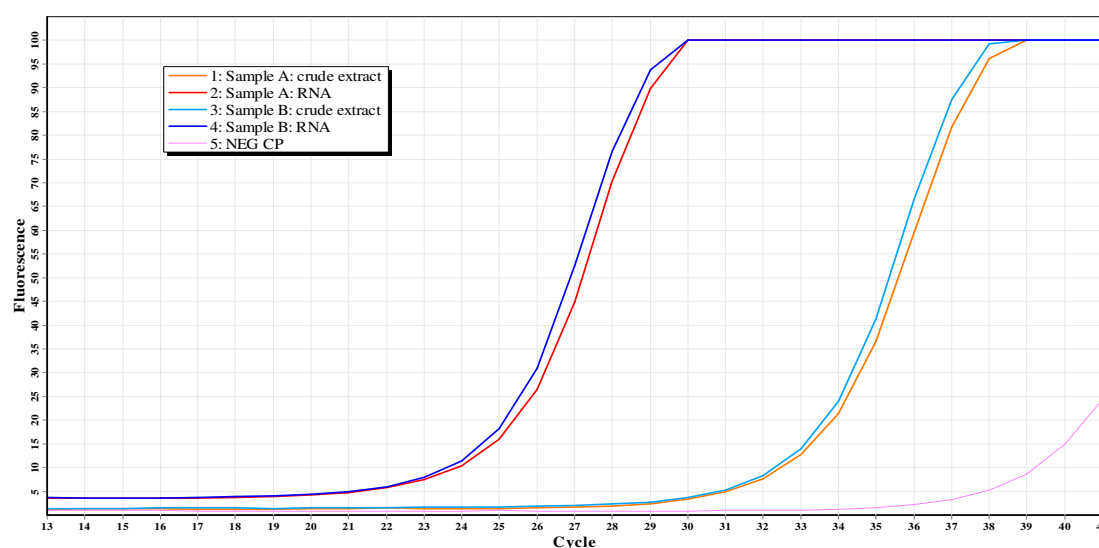
Figure 21: Amplification plot of qRT-PCR performed using a crude extract vs. purified RNA of grapevine Sample A and B respectively. C_q-values for a threshold of detection which was set at 0.03551 were as follows. Sample A: RNA = 19.18, crude extract = 25.46. Sample B: RNA = 18.79, crude extract = 24.50.
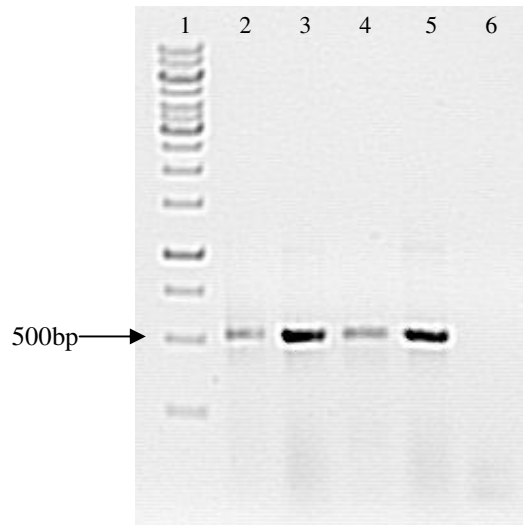
Figure 22: Conventional RT-PCR amplification performed using a crude extract vs. purified RNA of grapevine Sample A and B respectively. Lane 1 - GeneRuler™ 1kb DNA Ladder. Lane 2 and 4 - crude extract of Sample A and B respectively. Lane 3 and 5 – purified RNA of Sample A and B respectively.

The specificity plot of the qPCR products is illustrated in Figure 23. This graph indicates that specific products were obtained for all amplifications with the exception of the negative control. Slight variations in maximum temperature of peaks were observed.
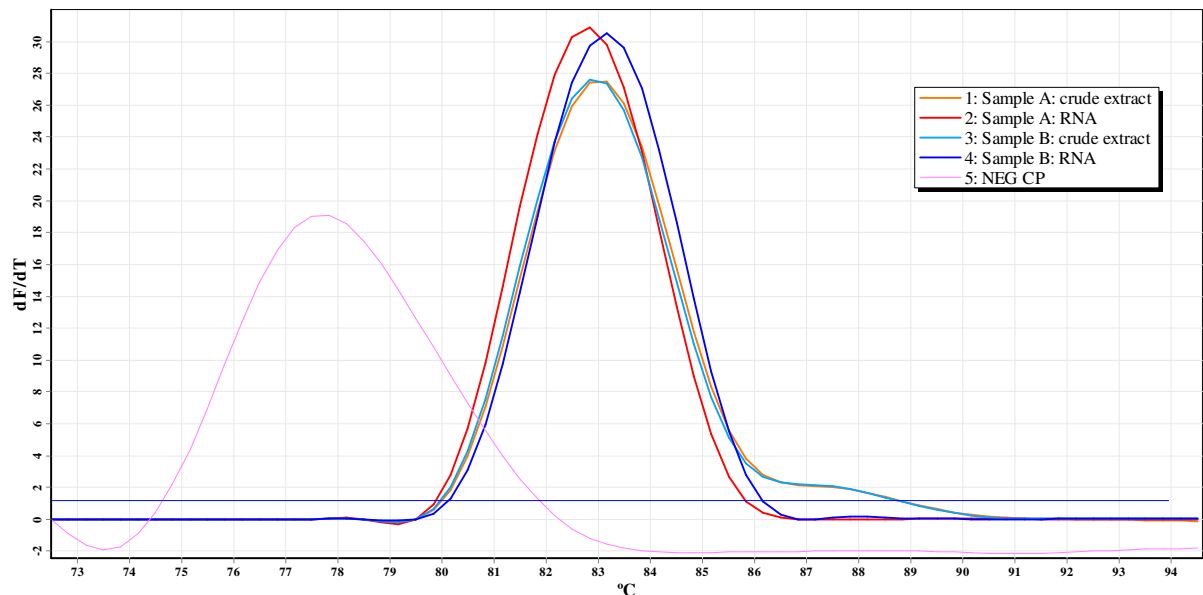
Figure 23: Specifcity plot of the derivative of fluorescence plotted against increase in temperature. Non-specific amplification (i.e. primer dimer) can be seen in the negative control.

4.3 Generation of RT-PCR amplicons used as template for qPCR-HRM

RT-PCR was performed with RNA isolated from a total of 96 vines (including negative controls). Each sample refers to the RNA extract from phloem and/or petiole material from 2-4 canes of a single grapevine plant. The list of arbitrarily named samples, farm of origin, sampling date and GRSPaV-diagnosis are given in Appendix B. The performance of three primer sets [RSP13 & RSP14 (RdRp), RSP9 & RSP10 (RdRp/TGBp1) and RSP21 and RSP22 (CP) (Figure 13)] was evaluated with RT-PCR for all the samples. Downstream characterization with qPCR-HRM was performed with a selection of 16 samples.

Various controls were incorporated during the generation of RT-PCR amplicons. Virus-free *in vitro* plantlets were maintained and used in every RNA extraction and cDNA synthesis to control for contaminants in extraction buffers and RT components. Water negative controls were also incorporated for first strand cDNA synthesis and PCR amplification. Where possible, RNA from a GRSPaV-infected vine was used as a positive control and as a calibrator sample for comparative quantification. Where GRSPaV-positive DNA was required, a plasmid DNA clone or PCR product was used as a positive control. Figure 24 is an example of the controls used to generate RT-PCR amplicons.
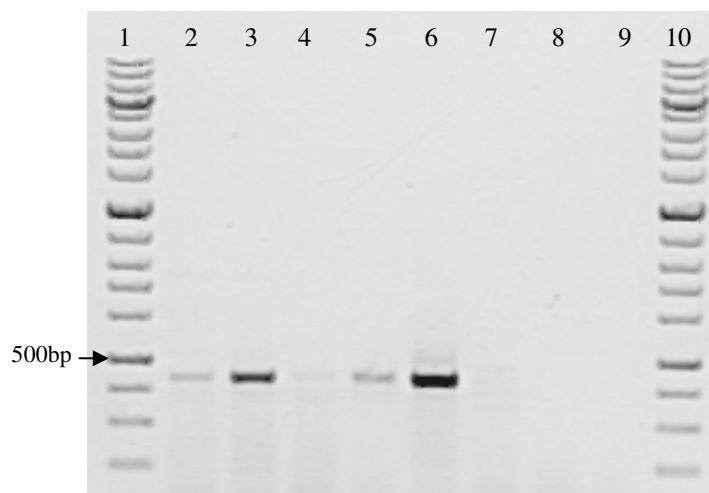
Figure 24: Two step RT-PCR of GRSPaV from a random selection of samples within the coat protein region (441bp) compared to four controls (Lanes 6-9). Lanes 1 and 10 - ZipRuler™ Express DNA Ladder Set, Lanes 2, 4 and 5 – weak amplification, Lane 3 – good amplification, Lane 6 - GRSPaV-positive plant, Lane 7 - Virus-free plantlet, Lane 8 – Negative control: water cDNA, Lane 9 – Negative control - water PCR.

GRSPaV positive samples produced varying amplification efficiency with the three primer sets evaluated (Figure 24 and Figure 25). The samples in both figures have been randomly selected. Varying amounts of amplification end-product was observed as measured by intensity of bands on an agarose gel. Different measures were exercised to improve amplification efficiency. These included the quantification and assessment of RNA extracts. Poor RNA produced poor amplification. Degraded RNA were subjected to subsequent RNA extractions with more successful amplification. Various reverse primers were evaluated for efficiency of priming reverse transcription. No differences were seen with different reverse primers. A higher amount of non-specific amplification was noticed when more than one primer was used in reverse transcription. Random priming (hexamers) of reverse transcription was not feasible for large-scale evaluation of primer sets due to cost of random priming reactions. Downstream qPCR-HRM assays consisted of nested reactions using diluted RT-PCR products. The varying amplification efficiency observed with RT-PCR did not influence the amplification efficiency or C_q-values of nested qPCR-HRM assays (Section 4.5).
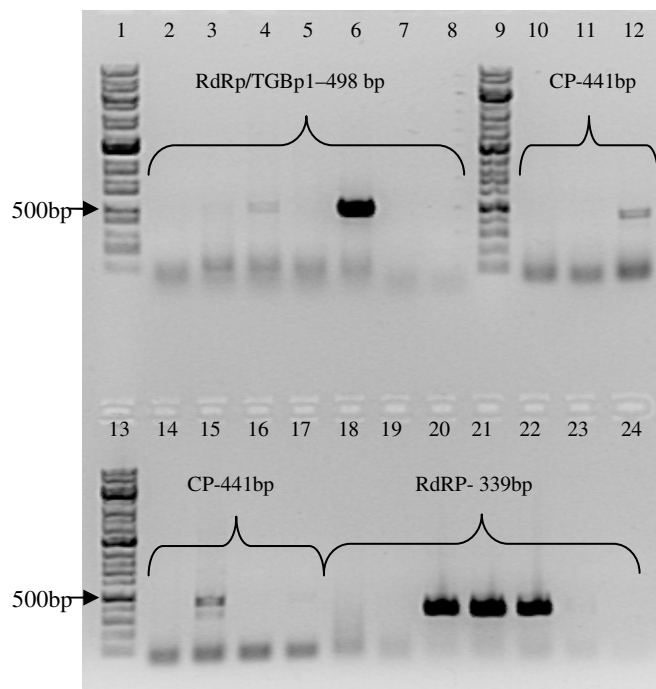
Figure 25: A random selection of four samples showing varying amplification efficiency with 3 primer sets. GRSPaV genomic regions and expected product sizes are annotated on the image. Water PCR negative controls as well as GRSPaV-infected plants and virus-free plantlets was included in each assay. Lanes 1, 9 and 13 - ZipRuler™ Express DNA Ladder Set. Lanes 6, 15 and 22 positive controls. Lanes 7, 16 and 23 – GRSPaV-negative plant. Lanes 8, 17 and 24 – water PCR

The efficiency of two other DNA polymerase enzymes [DreamTaq™ (Fermentas) and Ex Taq™ (Takara Bio)] was compared to the efficiency of KapaTaq™ amplification. Weaker amplification was seen with ExTaq™ and equal efficiency amplification was observed with DreamTaq™ (results not shown). All further amplifications were conducted with KapaTaq™. Primer and cDNA titrations were performed using serial dilutions of cDNA. Dilute cDNA (1:100) produced weak amplification. Most efficient amplification was seen with a dilution of 1:10. Optimal primer concentration was determined to be 0.25 µM. The most efficient amplification was observed when 5 cycles of PCR at an annealing temperature of 37°C was included prior to specific annealing cycles. This PCR program was thus applied to all subsequent amplifications.

4.4 Optimization of qPCR-HRM assay

All qPCR-HRM assays were performed in duplicate for each sample using diluted RT-PCR products. RT-PCR products were derived from total RNA extracts and subsequently diluted 1:500. The qPCR-HRM assay was performed to evaluate the genetic diversity within select regions of the GRSPaV genome. Selected samples were further characterized with Sanger sequencing to confirm the HRM data generated.

Four nested primer sets falling within areas targeted for diagnosis were initially designed and tested for suitability to qPCR-HRM. As mentioned previously, small amplicons (<400bp) are required for successful HRM analysis. Amplicons with delta-G values higher than -1 were preferred due to the low level of secondary structure formation. Analytical specificity of primers was experimentally determined as secondary melt domains (extra peaks) using the first derivative of fluorescence during the melt phase. Specificity of primers was also confirmed via agarose gel electrophoresis. Confirmation of specificity of primers to target regions of the GRSPaV genome was obtained by direct sequencing of RT-PCR products.

The primer pairs used for qPCR-HRM analysis are summarized in Table 5. The optimal annealing temperature for each primer pair was determined with gradient PCR over a range of 15°C (50-65°C). The assay was further optimized using a range of template, magnesium and primer titrations. The use of qPCR for amplification was advantageous, as detailed information about the quality of amplification was attained. Low amplification efficiencies (<1.4) resulted from poor nucleic acid quality or sub-optimal amplification. The integrity of RNA, as assessed by agarose gel electrophoresis was directly proportional to the amplification efficiency. The average amplification efficiencies observed for this study were between ~1.5 to ~1.9. All samples that amplified poorly were regarded as outliers of amplification and could not be used in HRM analysis.

4.4.1 Validation of qPCR-HRM technique

Plasmid cDNA clones were used to validate the qPCR-HRM technique. A selection of samples (1-8) was subjected to this analysis (

Table 12). RT-PCR was performed on the RNA extracts of 8 samples using primer set RSP9 & RSP10. RT-PCR products from this region spanning ORF 1 and 2 (498bp) of the GRSPaV genome were used for TA-cloning. Plasmid cDNA clones were subjected to sequencing and parallel nested qPCR-HRM reactions using primer sets RSP_910_HRM_3F & RSP_910_HRM_4R. A multiple alignment of the sequencing results are available in Appendix C. The sequencing results are summarized in

Table 12.

Optimized amplification is required for successful HRM analysis (Figure 26). It is recommended that C_q-values of duplicate samples be within 3 cycles of each other.
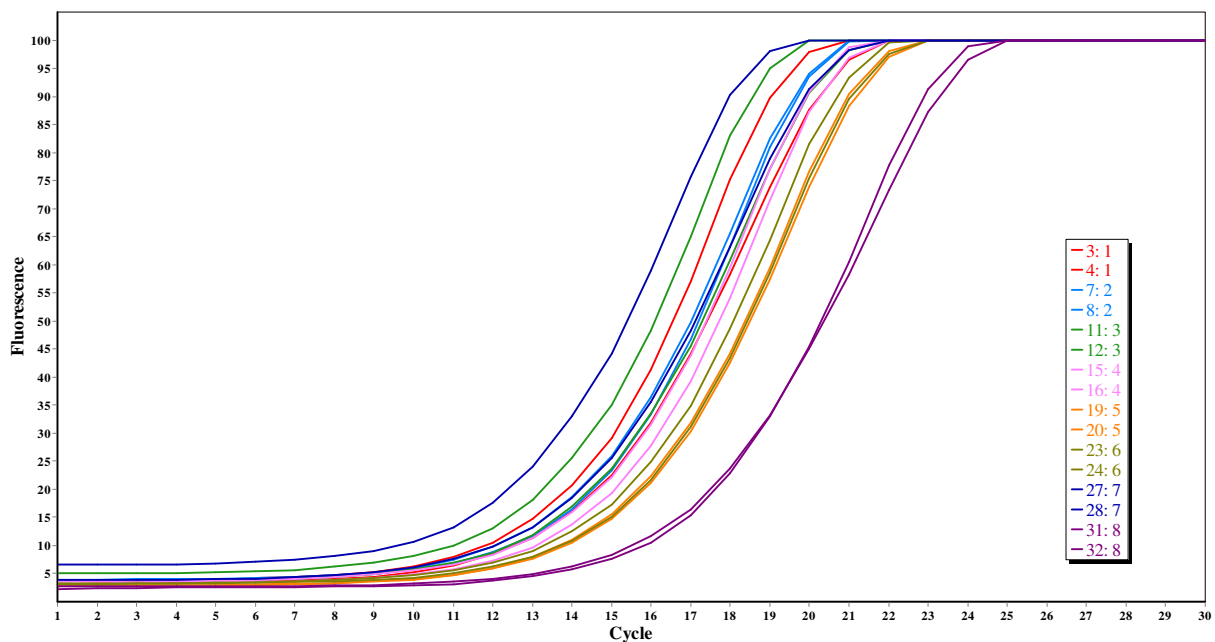
Figure 26: Amplification plot of a nested qPCR-HRM amplicon (140bp) of 8 samples performed in duplicate using plasmid DNA clones.

It is evident from Figure 27, that all reactions reached their maximum rate of fluorescence at some point during the reaction. Therefore, all reactions reached maximum amplification efficiency of 2. The average amplification efficiency was however 1.52±0.04. The take-off point is used by the software module to calculate this amplification efficiency. Both values are given in Table 11. The take-off point can be defined as that cycle where the amplification reaches 20% of the maximum rate of fluorescence increase. It is calculated from the second derivative of the increase in fluorescence during amplification.
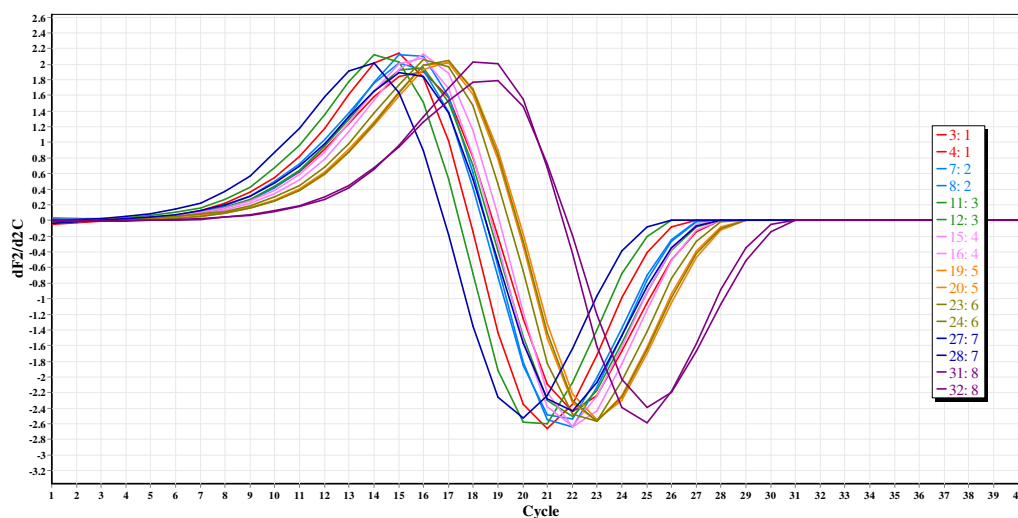
Figure 27: Graph of the second derivative of the increase in fluorescence during amplification of 8 cDNA clones. Peaks correspond to the maximum rate of fluorescence increase.

Table 11: Amplification efficiency and take-off values of 8 cDNA clones.

Sample #	Take Off Point	Amplification Efficiency
1	10.5	1.5
1	10.1	1.49
2	10.9	1.52
2	10.3	1.48
3	10.6	1.55
3	9.8	1.54
4	11	1.53
4	11.3	1.54
5	12	1.52
5	11.8	1.5
6	12	1.55
6	11.8	1.5
7	8.9	1.54
7	10.2	1.48
8	13.2	1.49
8	13.8	1.55

Table 11 highlights the reproducibility of the qPCR-HRM assay because intra-assay variance is limited. Sample duplicates have very similar take-off and amplification efficiency values which are a result of assay precision, true template estimation and pipetting accuracy.

The graph of the normalized melt profiles clearly shows a temperature shift from the dominant variant (Figure 28). The single nucleotide polymorphism at position 386T>C in Sample 2 and position 419G>A in Sample 8 produces a temperature shift of 0.5°C from the dominant variant. Sample 1 is a quasi-species of GRSPaV which was directly sequenced from the amplicon (cloning step omitted). It shows 2 ambiguities at positions 381 and 447 (
Table 12). Sample 1 displays a change in the gradient of its melt profile as compared to the dominant variants. Furthermore all duplicates of samples fall next to each other which also indicates short term assay precision. The results of the normalized melt profiles are thus validated by sequencing.
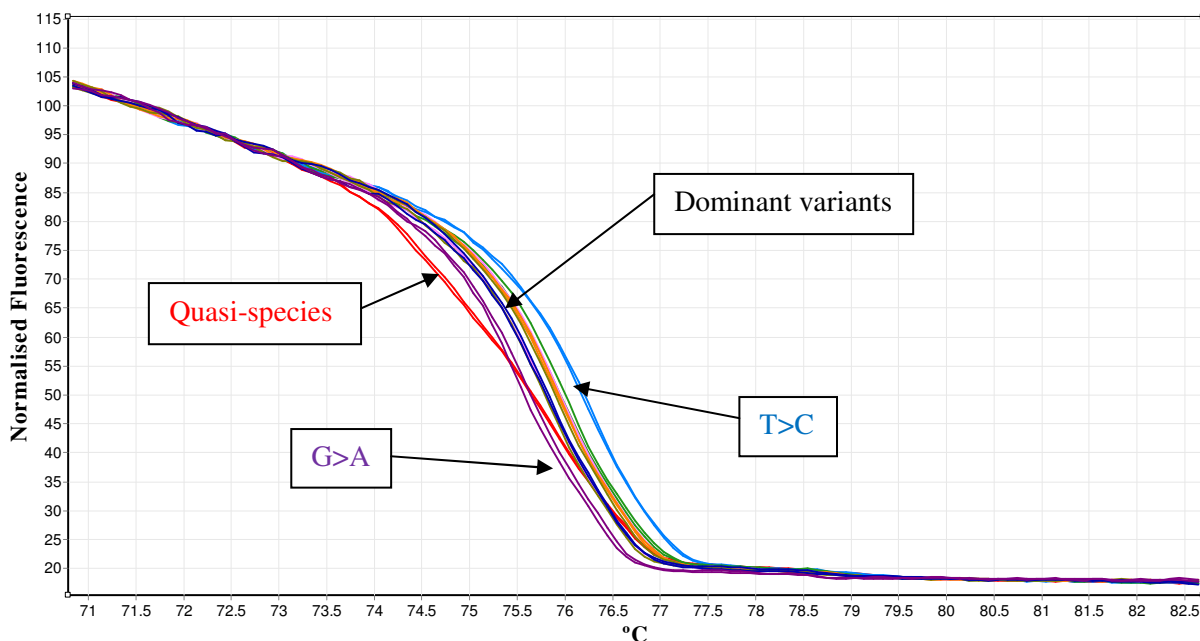
Figure 28: Normalized melt profiles of a nested qPCR-HRM amplicon (140bp) of 8 samples performed in duplicate using plasmid DNA clones. Normalization ranges: Pre-melt phase (78.84-72.16°C); post-melt phase (78.04-82.79°C). Variants are annotated: Quasi-species – mtX, T>C – mtC, G>A - mtA

The normalized melt profiles can be better visualized using the difference graph (Figure 29). The results displayed in Figure 28 and Figure 29 are summarized in
Table 12. It is evident from the difference graph (Figure 29) that Samples 1, 2 and 8 are significantly different to the reference genotype (Sample 4 represents the dominant variant in this instance). A significant difference is indicated by ΔF larger than 5. The samples confirmed by sequencing as being the dominant variants are not significantly different from the reference sample (ΔF<5). The amplicon used in qPCR-HRM assay for the RdRp region was also validated in this way. The amplicon used in the qPCR-HRM assay for the CP however, demonstrated some difficulties as outlined below.

Table 12: Summary of sequencing results of plasmid cDNA clones used to validate qPCR-HRM technique. Notation
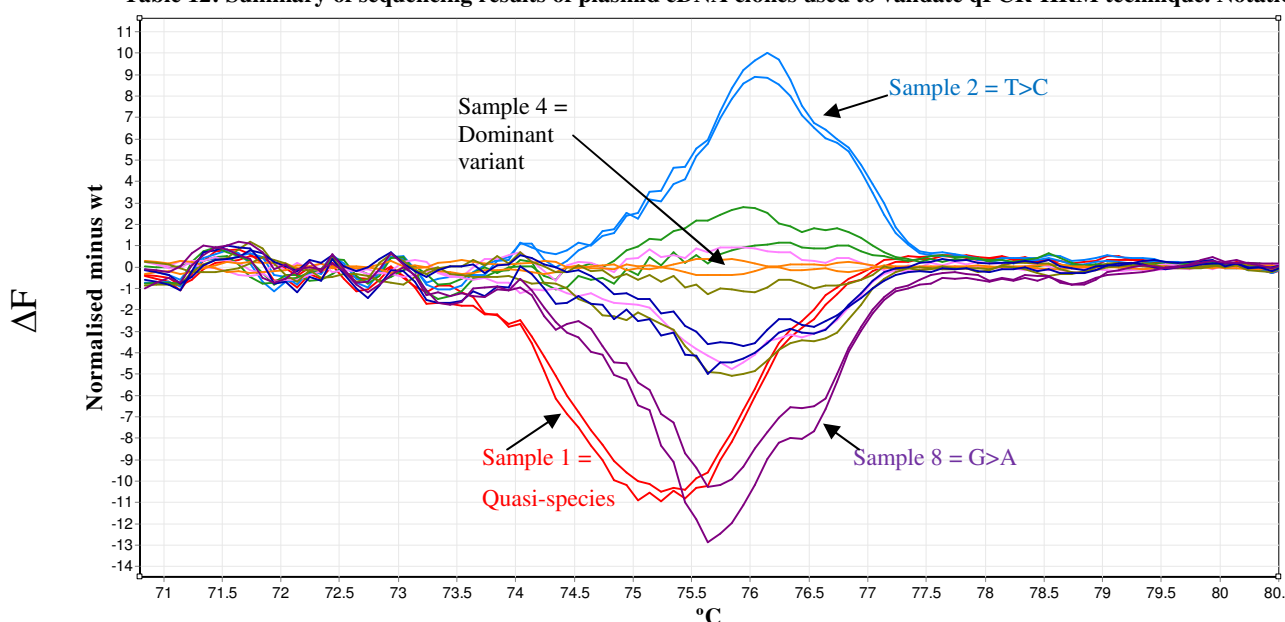
Figure 29: The difference graph of the normalized melt profiles subtracted from the normalized melt profile of the dominant variant in the assay. Variants are annotated as follows: Quasi-species – mtX, T>C – mtC, G>A - mtA for plasmids: pDRIVE=backbone, 910=cloned fragment, _2=RNA sample, -9=colony picked. Variants annotated in Figure 27 are as follows: Quasi-species – mtX, T>C – mtC, G>A – mtA.

Sample #	Sequencing Number	Sequencing template:	Position in diagnostic fragment 910				Variant
			381	386	419	447	
1	Vitis_0854	Amplicon - 1	G or T	T	G	A or G	mtX
2	Vitis_0855	pDRIVE910_**2**-9	G	C	G	A	mtC
3	Vitis_0856	pDRIVE910_**3**-9	G	T	G	A	Dominant
4	Vitis_0857	pDRIVE910_**4**-4	G	T	G	A	Dominant
5	Vitis_0858	pDRIVE910_**5**-9	G	T	G	A	Dominant
6	Vitis_0859	pDRIVE910_**6**-3	G	T	G	A	Dominant
7	Vitis_0860	pDRIVE910_**7**-4	G	T	G	A	Dominant
8	Vitis_0861	pDRIVE910_**8**-3	G	T	A	A	mtA

A multiple alignment of various published GRSPaV CP sequences showed that variation within this area was expected. The first nested primer set analyzed in the CP region (RSP_CP_HRM_1F and RSP_CP_HRM_2R) spanned a 130 bp region. The melt profile of selected samples within this region was adequate for analysis i.e. no secondary structure or melt domains. However, no significant temperature or shape shifts were observed when qPCR assays were performed (data not shown). Upon sequencing of a number of plasmid cDNA clones, the results revealed no variation within this 130bp region (data not shown). A different and perhaps larger region of analysis was thus required. It was decided to develop a second, larger HRM analysis region within the CP region with higher predicted variation. The HRM region given by (**RSP_2122_HRM_6F** and **RSP_2122_HRM_7R**) spanned 195bp within a different region of the CP. The regions within the genome of GRSPaV that was successfully validated in HRM analysis are displayed in Figure 14.

4.5 Evaluation of a panel of sequence characterized CP sequence variants using HRM analysis

A selection of 16 samples was used for screening with qPCR-HRM and subsequent sequencing in three regions of the GRSPaV genome. Two to five samples were randomly selected from each farm. It was ensured that the qPCR-HRM data analysis was done without any knowledge of the sequencing results. For the purposes of this section, both data sets (HRM and sequencing) of the CP region will be presented and compared.

The multiple alignment of the CP region (195bp) of the 16 samples that were subjected to HRM can be viewed in Appendix C. Overall, the region showed 72.3% nucleotide identity. This percentage corresponds to 56 positions where a SNP in at least one of the samples was found. A schematic representation of the nucleotide identities of the 16 samples sequenced relative to GRSPaV-SG1 is shown in Figure 30. This guide tree was built using the neighbor-joining method, which works on a matrix of distances between all the pairs of sequence aligned (Nei, 1987).
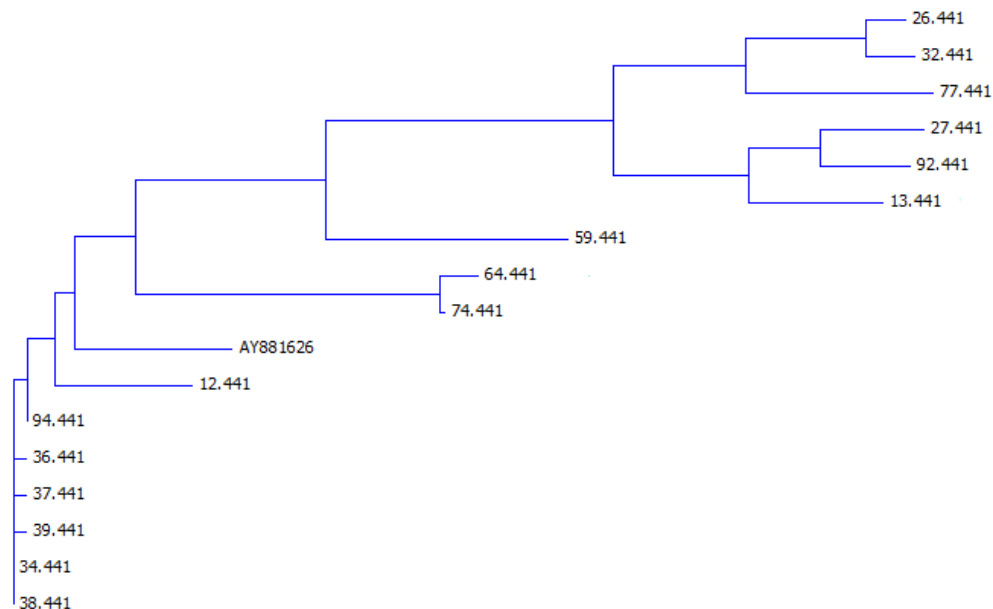
Figure 30: Schematic representation of nucleotide identities of 16 South African sequences (.441) used for qPCR-HRM and parallel sequencing relative to the Group II full-length reference isolate, GRSPaV-SG1 (Acc. No. AY881626). The radiations that are present broadly reflect the final HRM output data (Table 13).

The HRM analysis of data was confirmed by sequencing a panel of sequence variants. Figure 31 displays the nested amplification of a 195bp CP region of GRSPaV. C_q-values of all duplicates are in the region of 11-16 cycles. Amplification efficiency for qPCR-HRM assay is 1.77 ± 0.03 (max = 2).
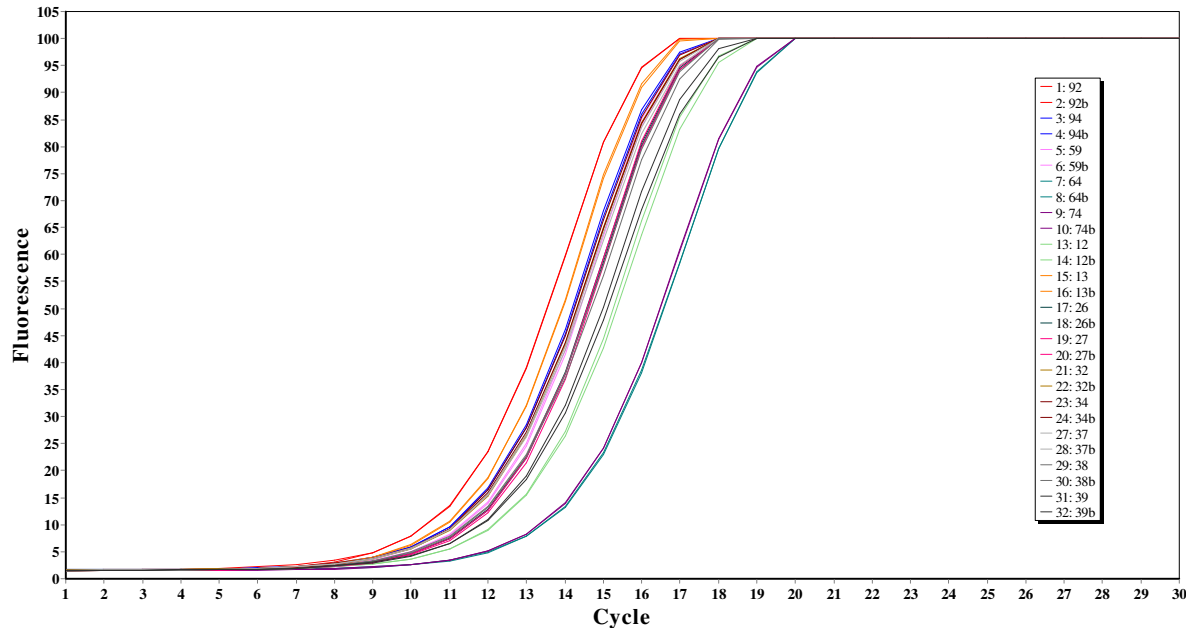
Figure 31: Amplification plot of an area within the CP region of 16 sequence-characterized samples performed in duplicate.

Figure 32 shows the normalized melt profiles of the above amplification. Temperature shifts are observed over a range of 1.5°C. The temperature shift represents the nucleotide base pair dissimilarities. Certain samples display a marked difference in slope e.g. Sample 59 (pink). These samples are speculated to be instances of mixed infection similar to the heterozygote
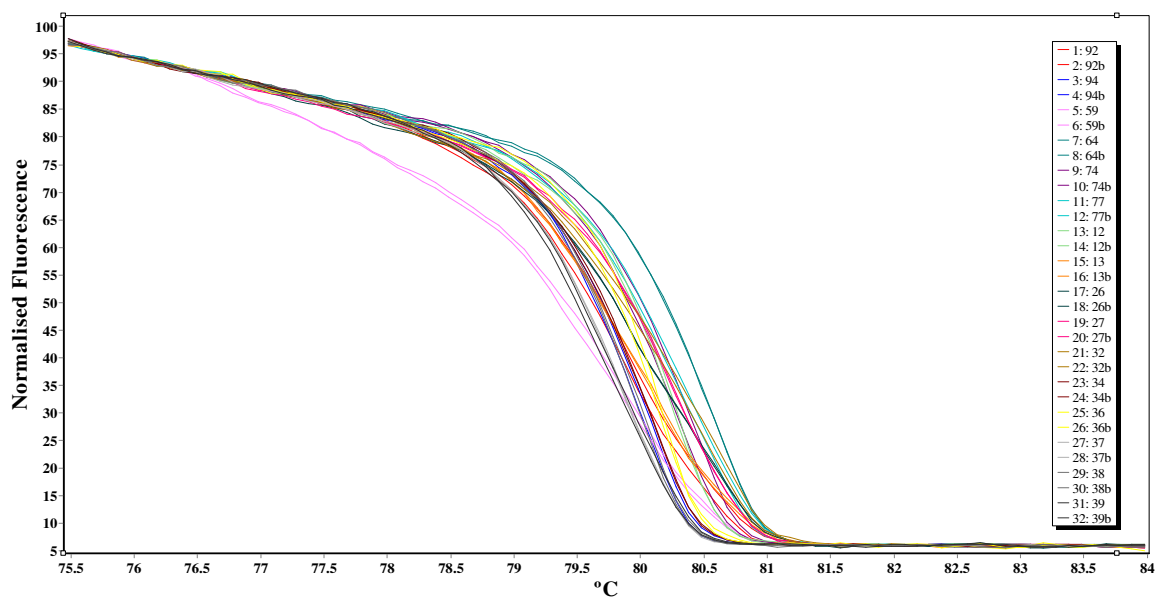
Figure 32: Normalized melt profiles of 16 sequence-characterized samples performed in duplicate. Normalization ranges: Pre-melt phase (75.48-76.48°C); post-melt phase (83.07-84.07°C).

73

nature of alleles of an organism. Mixed infections are represented by an ambiguity in sequence data above a threshold of 25%. The presence of mixed infections can only be verified with cloning of RT-PCR products followed by sequencing several of the cDNA clones (population cloning approach).

A single sample of each farm of origin was selected as the genotype to represent that particular farm (Tradouw –BD, Kanonkop – KK, Grondves – GV, Nietvoorbij – NVB). The allocation of genotypes by the user allows similar genotypes to be computed using the auto-calling software. A difference graph of the major genotypes found within this sample set is plotted in Figure 33. In the graph, the normalized melt profiles are subtracted from the normalized melt profile of a user-defined reference sample. In this graph the reference sample is that of the KK genotype. All genotypes differ significantly at $\Delta F > 5$. A second sample is included to illustrate its similarity to the reference sample i.e. $\Delta F \leq 5$. These two samples are thus both of the KK genotype at a confidence interval of 70%. It is also observed that multiple melt domains exist. A smaller temperature range can be applied to distinguish melt domains.
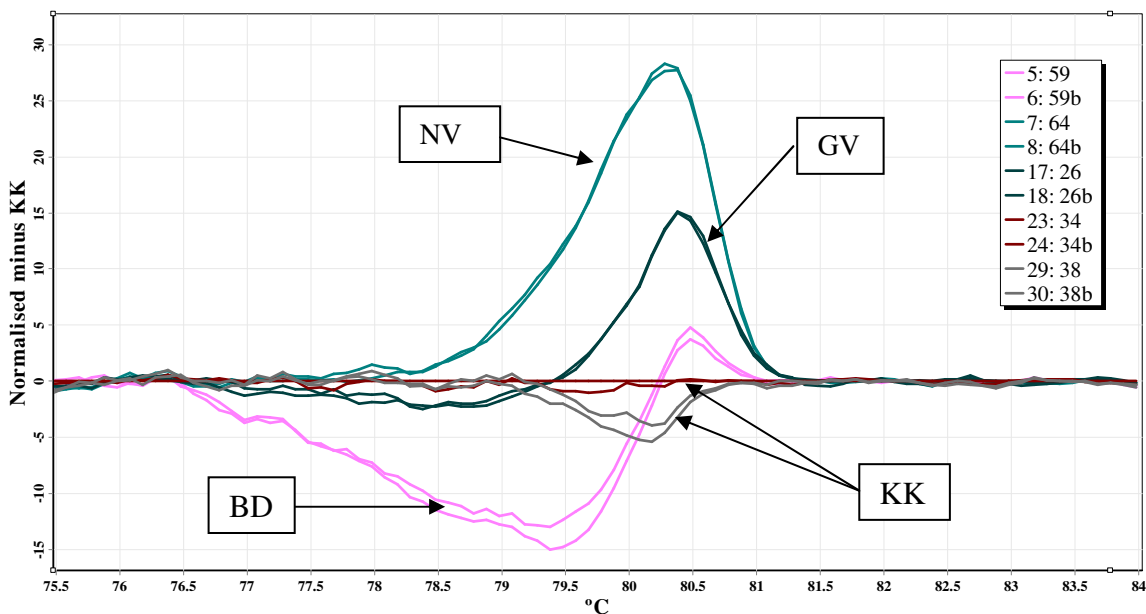
Figure 33: Difference graph of the major genotypes within the CP region of this sample set.

Figure 34 shows the difference graph of the entire panel of sequence characterized samples including the major genotypes displayed in Figure 33. The graph displays the range of sequence variants which was confirmed with sequencing.
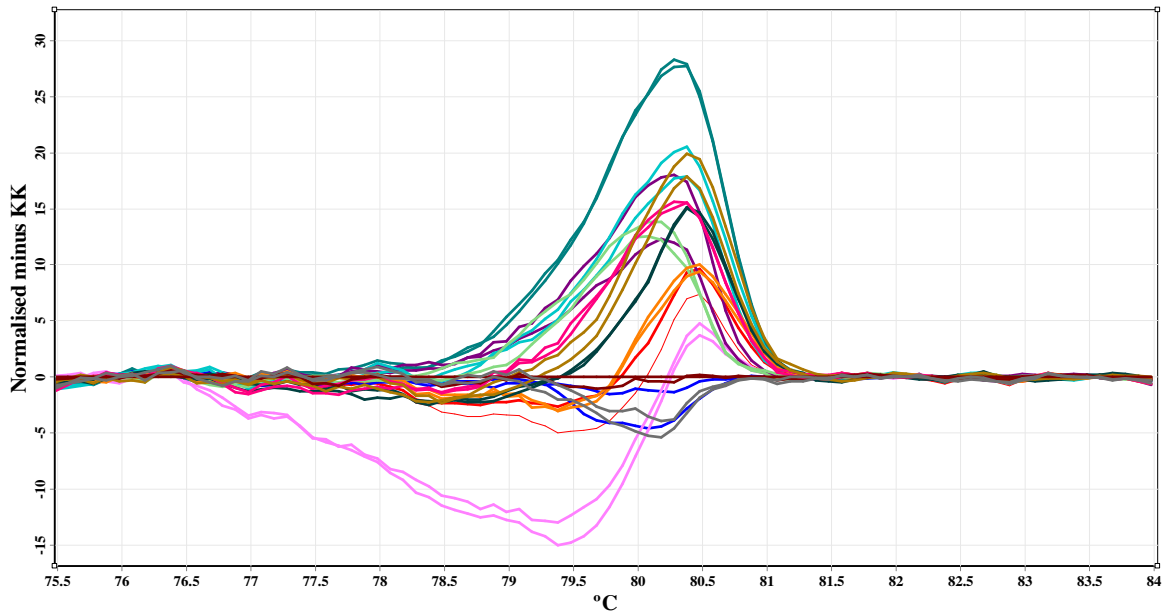
Figure 34: Difference graph of 16 sequence-characterized samples.

Table 13: Auto-calling of duplicate samples by RotorGene software using user-defined genotypes. Tradouw –BD, Kanonkop – KK, Grondves – GV, Nietvoorbij – NVB.

Tube No.	Colour	Name	Genotype	Farm of origin	Tube No.	Colour	Name	Genotype	Farm of origin
1		92	BD	BD	17		26	GV	GV
2		92	BD	BD	18		26	GV	GV
3		94	KK	BD	19		27	GV	GV
4		94	KK	BD	20		27	GV	GV
5		59	BD	NVB	21		32	GV	GV
6		59	BD	NVB	22		32	GV	GV
7		64	NVB	NVB	23		34	KK	KK
8		64	NVB	NVB	24		34	KK	KK
9		74	GV	NVB	25		36	KK	KK
10		74	GV	NVB	26		36	KK	KK
11		77	GV	NVB	27		37	KK	KK
12		77	NVB	NVB	28		37	KK	KK
13		12	GV	GV	29		38	KK	KK
14		12	GV	GV	30		38	KK	KK
15		13	BD	GV	31		39	KK	KK
16		13	BD	GV	32		39	KK	KK

Table 13 shows the summarized results from the auto-calling module of the software compared to the respective farm of origin of each sample. It is the final genotype output at a confidence level of 70%. It is observed that the majority of samples had the genotype representative of their farm of origin: 34, 36, 37, 38 and 39 group with KK genotype; 12, 26, 27 and 32 group with GV genotype; 64 and 92 are single samples representative of NVB and BD genotypes respectively. Five samples however (highlighted in grey) do not correspond with the genotype representing their farm of origin. Sample 94 originated from BD, but had a genotype more similar to those samples originating from KK. Sample 59 originated from NVB and Sample 13 from GV, but both samples had genotypes more similar to BD. Sample 74 originated from NVB, but had a genotype more similar to GV. Sample 77 was the only sample for which duplicates were not called accurately.

4.6 Phylogenetic Analyses

Phylogenetic analysis of sequenced RT-PCR amplicons was performed with a selection of GRSPaV sequences available in the GenBank database (Appendix A). This was performed to determine the phylogenetic relationship to each other and to variants published by other authors. Three regions were used for three separate phylogenetic analyses. The phylogenetic trees for the RdRp and TGBp1 regions are available in Appendix D. For the RdRp and the CP region, Portuguese and North American sequences contained in the phylogenetic analyses in Figure 9 and Figure 8 were included in the phylograms drawn for the current study. For the RdRp/TGBp1 region, Japanese sequences contained in the phylogenetic analysis in Figure 7 were used in this phylogenetic study. In all instances, sequences were selected to represent the four different phylogenetic groups that have been identified by other authors (Meng *et al.*, 2006; Nakaune *et al.*, 2006; Nolasco *et al.*, 2006).

The alignment matrix of the 3 regions of the GRSPaV genome with the PCMV outgroup introduced gaps of 2-5 base pairs. PCMV is the foveavirus which when aligned, produced the least number of gaps when compared to the other members of the genus *Foveavirus*. The heuristic searches retrieved between 8000 and 9500 trees that were used to generate a strict consensus tree for every region. One of the shortest trees for each region is represented in Figure 5 and Appendix D. Bootstrap values are indicated on the branches of the trees. The tree statistics for each of the three trees produced are tabulated below:

Table 14: Summarized statistics for the phylogenetic trees generated.

Phylogenetic tree	Tree length	Number of characters				Consistency index	Retention index
		Parsimony-informative	Parsimony-uninformative	Constant	Total		
CP	596	127	131	155	413	0,579	0,837
RdRp	413	97	82	110	289	0,579	0,803
RdRp/TGBp1	551	155	104	212	471	0,628	0,828
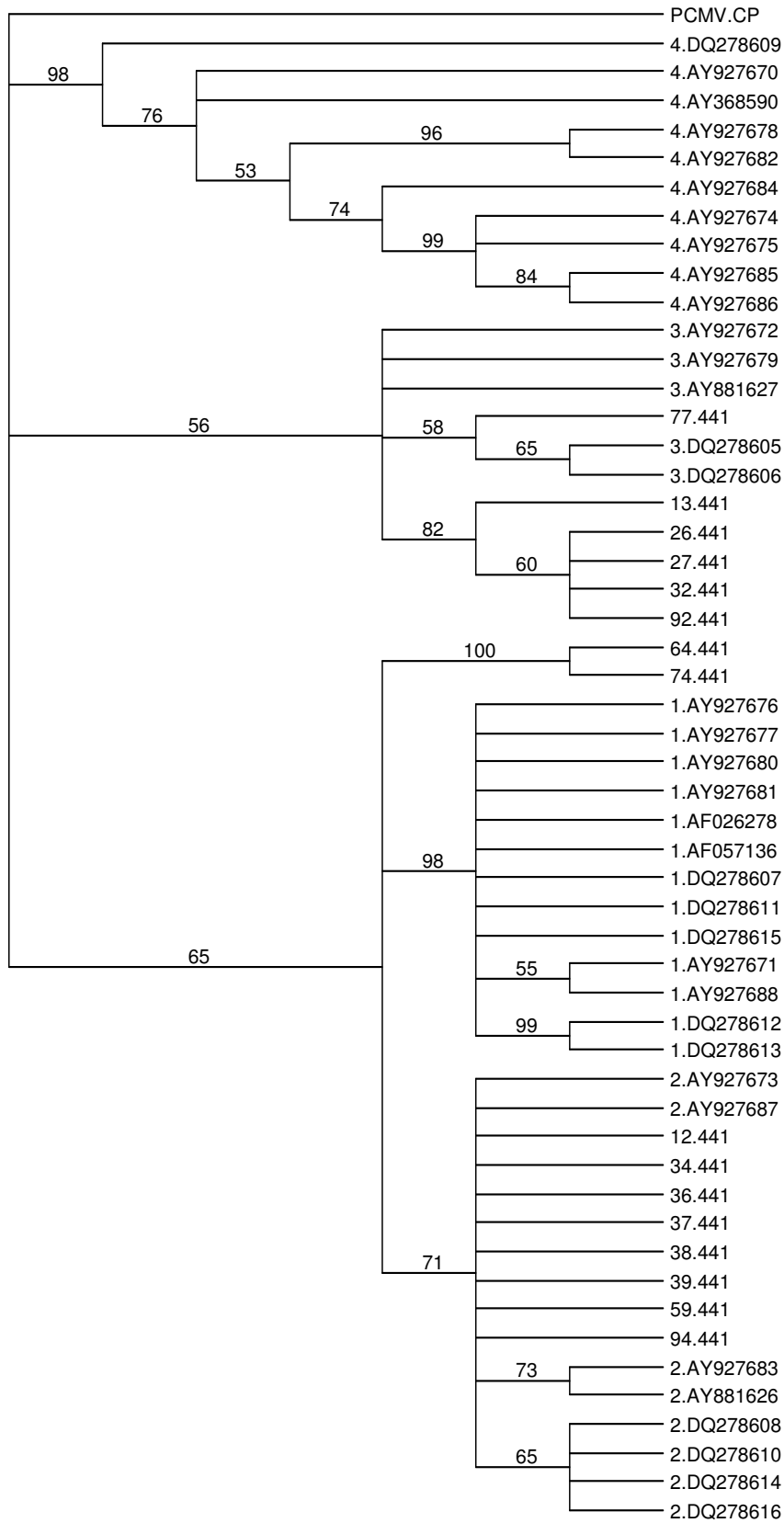
Figure 35: Phylogenetic tree for the partial CP region. SA sequences are indicated by .441. Bootstrap values are indicated above the respective branch. Branches with bootstrap values higher than 75 were considered well supported. Branches with bootstrap values lower than 60 were considered poorly supported. Genbank sequences are prefixed with relative phylogenetic group.

The purpose of the current study was to establish which of the phylogenetically distinct sequence variant groups (Groups I, II, III and IV) are the dominant sequence variants present in the sample set. The phylogenetic tree representing this analysis for the Coat Protein region is shown in Figure 35. It is observed that the majority of South African sequence variants radiate with groups II and III.

5. Discussion

5.1 Nucleic acid extraction

Optimal isolation of viral nucleic acids is crucial for conducting experimental work. Isolation and sample processing methods must be cost- and time effective and must guarantee nucleic acid integrity. The low yields of dsRNA obtained in this study were deemed inadequate for the purposes of the study. Total RNA was used as template for the remainder of the GRSPaV detection and characterization experiments.

Isolation of total RNA proved consistent with all plant material examined in terms of yield, integrity and reliability (Figure 18). DNase I treatment of RNA extract did not affect the yield of RNA significantly. The A_{260}/A_{280} and the A_{260}/A_{230} ratios of absorbance were within the recommended parameters described by the spectrophotometer manufacturer. The ratios obtained can thus be interpreted as a measure of nucleic acid quality and purity. However, the spectrophotometer does not have the ability to measure the integrity of RNA isolated. Agarose gel electrophoresis was thus used to assess the integrity of the RNA as depicted in Figure 18. Thawing and freezing of RNA was avoided. This preserved the stability of RNA at -80°C. Nevertheless, the integrity of RNA was examined with RT-PCR amplification using primers targeted to the *V. vinifera* gene ß-Tubulin. This internal control gave an indication of the suitability of RNA stored for longer periods of time to RT-PCR (Figure 19). All RNA samples showing poor amplification were discarded and RNA isolation was repeated.

5.2 Detection of GRSPaV

5.2.1 Crude virus extraction – GES method

Once optimized, this method of detection has some unique advantages. The technique is less time-consuming as reverse transcription and amplification can take place in a single tube. The method eliminates the need for nucleic acid extraction procedures, as plant sap can be used directly in a RT-PCR reaction. It is thus suitable for large-scale screening of vines of which the viral status is unknown. Furthermore, this approach to diagnosis is suitable for both conventional and quantitative PCR.

Unfortunately this procedure has disadvantages. High fidelity enzymes with proofreading capability are not suitable for use with this procedure. This may have influenced the reliability of amplification as mutations may have been incorporated, leading to an over-estimation of genetic diversity. Nevertheless, *Taq* DNA polymerases have very low error rates which influences the genetic diversity only minimally (Toi and Dwyer, 2008; Teycheney *et al*., 2005). Optimization of rapid direct one-tube RT-PCR can become challenging: non-specific amplification may be difficult to prevent and the inclusion of PCR-inhibitors is inevitable. This is evident from an amplification plot of RT-PCR reactions carried out on RNA and a crude plant extract. Because the amplification is viewed over time, it can be seen that amplification of purified RNA occurs much earlier than crude plant extract (as shown in Figure 21). The difference in C_q-values is also attributed to the difference in initial concentration of viral RNA molecules. The RNA included in the RT-PCR from the crude extract is diluted 100 fold as compared to purified RNA extracted from the same amount of plant material. This difference is due to the nature of the extraction procedures.

More efficient amplification with purified RNA is also seen with conventional PCR (Figure 22). Quantitative PCR analyses are thus well correlated to conventional end-point PCR analysis. In conclusion, a rapid and direct method of RT-PCR was found to be adequate for the purposes of establishing infection of GRSPaV using crude extract. The technique was thus used to screen all vines sampled in this study. RNA was isolated for selected vines to perform downstream amplification and characterization.

5.2.2   Multiple Primer sets

The knowledge on the genetic diversity of GRSPaV has allowed the design of universal primers that can be used for the diagnosis of GRSPaV. The approach suggested by Nolasco *et al*. (2000) was followed in this study. During a study to evaluate the sensitivity, specificity and positive predictive value of various primer pairs used for diagnosis, these researchers made several conclusions (Nolasco *et al*., 2000). Firstly, total RNA isolations are feasible as RT-PCR template in diagnosis. Secondly these researchers suggest the use of more than one primer pair in diagnosis, because combinations of primer pairs deliver the highest sensitivity. This is due to RNA viruses having naturally high variability which can affect the ability of a single primer pair to detect certain sequence variants.

Three primer sets were utilized to detect GRSPaV infection during this study. Samples were diagnosed negative for GRSPaV when RT-PCR results were negative for the three primer sets evaluated in this study (Figure 25). Samples were diagnosed positive for GRSPaV when RT-PCR results were positive for at least one primer set. There was no combination of primer sets that demonstrated significantly higher specificity. Diagnosis of RSP with more than one primer set becomes problematic because it increases the cost for detection of GRSPaV. A balance must be established which links cost-effectiveness to prudence. For applications such as certification of grapevines, the short term costs of accurate viral detection outweigh the long term costs of planting a diseased vineyard.

5.3 Optimization of qPCR-HRM assay

5.3.1   Amplification efficiency is template-dependant

The amplification efficiency was most influenced by the type of template used in the qPCR-HRM assay. The first template evaluated was purified total RNA. Successful qRT-PCR amplification of small amplicons (<200bp) was achieved using 200ng of total RNA. However, amplification efficiency varied greatly and C_q-values of replicates were dissimilar. RNA degraded over a period of time in storage at -80°C and produced poor amplification, despite avoiding freeze-thaw cycles. The RNA isolation procedure had to be repeated several times with the same samples to produce consistent results. HRM analysis is practically impossible with sub-optimal amplification and high C_q-values (Corbett, 2006).

The second template assessed for suitability as template for qPCR-HRM was the products of first-strand cDNA synthesis. These RNA-DNA hetroduplexes cannot be purified or quantified accurately. Furthermore, without the use of labeling of viral particles, the exact amount of viral RNA within any RNA extract is unknown. Difference in C_q-values could be introduced due to pipetting errors when cDNA is used, which is not a reflection of the quantity of viral RNA present. The risk of cross-contamination is also high. Together, these factors complicated the optimization of qPCR-HRM using RNA-DNA heteroduplexes.

The third template analyzed for suitability to qPCR-HRM was that of plasmid DNA. Plasmid DNA is easily obtained by TA-cloning of RT-PCR products and transformation of *E. coli.* An advantage of this approach is that a continual supply of a particular sequence variant can be

maintained in the laboratory through freezer cultures containing the cDNA clone. Sequencing of plasmid DNA is uni-directional and reliable. The qPCR-HRM analysis was highly successful and used to validate the qPCR-HRM technique as described in section 4.4.1. This approach however, does not take into consideration the quasi-species nature of the viral genome or the common phenomenon of mixed infections within vines. As mentioned earlier, the whole viral population is not represented unless a number of cDNA clones derived from a single RT-PCR product is sequenced. This approach was also not feasible for the large number of samples that was investigated in this study.

The final template analyzed was diluted RT-PCR products in a nested qPCR-HRM reaction. Results when using diluted RT-PCR product were superior to the results produced from any other template. Average amplification efficiencies approached 1.7. C_q-values lower than 25 cycles were attained in most cases (Figure 26 and Figure 31). This was expected as RT-PCR product represents uniform, high-quality template that is not prone to degradation. Purified PCR products (Zymoclean or Sureclean) did not produce different C_q-values than non-purified PCR products. This was expected as a large dilution ratio (1:500) renders purification null. Due to their size (~340-500bp) RT-PCR templates could be purified with ultra-filtration for sequencing to confirm variation within the nested amplicon. The highest reproducibility (long-term precision or inter-assay variance) and repeatability (short-term precision or intra-assay variance) was observed with this approach.

5.3.2   Optimization of melt phase

Once the efficiency of amplification was optimized, the temperature range of the melt phase could be adjusted. A relatively long temperature range (70°C-90°C) was used for all HRM-amplicons. This was done to allow adequate pre-and post-melt phases which were used for normalization. These phases on either side of the melt transition must ideally have a horizontal gradient for stronger confidence in auto-calling. Shorter temperature ranges may exclude certain melt domains. GC-rich regions of amplicons are known to have melt domains at higher temperatures (Corbett, 2006).

Secondary melt domains caused by GC-rich regions or secondary structures of DNA can significantly influence the melt profiles. During optimization of amplification, minimal template was included to reduce the formation of secondary structure during the melt phase.

HRM amplicons were also designed as small as possible to reduce the level of secondary structure formation. Other factors influencing the melt profiles were the salt concentration and saturation of fluorescent dye. Accurate pipetting was vital to obtain repeatability of qPCR-HRM assays. Duplicate samples displaying C_q-values in excess of 3 cycles of each other indicated poor short term precision and therefore inaccurate melt profiles. Fluorescent dyes with lower saturation e.g. SYBR Green I™ produced poor melt profiles.

5.3.3   Direct Sanger sequencing

The final data output during the characterization of South African sequence variants of GRSPaV was their respective electropherograms also known as chromatograms. These were generated by direct Sanger sequencing of RT-PCR products used as template for nested qPCR-HRM reactions. Multiple alignments of sequence data indicated the most common genotypes found. These were used to define genotypes for auto-calling by the software module. The sequencing results confirmed the HRM-data. Samples with similar melt profiles had similar sequences and were similarly auto-called by the software at a confidence interval of 70%.

Direct sequencing of RT-PCR products was performed to circumvent a costly population cloning and sequencing strategy. It is well-documented (Meng *et al*., 1998; Zhang *et al*., 1998) that GRSPaV cDNA clones derived from RT-PCR products are up to 82% identical. This is due to the common incidence of mixed infections within a single vine. Mixed infections or quasi-species within vines in this study were identified as ambiguities occurring above a threshold of 25% using a chromatogram (Applied Biosystems). By directly sequencing RT-PCR products, the whole population of viral genomes could be represented. A nucleotide position in a multiple alignment where the ambiguity representing both true bases is present, is a clear indication that both the nucleotides are present in the population of viral genomes (Appendix C). These ambiguities represent mixed infection or quasi-species.

Often ambiguities were seen at nucleotide positions where sequence variants belonging to different phylogenetic groups (I-IV) differ. This could also be an indication of a possible mixed infection. In such a case, the sequencing of several cDNA-clones of an RT-PCR product would confirm the different sequence variants present in a vine with a mixed infection. Other ambiguities are also incorporated in the virus genome during replication. The

error-prone replication mechanisms of viruses thus give rise to quasi-species: populations of similar viral genomes that accumulate over time due to high mutation rates. The mutations seen however are only representative of tolerated mutations.

5.4 Evaluation of a panel of sequence characterized CP sequence variants using HRM analysis

The main objective of this study was to develop a technique to detect GRSPaV genetic diversity. The technique required an unbiased (i.e. not sequence specific) approach. This was achieved with qPCR-HRM and the use of GRSPaV universal primer sets and dsDNA intercalating dye as opposed to more specific hydrolysis probes e.g. TaqMan®. The prerequisites included that the region(s) of the genome analyzed be an area which is representative of the genetic diversity of GRSPaV. To this end, three regions of the GRSPaV genome were examined (Figure 14). The CP and RdRp region were the most useful areas for this purpose. The most published sequence information is available for these areas (Meng, 2007).

The selection of samples for qPCR-HRM analysis and sequencing was based on a number of factors. Firstly, 2-5 samples collected from each of the four farms were included in the HRM analysis. This was done to establish any correlation of farm of origin to the genotype of a particular sequence variant. Secondly, samples showing distinct RT-PCR products for all three of the genomic regions examined were selected (Figure 25). This was done to compare the various phylogenetic trees produced during this study. Varying amplification efficiency observed with RT-PCR had no influence on C_q-values of qPCR-HRM assays. Lastly, the cost of the number of samples subjected to qPCR-HRM and sequencing was taken into account. These factors may have introduced a diversity-bias within the HRM results obtained. Samples showing amplification with only one or two of the three primer sets were not included in the HRM analysis. These samples may have represented more diverse sequence variants that were not detected with the three primer sets evaluated in this study. In future studies, possible diverse sequence variants can be confirmed with sequencing larger regions of the GRSPaV genome of these variants. Due to cost constraints, only 2-5 isolates from each farm was selected for HRM analysis and sequencing. This was sufficient for establishing standard, sequence-characterized melt profiles for comparison to future large scale HRM

analysis. For the purposes of the current study however, the parameters used for the selection of samples for qPCR-HRM analysis was adequate and warranted.

Some of the observations of the nucleotide identities are that samples originating from the same farms group together (Appendix C and Table 13). This is consistent with the findings of other researchers. It is for instance speculated that the presence of similar GRSPaV sequence variants are dependent on the cultivar, variety or clone of *V. vinifera* examined (Meng and Gonsalves, 2007a). Mixed infections occurring within a particular variety are then explained by cross-contamination via grafting. This suggestion is supported by a study performed by Meng *et al.* (2006) where distinct population structures present in scions were different to those present in rootstocks. Mixed infections of GRSPaV sequence variants of scions were much more common than in rootstocks displaying predominantly single infection (Meng *et al.*, 2006). To analyze large genetic diversity within the genome of GRSPaV, it is therefore recommended that a large number of cultivars and samples are examined. Such analyses require a technique such as qPCR-HRM which is suitable for large-scale application.

It is clear from the auto-calling results from Table 13 that duplicates of each sample are identified as replicates of each other. Furthermore there is 78% correlation between farm of origin and genotype identification. This shows that the qPCR-HRM assay of the CP region can accurately predict the sequence genotype by grouping samples of similar normalized melt profiles together (Figure 33 and Figure 34). Approximately 22% of samples analysed e.g. 13, 59, 74 and 94 (Table 13) showed that viral sequences present are more similar to other farms than their respective farms of origin. This result does not negate above conclusions as these vines may harbour multiple variants or variants that are more similar to variants from other farms. Sample 77 was the only sample for which its duplicates were auto-called differently. The first duplicate was called as GV genotype, the second duplicate was called as NVB genotype (Table 13). This discrepancy may be due to experimental error. It may also be due to an inability of the software to differentiate very closely related genotypes at a confidence percentage of 70%.

5.5 Phylogenetic analyses

The purpose of the current phylogenetic study was to confirm that the HRM data could be useful to determine the different genotypes. The phylogenetic results also establish which of the distinct sequence variant groups (Groups I, II, III and IV) are the dominant sequence variants present in the sample set. The three phylogenetic trees drawn up correlated to each other with few exceptions (Appendix D). However, less published sequence information is available for the RdRp and TGB region. Sequenced variants consistently radiated with their respective phylogenetic groups. The level of variation within the CP region was relatively low compared to the other two regions under analysis in this study. The partial RdRp region had the highest variability. This finding is consistent with literature (Nolasco *et al*., 2006), where GRSPaV CP sequences were found to be highly conserved. This area thus proves an ideal area for phylogenetic study. The results of the phylogenetic relationship of the CP are thus discussed below.

The consistency index (CI) and retention index (RI) values for the phylogenetic trees of the CP are 0.58 and 0.83 respectively (Table 14). This indicates an average confidence in the topographical layout of the trees. The trees retrieved with the heuristic search for the CP showed four clades. The sequence variants from this study group radiated with three of the four clades. Eight samples (12, 34, 36, 37, 38, 39, 59 and 94) radiated with medium support to Group II with a bootstrap value of 71. The majority of these samples are of the user-defined KK genotype. Six samples (13, 26, 27, 32 and 92) radiated to Group III with poor support of 56. The majority of these samples are of the GV or BD genotype. It is evident that the GV and BD genotypes are more closely related to each other than to the KK genotype. Two samples (64 and 74) appear to be mixed infection of Groups I and II. Further studies such as a population cloning approach are however required to elucidate the exact mixed infection occurring within these vines.

A possible explanation for the medium to poor support of sequenced variants to phylogenetic groups could be the size of the sequenced amplicons. The phylogenetic trees were produced from a total of 289 (RdRp), 413 (CP) and 471 (RdRp/TGBp1) characters. This represents only partial sequences of the GRSPaV genome. The number of parsimony-informative

characters were 97 (RdRp), 127 (CP) and 155 (RdRp/TGBp1). These regions may have been too small to produce phylogenetic analyses with strong support.

The published GRSPaV sequences are derived from cDNA clones, whereas the sequences produced by the current study are derived from RT-PCR products. Previous studies produced sequences with minimal ambiguities because an expensive and time-consuming population cloning approach was used. The sequences produced from RT-PCR products however contain the ambiguities which are representative of the whole GRSPaV population present in a vine. This may be another explanation for the medium to poor support of the sequenced samples to a particular phylogenetic group. The program (PAUP) used for analysis takes both bases of an ambiguity into account during the heuristic search for phylogenetic relationships. This may have caused difficulty in some of the samples during the analysis to assign a sequenced sample to a single phylogenetic group.

It can be deduced from the phylogenetic tree of the CP, that sequence variants from Groups II are more common in this sample set. This result was corroborated by a concurrent metagenomic sequence study performed on the same sample group (Coetzee *et al*., 2009). The concurrent study elucidated a full-length sequence of GRSPaV from an environmental isolate. The sequence was similar to GRSPaV-SG1, the full-length representative sequence of Group II. An accurate description of symptoms of plants sampled was not recorded at field collections. The results of this study therefore do not indicate the association of a particular sequence variant with a particular disease or symptom. As mentioned above the dominant sequence variants found within this sample set radiated with Group II sequence variants. Meng *et al*. (2005) demonstrated experimentally that the single infection of GRSPaV-SG1 is asymptomatic. An implication of this finding for the current study could be that GRSPaV is not the only viral component necessary for vines to show decline symptoms. However, accurate association studies of several grapevine-infecting viruses and viroids with disease symptoms must be performed to establish the etiology of Shiraz decline. For the purposes of the current study, the phylogenetic analysis was adequate. The results indicated the major sequence variants found in the sample set and confirmed HRM analysis as a tool for sequence variant determination.

6. Conclusion

Viral diseases affect vineyards negatively. This has economic implications for the facets of the South African grape and wine industry such as tourism, local beverage production as well as fruit and wine export. Investigation into the disease-causing agents that affect grapevines is valuable because it improves our understanding of viral disease.

The first aim of this study was to reliably and rapidly detect GRSPaV in grapevine. This was successfully achieved on a large scale using crude plant extracts in both quantitative and conventional RT-PCR. Several viral nucleic acid extraction procedures were attempted. Low yields of dsRNA were deemed inadequate for this study. The feasibility of total RNA extracts for RT-PCR template was evaluated. This template was found to be adequate, provided that more than one primer set was used. All RNA samples that produced poor amplification were discarded and RNA isolation was repeated.

The second aim of this study was to optimize and establish a technique to detect GRSPaV sequence variants in South African vines. This aim required a technique that is not sequence-specific and is capable of differentiating the various GRSPaV sequence variants. The qPCR-HRM assays developed during this study provided such a technique.

Several templates such as RNA, RNA-DNA heteroduplexes, cloned cDNA and diluted PCR product was evaluated for their usefulness in qPCR-HRM assays. Diluted RT-PCR products and cloned cDNA delivered the most consistent amplification plots and melt profiles. Cloned cDNA fragments were used to validate the technique but were considered unsuitable for strain determination of GRSPaV. The RT-PCR products of sixteen GRSPaV infected samples were subjected to qPCR-HRM and concurrent direct sequencing. The sequencing confirmed the qPCR-HRM melt profiles and auto-calling data: samples with similar melt profiles were also similar in sequence. Genotypes could be reliably assigned to certain groups of samples and was phylogenetically correlated to published sequences.

The current study prompts further investigation into the genetic diversity of GRSPaV. Factors such as the use of enzymes lacking proof-reading ability could lead to an overestimation of genetic diversity. The criteria applied to samples selected for HRM analysis could also lead to poor deductions about genetic diversity. Nonetheless, GRSPaV-infected samples can in the

future be subjected to qPCR-HRM assays developed during this study. This can be performed to establish similarity to known genotypes and therefore phylogenetic groups. Phylogenetic analyses revealed that the major sequence variants found in South African vines belong to Groups II and III. Mixed infection of sequence variants and quasi-species were a common occurrence. The assay will also be useful in establishing correlation of specific groups of genotypes to different phenotypical expression of viral disease. This will provide insight into the etiology of diseases associated with GRSPaV.

Appendix A

A table of the accession numbers, genomic region, sequence length, geographic origin, submitting author and year of submission of GRSPaV sequences that is available from Genbank and was used in this study.

Acc no	Length	Region	Country	1st Authour	Year Published
AB222858	202	CP	Japan	Nakaune	2006
AB222859	202	CP	Japan	Nakaune	2006
EU180590	381	CP	France	Sempe	2007
EU180591	381	CP	France	Sempe	2007
EU180592	381	CP	France	Sempe	2007
EU180593	381	CP	France	Sempe	2007
FJ577805	441	CP	Missouri, US	Lunden/Meng	2008
FJ577806	441	CP	Missouri, US	Lunden/Meng	2008
FJ577807	441	CP	Missouri, US	Lunden/Meng	2008
FJ577808	441	CP	Missouri, US	Lunden/Meng	2008
FJ577809	441	CP	Missouri, US	Lunden/Meng	2008
DQ278605	441	CP	Canada	Meng	2006
DQ278606	441	CP	Canada	Meng	2006
DQ278607	441	CP	Canada	Meng	2006
DQ278608	441	CP	Canada	Meng	2006
DQ278609	441	CP	Canada	Meng	2006
DQ278610	441	CP	Canada	Meng	2006
DQ278611	441	CP	Canada	Meng	2006
DQ278612	441	CP	Canada	Meng	2006
DQ278613	441	CP	Canada	Meng	2006
DQ278614	441	CP	Canada	Meng	2006
DQ278615	441	CP	Canada	Meng	2006
DQ278616	441	CP	Canada	Meng	2006
AM180432	606	CP	California	Lima	2006
AM180417	617	CP	California	Lima	2006
AM180444	650	CP	California	Lima	2006
AM180428	669	CP	California	Lima	2006
AM180418	670	CP	California	Lima	2006
AM180419	670	CP	California	Lima	2006
AM180420	670	CP	California	Lima	2006
AM180421	670	CP	California	Lima	2006
AM180422	670	CP	California	Lima	2006
AM180423	670	CP	California	Lima	2006

AM180424	670	CP	California	Lima	2006
AM180425	670	CP	California	Lima	2006
AM180426	670	CP	California	Lima	2006
AM180427	670	CP	California	Lima	2006
AM180429	670	CP	California	Lima	2006
AM180430	670	CP	California	Lima	2006
AM180431	670	CP	California	Lima	2006
AM180433	670	CP	California	Lima	2006
AM180434	670	CP	California	Lima	2006
AM180435	670	CP	California	Lima	2006
AM180436	670	CP	California	Lima	2006
AM180437	670	CP	California	Lima	2006
AM180438	670	CP	California	Lima	2006
AM180439	670	CP	California	Lima	2006
AM180440	670	CP	California	Lima	2006
AM180441	670	CP	California	Lima	2006
AM180442	670	CP	California	Lima	2006
AM180443	670	CP	California	Lima	2006
AB331418	780	CP	Japan	Nakaune	2008
AB331419	780	CP	Japan	Nakaune	2008
AB331420	780	CP	Japan	Nakaune	2008
AB331421	780	CP	Japan	Nakaune	2008
AB331422	780	CP	Japan	Nakaune	2008
AB331423	780	CP	Japan	Nakaune	2008
AB331424	780	CP	Japan	Nakaune	2008
AB331426	780	CP	Japan	Nakaune	2008
AB331427	780	CP	Japan	Nakaune	2008
AB331428	780	CP	Japan	Nakaune	2008
AB331429	780	CP	Japan	Nakaune	2008
AB331430	780	CP	Japan	Nakaune	2008
AB331431	780	CP	Japan	Nakaune	2008
AB331432	780	CP	Japan	Nakaune	2008
AB331433	780	CP	Japan	Nakaune	2008
AB331434	780	CP	Japan	Nakaune	2008
AB331435	780	CP	Japan	Nakaune	2008
AB331436	780	CP	Japan	Nakaune	2008
AB331437	780	CP	Japan	Nakaune	2008
AB331438	780	CP	Japan	Nakaune	2008
AB331439	780	CP	Japan	Nakaune	2008
AB331440	780	CP	Japan	Nakaune	2008
AB331441	780	CP	Japan	Nakaune	2008
AY927670	780	CP	Portugal	Nolasco	2006
AY927671	780	CP	Portugal	Nolasco	2006

AY927672	780	CP	Portugal	Nolasco	2006
AY927673	780	CP	Portugal	Nolasco	2006
AY927674	780	CP	Portugal	Nolasco	2006
AY927675	780	CP	Portugal	Nolasco	2006
AY927676	780	CP	Portugal	Nolasco	2006
AY927677	780	CP	Portugal	Nolasco	2006
AY927678	780	CP	Portugal	Nolasco	2006
AY927679	780	CP	Portugal	Nolasco	2006
AY927680	780	CP	Portugal	Nolasco	2006
AY927681	780	CP	Portugal	Nolasco	2006
AY927682	780	CP	Portugal	Nolasco	2006
AY927683	780	CP	Portugal	Nolasco	2006
AY927684	780	CP	Portugal	Nolasco	2006
AY927685	780	CP	Portugal	Nolasco	2006
AY927686	780	CP	Portugal	Nolasco	2006
AY927687	780	CP	Portugal	Nolasco	2006
AY927688	780	CP	Portugal	Nolasco	2006
EF636803	780	CP	Brazil	Radaelli	2007
EF636804	780	CP	Brazil	Radaelli	2007
EF690380	780	CP	Brazil	Radaelli	2007
EF690381	780	CP	Brazil	Radaelli	2007
EF690382	780	CP	Brazil	Radaelli	2007
EF690383	780	CP	Brazil	Radaelli	2007
EF690384	780	CP	Brazil	Radaelli	2007
EU040204	780	CP	Brazil	Radaelli	2007
EU204913	780	CP	Brazil	Radaelli	2007
DQ364979	867	CP	Italy	Terlizzi	2006
DQ364980	867	CP	Italy	Terlizzi	2006
DQ364981	867	CP	Italy	Terlizzi	2006
DQ364982	867	CP	Italy	Terlizzi	2006
DQ364983	867	CP	Italy	Terlizzi	2006
DQ364984	867	CP	Italy	Terlizzi	2006
DQ364985	867	CP	Italy	Terlizzi	2006
DQ364986	867	CP	Italy	Terlizzi	2006
DQ364987	867	CP	Italy	Terlizzi	2006
DQ364988	867	CP	Italy	Terlizzi	2006
DQ364989	867	CP	Italy	Terlizzi	2006
DQ364990	867	CP	Italy	Terlizzi	2006
DQ364991	867	CP	Italy	Terlizzi	2006
DQ364992	867	CP	Italy	Terlizzi	2006
DQ364993	867	CP	Italy	Terlizzi	2006
DQ364994	867	CP	Italy	Terlizzi	2006
DQ364995	867	CP	Italy	Terlizzi	2006

DQ443732	905	CP	Brazil	Pereira	2006
AY881627	8743	FL - BS	NY, USA	Meng	2005
AF057136	8744	FL - GRSPaV1	NY, USA	Meng	1998
AY368172	8743	FL - PN	California	Rowhani	2003
AF026278	8725	FL - RSPaV	California	Zhang	1998
AY881626	8742	FL - SG1	NY, USA	Meng	2005
AY368590	8742	FL - SY	California	Lima	2006
AJ457983	161	RdRP	Greece	Dovas/Katis	2002
DQ864489	197	RdRP	South Africa	Goszczynski	2006
EU247951	199	RdRP	South Africa	Goszczynski	2006
EU247952	199	RdRP	South Africa	Goszczynski	2006
FJ884327	199	RdRP	South Africa	Goszczynski	2006
FJ884328	199	RdRP	South Africa	Goszczynski	2006
FJ884333	199	RdRP	South Africa	Goszczynski	2006
FJ884334	199	RdRP	South Africa	Goszczynski	2006
FJ884335	199	RdRP	South Africa	Goszczynski	2006
DQ278626	338	RdRP	Canada	Meng	2006
DQ278637	338	RdRP	Canada	Meng	2006
DQ278617	339	RdRP	Canada	Meng	2006
DQ278618	339	RdRP	Canada	Meng	2006
DQ278620	339	RdRP	Canada	Meng	2006
DQ278621	339	RdRP	Canada	Meng	2006
DQ278622	339	RdRP	Canada	Meng	2006
DQ278623	339	RdRP	Canada	Meng	2006
DQ278624	339	RdRP	Canada	Meng	2006
DQ278625	339	RdRP	Canada	Meng	2006
DQ278626	339	RdRP	Canada	Meng	2006
DQ278627	339	RdRP	Canada	Meng	2006
DQ278628	339	RdRP	Canada	Meng	2006
DQ278629	339	RdRP	Canada	Meng	2006
DQ278630	339	RdRP	Canada	Meng	2006
DQ278631	339	RdRP	Canada	Meng	2006
DQ278632	339	RdRP	Canada	Meng	2006
DQ278633	339	RdRP	Canada	Meng	2006
DQ278634	339	RdRP	Canada	Meng	2006
DQ278635	339	RdRP	Canada	Meng	2006
DQ278636	339	RdRP	Canada	Meng	2006
DQ278638	339	RdRP	Canada	Meng	2006
DQ278639	339	RdRP	Canada	Meng	2006
DQ278640	339	RdRP	Canada	Meng	2006
DQ278641	339	RdRP	Canada	Meng	2006
DQ278642	339	RdRP	Canada	Meng	2006
DQ278643	339	RdRP	Canada	Meng	2006

DQ278644	339	RdRP	Canada	Meng	2006
DQ278645	339	RdRP	Canada	Meng	2006
DQ278646	339	RdRP	Canada	Meng	2006
DQ278647	339	RdRP	Canada	Meng	2006
DQ278648	339	RdRP	Canada	Meng	2006
DQ278649	339	RdRP	Canada	Meng	2006
DQ278650	339	RdRP	Canada	Meng	2006
EU271800	559	RdRP	Australia	Habili	2006
EU271795	561	RdRP	Australia	Habili	2006
EU271793	563	RdRP	Australia	Habili	2006
EU271790	572	RdRP	Australia	Habili	2006
EU271791	574	RdRP	Australia	Habili	2006
EU271792	575	RdRP	Australia	Habili	2006
EU271794	575	RdRP	Australia	Habili	2006
EU271796	575	RdRP	Australia	Habili	2006
EU271797	575	RdRP	Australia	Habili	2006
EU271798	575	RdRP	Australia	Habili	2006
EU271799	575	RdRP	Australia	Habili	2006
EU271801	575	RdRP	Australia	Habili	2006
EU271802	576	RdRP	Australia	Habili	2006
AM180543	618	RdRP	California	Lima	2006
AM180518	664	RdRP	California	Lima	2006
AM180519	664	RdRP	California	Lima	2006
AM180520	664	RdRP	California	Lima	2006
AM180521	664	RdRP	California	Lima	2006
AM180522	664	RdRP	California	Lima	2006
AM180523	664	RdRP	California	Lima	2006
AM180524	664	RdRP	California	Lima	2006
AM180525	664	RdRP	California	Lima	2006
AM180526	664	RdRP	California	Lima	2006
AM180527	664	RdRP	California	Lima	2006
AM180528	664	RdRP	California	Lima	2006
AM180529	664	RdRP	California	Lima	2006
AM180530	664	RdRP	California	Lima	2006
AM180531	664	RdRP	California	Lima	2006
AM180532	664	RdRP	California	Lima	2006
AM180533	664	RdRP	California	Lima	2006
AM180534	664	RdRP	California	Lima	2006
AM180535	664	RdRP	California	Lima	2006
AM180536	664	RdRP	California	Lima	2006
AM180537	664	RdRP	California	Lima	2006
AM180538	664	RdRP	California	Lima	2006
AM180539	664	RdRP	California	Lima	2006

AM180540	664	RdRP	California	Lima	2006
AM180541	664	RdRP	California	Lima	2006
AM180542	664	RdRP	California	Lima	2006
AM181038	664	RdRP	California	Lima	2006
AY340585	828	RdRP	Brazil	Espinha	2003
AY244640	831	RdRP	Brazil	Fajardo	2004
AB277783	2876	RdRP & TGB	Japan	Nakaune	2006
AB277784	2876	RdRP & TGB	Japan	Nakaune	2006
AB277785	2876	RdRP & TGB	Japan	Nakaune	2006
AB277786	2876	RdRP & TGB	Japan	Nakaune	2006
AB277787	2876	RdRP & TGB	Japan	Nakaune	2006
AB277788	2876	RdRP & TGB	Japan	Nakaune	2006
EF105294	2680	RdRP & TGP	Canada	Meng	1999

Appendix B

The list of arbitrarily named samples, farm of origin, sampling date and material and GRSPaV-diagnosis. Samples used in qPCR-HRM assays are indicated

	Sample Name	Farm of origin	Harvest period	Phloem/ Peiolet	RNA conc. (ng/µl)	GRSPaV diagnosis	qPCR-HRM
1	pooled	Kanonkop	Jan 09	Both		Pos	
2	pooled	Kanonkop	Jan 09	Both		Pos	
3	2:31	Kanonkop	Nov 08	Both	Y	Pos	
4	3:28	Kanonkop	Nov 08	Both	Y	Pos	
5	4:14	Kanonkop	Nov 08	Both	NO	Pos	
6	4:19	Kanonkop	Nov 08	Both	Y	Pos	
7	4:35	Kanonkop	Nov 08	Both	Y	Pos	
8	5:14	Kanonkop	Nov 08	Both	Y	Pos	
9	6:4	Kanonkop	Nov 08	Both	Y	Pos	
10	8:34	Kanonkop	Nov 08	Both	Y	Pos	
11	4:2	Nietvoorbij	May 08	Phloem	NO	inconclusive	
12	**1:1**	**Vititec**	**May 08**	**Phloem**	**Y**	**Pos**	✔
13	**10:5**	**Grondves**	**May 09**	**Phloem**	**Y**	**Pos**	✔
14	8:14	Grondves	May 09	Phloem	Y	Neg	
15	6:22	Grondves	May 09	Phloem	Y	Neg	
16	4:2	Grondves	May 09	Phloem	Y	Pos	
17	4:3	Grondves	May 09	Phloem	Y	Neg	
18	4:11	Grondves	May 09	Phloem	Y	Neg	
19	4:14	Grondves	May 09	Phloem	Y	Pos	
20	4:26	Grondves	May 09	Phloem	Y	Neg	
21	4:27	Grondves	May 09	Phloem	Y	Neg	
22	6:17	Grondves	May 09	Phloem	360.12	Neg	
23	7:16	Grondves	May 09	Phloem	Y	Pos	
24	7:18	Grondves	May 09	Phloem	Y	Neg	
25	7:24	Grondves	May 09	Phloem	Y	Neg	
26	**8:2**	**Grondves**	**May 09**	**Phloem**	**Y**	**Pos**	✔
27	**8:3**	**Grondves**	**May 09**	**Phloem**	**Y**	**Pos**	✔
28	8:14	Grondves	May 09	Phloem	Y	Neg	
29	8:20	Grondves	May 09	Phloem	Y	Neg	
30	8:24	Grondves	May 09	Phloem	267.31	Neg	
31	9:20	Grondves	May 09	Phloem	Y	Neg	
32	**9:17**	**Grondves**	**May 09**	**Phloem**	**115.16**	**Pos**	✔
33	10:12	Grondves	May 09	Phloem	Y	NEG	
34	**6:13**	**Kanonkop**	**Nov 08**	**Phloem**	**Y**	**Pos**	✔

35	7:21	Kanonkop	Nov 08	Phloem	Y	Pos	
36	**7:24**	**Kanonkop**	**Nov 08**	**Phloem**	**Y**	**Pos**	✔
37	**9:10**	**Kanonkop**	**Nov 08**	**Phloem**	**Y**	**Pos**	✔
38	**9:17**	**Kanonkop**	**Nov 08**	**Phloem**	**Y**	**Pos**	✔
39	**10:9**	**Kanonkop**	**Nov 08**	**Phloem**	**Y**	**Pos**	✔
40	1:22	Kanonkop	Feb 08	Petioles		Pos	
41	2:21	Kanonkop	Feb 09	Petioles		Pos	
42	2:31	Kanonkop	Feb 09	Petioles		Pos	
43	3:28	Kanonkop	Feb 09	Petioles		Pos	
44	4:12	Kanonkop	Feb 09	Petioles		Pos	
45	4:19	Kanonkop	Feb 09	Petioles		Pos	
46	4:35	Kanonkop	Feb 09	Petioles		Pos	
47	5:14	Kanonkop	Feb 09	Petioles		Pos	
48	6:4	Kanonkop	Feb 09	Petioles		Pos	
49	6:13	Kanonkop	Feb 09	Petioles		Pos	
50	7:21	Kanonkop	Feb 09	Petioles		Pos	
51	7:24	Kanonkop	Feb 09	Petioles		Pos	
52	8:34	Kanonkop	Feb 09	Petioles		Pos	
53	9:10	Kanonkop	Feb 09	Petioles		Pos	
54	9:17	Kanonkop	Feb 09	Petioles		Pos	
55	10:9	Kanonkop	Feb 09	Petioles		Pos	
56	1:2	Nietvoorbij	June 09	Phloem	112.70	Neg	
57	2.2	Nietvoorbij	June 09	Phloem	235.98	Neg	
58	2.3	Nietvoorbij	June 09	Phloem	140.82	Neg	
59	**3.2**	**Nietvoorbij**	**June 09**	**Phloem**	**385.31**	**Pos**	✔
60	3.3	Nietvoorbij	June 09	Phloem	140.97	Neg	
61	4.2	Nietvoorbij	June 09	Phloem	133.21	NEG	
62	4.3	Nietvoorbij	June 09	Phloem	271.65	NEG	
63	5.2	Nietvoorbij	June 09	Phloem	137.55	Neg	
64	**5.3**	**Nietvoorbij**	**June 09**	**Phloem**	**292.35**	**Pos**	✔
65	6.2	Nietvoorbij	June 09	Phloem	196.54	Neg	
66	6.3	Nietvoorbij	June 09	Phloem	323.02	Neg	
67	7.2	Nietvoorbij	June 09	Phloem	106.19	Neg	
68	7.3	Nietvoorbij	June 09	Phloem	105.59	Neg	
69	8.2	Nietvoorbij	June 09	Phloem	98.51	Neg	
70	8.3	Nietvoorbij	June 09	Phloem	381.30	Neg	
71	9.2	Nietvoorbij	June 09	Phloem	180.40	Neg	
72	9.3	Nietvoorbij	June 09	Phloem	100.69	Neg	
73	10.2	Nietvoorbij	June 09	Phloem	129.43	Neg	
74	**10.3**	**Nietvoorbij**	**June 09**	**Phloem**	**325.25**	**Pos**	✔
75	11.2	Nietvoorbij	June 09	Phloem	323.62	Neg	
76	11.3	Nietvoorbij	June 09	Phloem	167.76	Neg	
77	**12.2**	**Nietvoorbij**	**June 09**	**Phloem**	**175.88**	**Pos**	✔

78	12.3	Nietvoorbij	June 09	Phloem	168.38	Neg	
79	13.2	Nietvoorbij	June 09	Phloem	110.40	Neg	
80	13.3	Nietvoorbij	June 09	Phloem	109.91	Neg	
81	14.2	Nietvoorbij	June 09	Phloem	211.16	Neg	
82	14.3	Nietvoorbij	June 09	Phloem	364.84	Neg	
83	15.2	Nietvoorbij	June 09	Phloem	134.40	Neg	
84	15.3	Nietvoorbij	June 09	Phloem	91.18	Neg	
85	16.2	Nietvoorbij	June 09	Phloem	105.35	Neg	
86	16.3	Nietvoorbij	June 09	Phloem	223.84	Neg	
87	17.2	Nietvoorbij	June 09	Phloem	98.79	Neg	
88	17.3	Nietvoorbij	June 09	Phloem	102.48	Neg	
89	17.4	Nietvoorbij	June 09	Phloem	98.85	Neg	
90	R	Dewetshof	July 09	Leaf	54.14	NEG	
91	Big	Tradouw	July 09	Petioles	-	Pos	
92	Big - A	Tradouw	July 09	Phloem	170.78	Pos	
92	**Big - B**	**Tradouw**	**July 09**	**Phloem**	**214.84**	**Pos**	✔
93	Small	Tradouw	July 09	Petioles	-	Pos	
94	**Small - A**	**Tradouw**	**July 09**	**Phloem**	**264.87**	**Pos**	✔
94	Small - B	Tradouw	July 09	Phloem	250.46	Pos	
95	95	*In vitro* plantlet	July 09	Leaf	179.61	NEG	
96	96	*In vitro* plantlet	July 09	Leaf	137.15	NEG	

Appendix C

Multiple alignment of plasmid cDNA clones used for validation of qPCR-HRM technique. Arrows indicate primer binding sites for nested qPCR-HRM assay

Sequencing Number	Plasmid	Position in diagnostic fragment 910				Variant
		381	386	419	447	
Vitis_0854	pDRIVE910_**1**-9	G or T	T	G	A or G	mtX
Vitis_0855	pDRIVE910_**2**-9	G	C	G	A	mtC
Vitis_0856	pDRIVE910_**3**-9	G	T	G	A	wt
Vitis_0857	pDRIVE910_**4**-4	G	T	G	A	wt
Vitis_0858	pDRIVE910_**5**-9	G	T	G	A	wt
Vitis_0859	pDRIVE910_**6**-3	G	T	G	A	wt
Vitis_0860	pDRIVE910_**7**-4	G	T	G	A	wt
Vitis_0861	pDRIVE910_**8**-3	G	T	A	A	mtA

Multiple alignment of sequences of RT-PCR templates used for the qPCR-HRM assay in the CP region. Arrows indicate primer binding sites for nested qPCR-HRM assay.
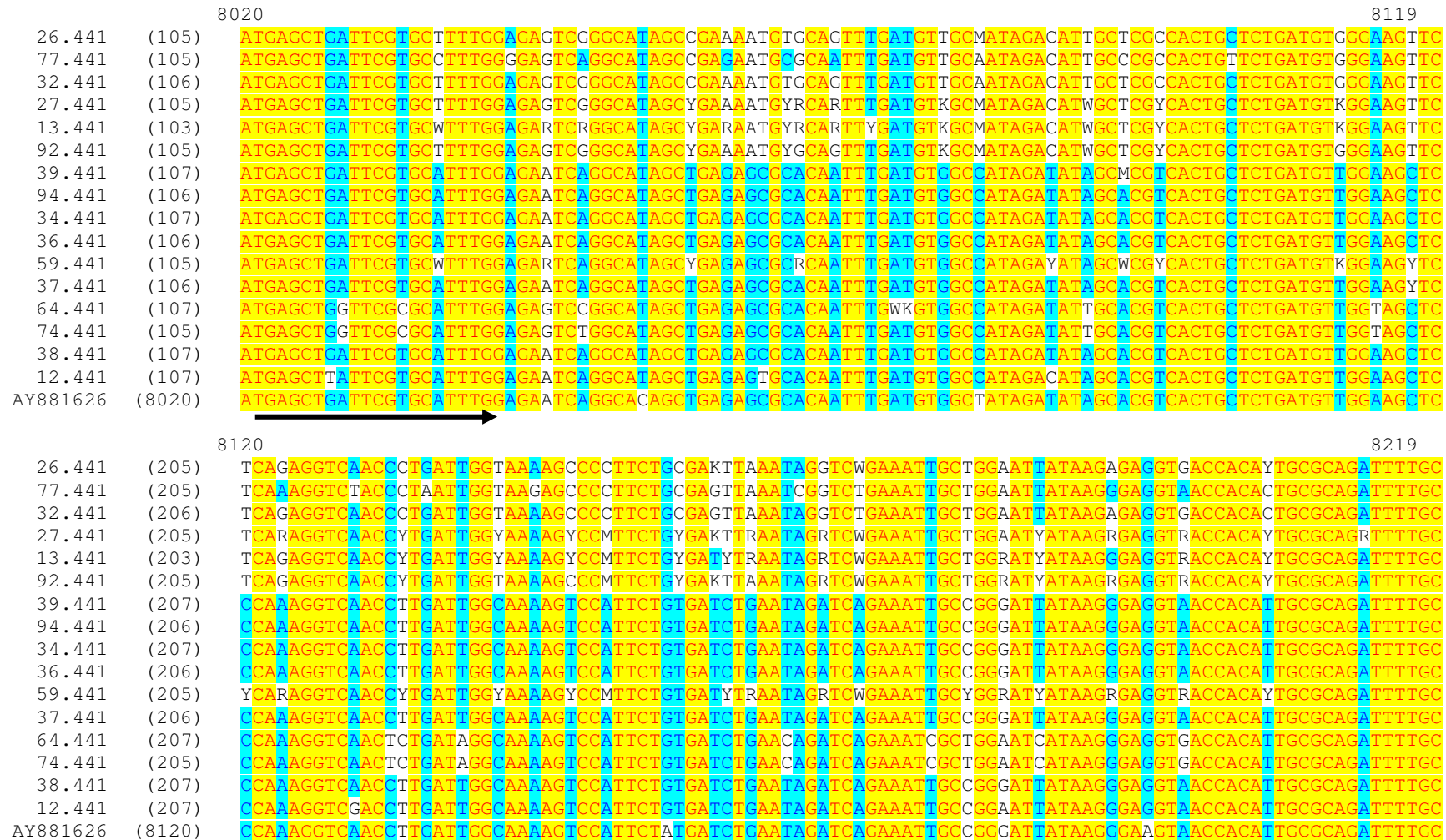
Appendix D

Phylogenetic tree (Bootstrap) of RdRP region of GRSPaV (RSP13 and RSP_1314_HRM_5R)

Bootstrap

```
                                                              PCMV.RdRP
                                                              77.339
      78                                                      4.DQ278623
                    55                                        4.DQ278634
                              74                              4.DQ278636
                                                              4.AY368590
                                                              2.DQ278637
                                                              2.DQ278618
                                                              1.DQ278621
                                                              1.DQ278622
                                                              2.DQ278627
                                                              1.DQ278628
                                                              2.DQ278629
                                                              1.DQ278630
                                                              1.DQ278631
                                                              1.DQ278632
                                                              1.DQ278638
                                                              2.DQ278639
                                                              1.DQ278641
                                                              1.DQ278642
                                                              3.DQ278644
                                                              1.DQ278645
                                                              1.DQ278648
                                                              2.DQ278650
                                                              1.AF057136
                                                              12.339
                                                              13.339
      94                                                      26.339
                                                              27.339
                                                              92.339
                    91                                        2.DQ278640
                              57                              2.DQ278626
                                                              2.DQ278624
                         80                                   2.DQ278617
                                                              64.339
                                                              74.339
                    93                                        2.DQ278635
                              88                              2.DQ278620
                                                              2.AY881626
                                                              36.339
                                                              38.339
                    73                                        39.339
                                                              59.339
                                                              94.339
                              76                              34.339
                                                              37.339
                                                              3.DQ278625
                                                              3.DQ278633
                                                              3.DQ278643
                    69                                        3.DQ278647
                                                              3.AY881627
                                                              32.339
                              62                              3.DQ278646
                                                              3.DQ278649
```

102

Phylogenetic tree (Bootstrap) of RdRP/TGBp1 region of GRSPaV (RSP_910_HRM_4R and RSP_910_HRM_3F)
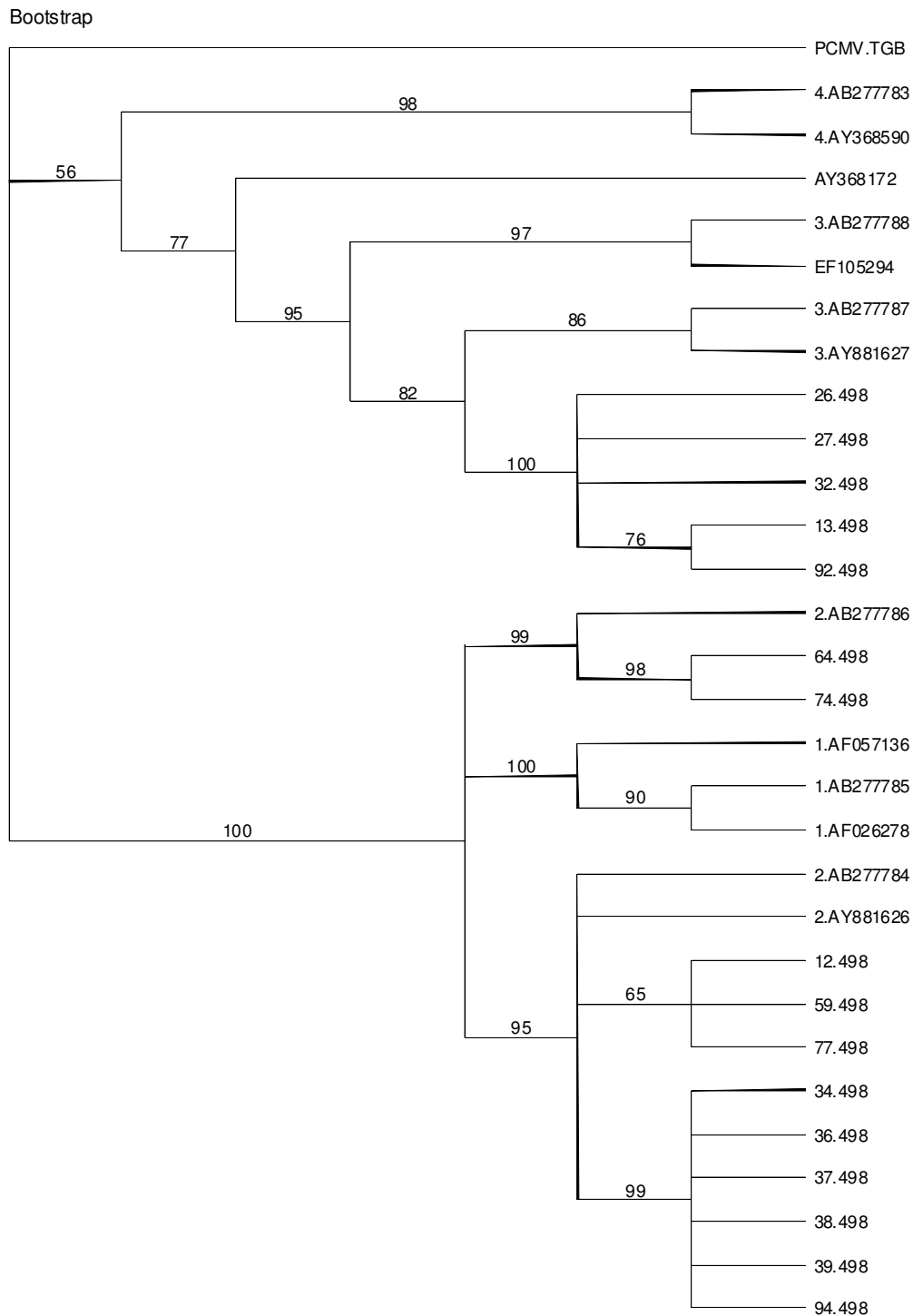
Bootstrap

Phylogenetic trees for the partial RdRp and TGB regions. South African sequences are indicated by .339 and .498 respectively. Bootstrap values are indicated above the respective branch. Branches with bootstrap values higher than 75 were considered well supported. Branches with bootstrap values lower than 60 was considered poorly supported. Genbank sequences are prefixed with relative phylogenetic group if classified by previous authors.

References

Adams, M.J., Antoniw, J.F., Bar-Joseph, M., Brunt, A.A., Candresse, T., Foster, G.D., *et al*, 2004. Virology division news: The new plant virus family *Flexiviridae* and assessment of molecular criteria for species demarcation. Archives of Virology. 149, 1045-1060.

Al Rwahnih, M., Daubert, S., Golino, D., Rowhani, A., 2009. Deep sequencing analysis of RNAs from a grapevine showing Syrah Decline symptoms reveals a multiple virus infection that includes a novel virus. Virology 387, 395-401.

Altschul, S.F., Gish, W., Miller, W., Myers, E.W., Lipman, D.J., 1990. Basic local alignment search tool. Journal of Molecular Biology. 215, 403-410.

Battany, M., Rowhani, A., Golino, D., 2004. Syrah in California—decline or disorder. Practical Winery and Vineyard 26, 20-35.

Bayne, E.H., Rakitina, D.V., Morozov, S.Y., Baulcombe, D.C., 2005. Cell-to-cell movement of potato potexvirus X is dependent on suppression of RNA silencing. Plant Journal 44, 471.

Beuve, M., Moury, B., Silmont, A., Sempé-Ignatovic, L., Hemmer, C., Lemaire, O., 2009. Viral sanitary status and genetic diversity of *Rupestris stem pitting-associated virus* in french syrah clones exhibiting various susceptibility levels to decline. In Extended Abstracts 16th Meeting of ICVG, 346-347.

Bianco, P.A., Zorloni, A., De Biasi, C., Belli, G., 2009. Preliminary investigations on a Syrah Decline in central Italy. In Extended Abstracts 16th Meeting of ICVG, 348-349.

Borgo, M., Anaclerio, F., Bertazzon, N., Angelini, E., 2006. The relationship between *Grapevine rupestris stem pitting-associated virus* and Rupestris stem pitting and Vein necrosis diseases. In Extended Abstracts 15th Meeting of ICVG, 75-76.

Borgo, M., Bertazzon, N., Anaclerio, F., Angelini, E., 2009. Different variants of GSPaV are associated to diverse diseases in grapevine. In Extended Abstracts 16th Meeting of ICVG, 327-328.

Bouyahia, H., Boscia, D., Savino, V., Notte, P., Pirolo, C., Castellano, M., *et al*, 2005. *Grapevine rupestris stem pitting-associated virus* is linked with grapevine Vein necrosis. Vitis 44, 133-137.

Bouyahia, H., Della Bartola, M., Materazzi, A., Triolo, E., 2009. Molecular characterisation of biologically divergent strains of GRSPaV. In Extended Abstracts 16th Meeting of ICVG, 329-330.

Bustin, S.A., Benes, V., Garson, J.A., Hellemans, J., Huggett, J., Kubista, M., *et al*, 2009. The MIQE guidelines: Minimum information for publication of quantitative real-time PCR experiments. Clinical Chemistry 55, 611.

Casati, P., Minafra, A., Rowhani, A., Bianco, P.A., 2003. Further data on molecular characterisaton of *Grapevine rupestris stem pitting-associated virus*. In Extended Abstracts 14th Meeting ICVG, 130.

Coetzee, B., Freeborough, M., Maree, H.J., Celton, J., Rees, D.J.G., Burger, J.T., 2009. Virome of a vineyard: Ultra deep sequencing analysis of diseased grapevines. In Extended Abstracts 16th Meeting of ICVG, 216-217.

Conti, M., Milne, R.G., Luisoni, E., Boccardo, G., 1980. A closterovirus from a stem-pitting-diseased grapevine. Phytopathology 70, 394-399.

Corbett Life Science, 2006. High Resolution Melt Assay Design and Analysis. CorProtocol 6000-1-July06.

Credi, R., Babini, A.R., 1997. Effects of virus and virus-like infections on growth, yield, and fruit quality of albana and trebbiano romagnolo grapevines. American Journal of Enology and Viticulture 48, 7-12.

Demeke, T., Adams, R.P., 1992. The effects of plant polysaccharides and buffer additives on PCR. BioTechniques 12, 332-334.

Dovas, C.I., Katis, N.I., 2003. A spot nested RT-PCR method for the simultaneous detection of members of the vitivirus and foveavirus genera in grapevine. Journal of Virological Methods 107, 99-106.

Drake, J.W., Holland, J.J., 1999. Mutation rates among RNA viruses. Proceedings of the National Academy of Sciences 96, 13910-13913.

Engelbrecht, D.J., Kasdorf, G.G.F., Mare, F.A., 1991. Field spread of stem-grooving diseases in South African grapevines. Phytophylactica 23, 239-240.

Engelbrecht, D.J., Nel, A.C., 1971. A graft-transmissible stem grooving of grapevines in the Western Cape province (South Africa) resembling legno riccio (rugose wood). Phytophylactica 3, 93-96.

Flaherty, D.L., 1992. Grape pest management. In: Flaherty, D.L., Christensen, L.P., Lanini, W.T., Marois, J.J. and Phillips, P.A. and Wilson L.T. (Eds.), Grape virus diseases. Division of Agriculture and Natural Resources, University of California, Oakland, California, pp. 101-110.

Fletcher, G., 1995. Incidence of stem pitting increasing in sunraysia vineyards. Australian Grapegrower & Winemaker 377, 49–50.

Gambino, G., Bondaz, J., Gribaudo, I., 2006. Detection and elimination of viruses in callus, somatic embryos and regenerated plantlets of grapevine. European Journal of Plant Pathology 114, 397-404.

Gambino, G., Gribaudo, I., 2006. Simultaneous detection of nine grapevine viruses by multiplex reverse transcription-polymerase chain reaction with coamplification of a plant RNA as internal control. Phytopathology 96, 1223-1229.

Goheen, A.C., 1988. Compendium of grape diseases. In: Pearson, R.C. and Goheen, A.C. (Eds.), Rupestris stem pitting, pp. 53.

Goheen, A.C., 1989. Virus diseases and grapevine selection. American Journal of Enology and Viticulture 40, 67-72.

Goldbach, R., Bucher, E., Prins, M., 2003. Resistance mechanisms to plant viruses: An overview. Virus Research 92, 207-212.

Goszczynski, D.E., 2007. Investigation of association of viruses of *viti-* and *foveaviruses* genera with Shiraz disease and Shiraz (syn. Syrah) decline in South Africa. In Proceedings of the Syrah Vine Health Symposium, 8-11.

Goszczynski, D.E., Jooste, A.E.C., 2002. The application of single-strand conformation polymorphism (SSCP) technique for the analysis of molecular heterogeneity of grapevine virus A. Vitis 41, 77-82.

Graniti, A., Ciccarone, A., 1961. Osservazioni su alterazioni virosiche e virus-simili della vite in puglia. Not.mal.piante 55, 99-102.

Gribaudo, I., Gambino, G., Cuozzo, D., Mannini, F., 2006. Attempts to eliminate *Grapevine rupestris stem pitting-associated virus* from grapevine clones. Journal of Plant Pathology 88, 293-298.

Habili, N., Davies, R., Randles, J., 2009. Detection of viruses in seeds of infected grapevines with and emphasis on *Grapevine rupestris stem pitting-associated virus*. In Extended Abstracts 16th Meeting of ICVG, 46-47.

Habili, N., Farrokhi, N., Lima, M., Nicholas, P., Randles, J., 2006. Distribution of *Rupestris stem-pitting-associated virus* variants in two Australian vineyards showing different symptoms. Annals of Applied Biology 148, 91-96.

Hall, T.A., 1999. BioEdit: A user-friendly biological sequence alignment editor and analysis program for windows 95/98/NT. In Nucleic Acids Symposium Series, 95-98.

Hewitt, W.B., Neja, R., 1971. Grapevine bark and wood pitting disease found in California. Plant Disease Reporter 55, 860-861.

Hofinger, B.J., Jing, H.C., Hammond-Kosack, K.E., Kanyuka, K., 2009. High-resolution melting analysis of cDNA-derived PCR amplicons for rapid and cost-effective

identification of novel alleles in barley. Theoretical and Applied Genetics 119, 851-865.

Hren, M., Boben, J., Rotter, A., Kralj, P., Gruden, K., Ravnikar, M., 2007. Real-time PCR detection systems for Flavescence dorée and Bois noir phytoplasmas in grapevine: comparison with conventional PCR detection and application in diagnostics. Plant Pathology 56, 785-796.

Hu, J.S., Gonsalves, D., Teliz, D., 1990. Characterization of closterovirus-like particles associated with grapevine leafroll disease. Journal of phytopathology 128, 1-14.

Hull, R., 2001. Matthews' plant virology. Academic Press. San Diego, California.

Korimbocus, J., Coates, D., Barker, I., Boonham, N., 2002. Improved detection of *Sugarcane yellow leaf virus* using a real-time fluorescent (TaqMan[®]) RT-PCR assay. Journal of virological methods 103, 109-120.

Legin, R., Vuittenez, A., 1973. Comparaison des symptomes et transmission par greffage d'une mosaique nervaire de *vitis vinifera,* de la marbrure de V. *rupestris* et d'une affection necrotique des nervures de l'hybride *rup.-berl.* 110R. Rivista di patologia vegetale, ser. IV 9, 57-63.

Li, Z., Martelli, G.P., Prota, U., 1989. A preliminary account of virus and virus-like disease of grapevines in the people's republic of China. In Extended Abstracts 9th Meeting ICVG, 57-78.

Lima, M., Alkowni, R., Uyemoto, J.K., Rowhani, A., 2009. Genomic study and detection of a new variant of *Grapevine rupestris stem pitting-associated* virus in declining California Pinot noir grapevines. Journal of Plant Pathology 91, 155-162.

Lima, M.F., Rosa, C., Golino, D.A., Rowhani, A., 2006. Detection of *rupestris stem pitting-associated virus* in seedlings of virus-infected maternal grapevine plants. In Extended Abstracts 15th Meeting of ICVG, 244-245.

Lima, M., Alkowni, R., Uyemoto, J., Golino, D., Osman, F., Rowhani, A., 2006. Molecular analysis of a California strain of *Rupestris stem pitting-associated virus* isolated from declining Syrah grapevines. Archives of Virology. 151, 1889-1894.

Ling, K.S., Zhu, H.Y., Gonsalves, D., 2008. Resistance to *Grapevine leafroll-associated virus 2* is conferred by post-transcriptional gene silencing in transgenic *Nicotiana benthamiana*. Transgenic Research 17, 733-740.

López, R., Asensio, C., Guzman, M.M., . Boonham, N., 2006. Development of real-time and conventional RT-PCR assays for the detection of *Potato yellow vein virus* (PYVV). Journal of Virological Methods 136, 24-29.

Lunello, P., Mansilla, C., Conci, V., Ponz, F., 2004. Ultra-sensitive detection of two garlic potyviruses using a real-time fluorescent (TaqMan®) RT-PCR assay. Journal of Virological Methods 118, 15-21.

Mackay, I.M., Arden, K.E., Nitsche, A., 2002. Real-time PCR in virology. Nucleic Acids Research 30, 1292.

Malan, S., Freeborough, M., Burger, J., 2009. Real-time PCR for sensitive reliable grapevine virus detection. In Extended Abstracts 16th Meeting of ICVG, 48-49.

Martelli, G.P., 1993. Rugose wood complex. In: Martelli, G.P. (Ed.) Graft-transmissible diseases of grapevines: Handbook for detection and diagnosis. International council for the study of viruses and virus diseases of the Grapevine/Food and Agriculture Organization of the United Nations. Rome, Italy: 45-53.

Martelli, G.P., 2009. Grapevine virology highlights. In Extended Abstracts 16th Meeting of ICVG, 15-23.

Martelli, G.P., Adams, M.J., Kreuze, J.F., Dolja, V.V., 2007. Family flexiviridae: A case study in virion and genome plasticity. Annual Review of Phytopathology 45, 73-100.

Martelli, G.P., Boudon-Padieu, E., 2006. Directory of infectious diseases of grapevines and viroses and virus-like diseases of the grapevine: Bibliographic report 1998-2004. Options méditerranéennes, ser.B 55.

Martelli, G.P., Jelkmann, W., 1998. *Foveavirus*, a new plant virus genus. Archives of Virology 143, 1245-1249.

Meng, B., Credi, R., Petrovic, N., Tomazic, I., Gonsalves, D., 2003. Antiserum to recombinant virus coat protein detects *Rupestris stem pitting-associated virus* in grapevines. Plant Disease 87, 515-522.

Meng, B., Gonsalves, D., 2003. *Rupestris stem pitting-associated virus* of grapevines: Genome structure, genetic diversity, detection, and phylogenetic relationship to other plant viruses. Current Topics in Virology 3, 125–135.

Meng, B., Gonsalves, D., 2007a. *Grapevine rupestris stem pitting-associated virus*. In: Rao, G.P., Myrta, A., Ling, K.-S. (Eds.) Characterization, diagnosis and management of plant viruses. Stadium Pres LLC. Texas,USA: 201-222.

Meng, B., Gonsalves, D., 2007b. *Grapevine rupestris stem pitting-associated virus*: A decade of research and future perspectives. Plant Viruses 1, 52-62.

Meng, B., Goszczynski, D., Gonsalves, D., 2000. Detection of *Rupestris stem pitting-associated virus* in the indicator *Vitis rupestris* "St. George" and sequence analysis. In Extended Abstracts 13th Meeting ICVG, 35-36.

Meng, B., Johnson, R., Peressini, S., Forsline, P.L., Gonsalves, D., 1999. *Rupestris stem pitting-associated virus-1* is consistently detected in grapevines that are infected with rupestris stem pitting. European Journal of Plant Pathology 105, 191-199.

Meng, B., Li, C., Wang, W., Goszczynski, D., Gonsalves, D., 2005. Complete genome sequences of two new variants of *Grapevine rupestris stem pitting-associated virus* and comparative analyses. Journal of General Virology 86, 1555-1560.

Meng, B., Pang, S., Forsline, P., McFerson, J., Gonsalves, D., 1998. Nucleotide sequence and genome structure of *Grapevine rupestris stem pitting-associated virus*-1 reveal similarities to apple stem pitting virus. Journal of General Virology 79, 2059-2069.

Meng, B., Rebelo, A.R., Fisher, H., 2006. Genetic diversity analyses of *Grapevine rupestris stem pitting-associated virus* reveal distinct population structures in scion versus rootstock varieties. Journal of General Virology 87, 1725-1733.

Meng, B., Zhu, H.Y., Gonsalves, D., 1999. *Rupestris stem pitting-associated virus-1* consists of a family of sequence variants. Archives of Virology 144, 2071-2085.

Minafra, A., Boscia, D., 2003. An overview of rugose wood-associated viruses: 2000-2003. In Extended Abstracts 14th Meeting of ICVG, 116-119.

Minafra, A., Casati, P., Elicio, V., Rowhani, A., Saldarelli, P., Savino, V., *et al*, 2000. Serological detection of *Grapevine rupestris stem pitting-associated virus* (GRSPaV) by a polyclonal antiserum to recombinant virus coat protein. Vitis 39, 115-118.

Morozov, S.Y., Solovyev, A.G., 2003. Triple gene block: Modular design of a multifunctional machine for plant virus movement. Journal of General Virology 84, 1351-1366.

Murashige, T., Skoog, F., 1962. A revised medium for rapid growth and bioassays with tobacco tissue cultures. Physiologia Plantarum 15, 473-497.

Myrta, A., Potere, O., Crescenzi, A., Nuzzaci, M., Boscia, D., 2000. Properties of two monoclonal antibodies specific to the cherry strain of *Plum pox virus*. Journal of Plant Pathology 82, 95-101.

Nakaune, R., Inoue, K., Nasu, H., Kakogawa, K., Nitta, H., Imada, J., *et al*, 2008. Detection of viruses associated with rugose wood in japanese grapevines and analysis of genomic variability of *Rupestris stem pitting-associated virus*. Journal of General Plant Pathology 74, 156-163.

Nakaune, R., Inoue, K., Nasu, H., Kakogawa, K., Nitta, H., Nakano, M., 2006. Etiology of Rugose wood disease in Japanese grapevines. In Extended Abstracts 15th Meeting of ICVG, 237-238.

Nakaune, R., Nakano, M., 2006. Efficient methods for sample processing and cDNA synthesis by RT-PCR for the detection of grapevine viruses and viroids. Journal of Virological Methods 134, 244-249.

Nassuth, A., Pollari, E., Helmeczy, K., Stewart, S., Kofalvi, S.A., 2000. Improved RNA extraction and one-tube RT-PCR assay for simultaneous detection of control plant RNA plus several viruses in plant extracts. Journal of Virological Methods 90, 37-49.

Nei, M., 1987. Molecular evolutionary genetics. Columbia Univ Press. New York.

Nolasco, G., Mansinho, A., Santos, M.T., Soares, C., Sequeira, Z., Sequeira, C., *et al.*, 2000. Large scale evaluation of primers for diagnosis of *Rupestris stem pitting-associated virus-1*. European Journal of Plant Pathology 106, 311-318.

Nolasco, G., Santos, C., Petrovic, N., Teixeira Santos, M., Cortez, I., Fonseca, F., *et al.*, 2006. *Rupestris stem pitting-associated virus* isolates are composed by mixtures of genomic variants which share a highly conserved coat protein. Archives of Virology 151, 83-96.

Orecchia, M., Nölke, G., Saldarelli, P., Dell'Orco, M., Uhde-Holzem, K., Sack, M., *et al.*, 2008. Generation and characterization of a recombinant antibody fragment that binds to the coat protein of *Grapevine leafroll-associated virus 3*. Archives of Virology 153, 1075-1084.

Osman, F., Leutenegger, C., Golino, D., Rowhani, A., 2007. Real-time RT-PCR (TaqMan®) assays for the detection of *Grapevine leafroll-associated viruses 1–5* and *9*. Journal of Virological Methods 141, 22-29.

Osman, F., Leutenegger, C., Golino, D.A., Rowhani, A., 2009. Comparison of high throughput low density arrays, RT-PCR and real-time TaqMan® RT-PCR in the detection of grapevine viruses. In Extended Abstracts 16th Meeting of ICVG, 36-37.

Osman, F., Rowhani, A., 2006. Application of a spotting sample preparation technique for the detection of pathogens in woody plants by RT-PCR and real-time PCR (TaqMan®). Journal of Virological Methods 133, 130-136.

Osman, F., Rowhani, A., 2008. Real-time RT-PCR (TaqMan®) assays for the detection of viruses associated with rugose wood complex of grapevine. Journal of Virological Methods 154, 69-75.

Paynter, R.W., 1981. Modification of the beer-lambert equation for application to concentration gradients. Surface and Interface Analysis 3, 186-187.

Petrovic, N., Meng, B., Ravnikar, M., Mavric, I., Gonsalves, D., 2003. First detection of rupestris stem pitting-associated virus particles by antibody to a recombinant coat protein. Plant Disease 87, 510-514.

Petrovic, N., Penev, B., Krastanova, T., Meng, B., Gonsalves, D., 2000. Distribution of *Rupestris stem pitting-associated virus* in greenhouse and field grown *Vitis rupestris* "St. George". In Extended Abstracts 13th Meeting ICVG, 35-36.

Prosser, S.W., Goszczynski, D.E., Meng, B., 2007. Molecular analysis of double-stranded RNAs reveals complex infection of grapevines with multiple viruses. Virus Research 124, 151-159.

Rebelo, A.R., Niewiadomski, S., Prosser, S.W., Krell, P., Meng, B., 2008. Subcellular localization of the triple gene block proteins encoded by a foveavirus infecting grapevines. Virus Research 138, 57-69.

Reisch, B.I., Pratt, C., 1996. Fruit breeding, volume II: Vine and small fruits crops. In: Janick J. and Moore J.N. (Eds.) Grapes. John Wiley and Sons Inc.: 297-369.

Renault-Spilmont, A.S., Grenan, S., Boursiquot, J.M., 2003. Syrah decline in French vineyards. In Extended Abstracts 14th Meeting ICVG, 144.

Rowhani, A., Zhang, Y.P., Chin, J., Minafra, A., Golino, D.A., Uyemoto, J.K., 2000. *Grapevine rupestris stem pitting-associated virus*: Population diversity, titer in the host and possible transmission vector. In Extended Abstracts 13th Meeting ICVG, 37.

Saldarelli, P., 2009. Flexiviruses: A grapevine point of view. In Extended Abstracts 16th Meeting of ICVG, 324-326.

Sambrook, J., Fritsch, E.F., Maniatis, T., 1989. Molecular cloning. Cold Spring Harbor Laboratory Press Cold Spring Harbor. New York.

Santos, C., Santos, M.T., Cortez, I., Boben, J., Petrovic, N., Sequeira, O.A., *et al*, 2003. Analysis of the genomic variability and design of an asymmetric PCR ELISA asay for the broad detection of *Grapevine rupestris stem pitting-associated virus*. In Extended Abstracts 14th Meeting ICVG, 126-127.

Saponari, M., Manjunath, K., Yokomi, R.K., 2008. Quantitative detection of *Citrus tristeza virus* in citrus and aphids by real-time reverse transcription-PCR (TaqMan®). Journal of Virological Methods 147, 43-53.

Savino, V., Boscia, D., Martelli, G.P., 1989. Rugose wood complex of grapevine: Can grafting to *Vitis* indicators discriminate between diseases. In Extended Abstracts 9th Meeting ICVG, 91-94.

Skiada, F., Maliogka, V.I., Eleftheriou, E.P., Katis, N.I., 2009. Advances on the eradication of *Grapevine rupestris stem pitting-associated virus* (GRSPaV) from *Vitis vinifera* explants. In Extended Abstracts 16th Meeting of ICVG, 262-263.

Skiada, F.G., Grigoriadou, K., Maliogka, V.I., Katis, N.I., Eleftheriou, E.P., 2009. Elimination of *Grapevine leafroll-associated virus 1* and *Grapevine rupestris stem pitting-associated virus* from grapevine cv. agiorgitiko, and a micropropagation

protocol for mass production of virus-free plantlets. Journal of Plant Pathology 91, 177-184.

Soares, C., Mansino, A., Teixeira Santos, M., Sequeira, O.A., Nolasco, G., 2000. Studying the genomic variability of *Rupestris stem pitting-associated virus 1*. In Extended Abstracts 13th Meeting ICVG, 41-42.

South African Wine Industry Statistics 33, May 2009. (www.sawis.co.za)

Steger, G., 1994. Thermal denaturation of double-stranded nucleic acids: Prediction of temperatures critical for gradient gel electrophoresis and polymerase chain reaction. Nucleic Acids Research 22, 2760.

Stewart, S., Nassuth, A., 2001. RT-PCR based detection of *Rupestris stem pitting-associated virus* within field-grown grapevines throughout the year. Plant Disease 85, 617-620.

Swofford, D.L., 2003. PAUP: Phylogenetic analysis using parsimony. v4.0. Sinaur associates. Sunderland, Massachusetts.

Teliz, D., Valle, P., Goheen, A.C., Luevano, S., 1980. Grape corky bark and Stem pitting in mexico. I. Occurrence, natural spread, distribution, effect on yield and evaluation of symptoms in 128 grape cultivars. In Extended Abstracts 7th Meeting of ICVG, 51-64.

Terlizzi, F., Credi, R., 2003. Partial molecular characterization of Italian *Grapevine rupestris stem pitting-associated virus* isolates. In Extended Abstracts 14th Meeting ICVG, 133-134.

Teycheney, P.Y., Laboureau, N., Iskra-Caruana, M.L., Candresse, T., 2005. High genetic variability and evidence for plant-to-plant transfer of *Banana mild mosaic virus*. Journal of General Virology 86, 3179-3187.

Toi, C.S., Dwyer, D.E., 2008. Differentiation between vaccine and wild-type *Varicella-zoster virus* genotypes by high-resolution melt analysis of single nucleotide polymorphisms. Journal of Clinical Virology 43, 18-24.

Tzanetakis, I.E., Martin, R.R., 2008. A new method for extraction of double-stranded RNA from plants. Journal of Virological Methods 149, 167-170.

Tzeng, H.L., Tzeng, D.D., Goheen, A.C., 1993. Anatomical and tissue culture studies of rupestris. Botanical Bulletin of Academia Sinica 34, 73.

Van Eeden, C., 2004. The construction of gene silencing transformation vectors for the introduction of multiple-virus resistance in grapevines, Stellenbosch University. Stellenbosch, South Africa.

Varga, A., James, D., 2005. Detection and differentiation of *Plum pox virus* using real-time multiplex PCR with SYBR green and melting curve analysis: A rapid method for strain typing. Journal of Virological Methods 123, 213-220.

Varga, A., James, D., 2006. Real-time RT-PCR and SYBR green I melting curve analysis for the identification of *Plum pox virus* strains C, EA, and W: Effect of amplicon size, melt rate, and dye translocation. Journal of Virological Methods 132, 146-153.

Wang, D., Maule, A.J., 1994. A model for seed transmission of a plant virus: Genetic and structural analyses of pea embryo invasion by *Pea seed-borne mosaic virus*. The Plant Cell 6, 777-787.

Wetzel, T., Candresse, T., Ravelonandro, M., Dunez, J., 1991. A polymerase chain reaction assay adapted to *Plum pox potyvirus* detection. Journal of Virological Methods 33, 355-365.

White, E.J., Venter, M., Hiten, N.F., Burger, J.T., 2008. Modified cetyltrimethylammonium bromide method improves robustness and versatility: The benchmark for plant RNA extraction. Biotechnology Journal 3, 1424-1428.

White, H., Potts, G., 2006. Mutation scanning by high resolution melt analysis. Evaluation of rotor-gene 6000 (Corbett Life Science), HR-1 and 384 well light scanner (Idaho Technology). National Genetics Reference Laboratory. Wessex, 1-26.

Wines of South Africa (WOSA), September 2004. The macroeconomic impact of the wine industry on the Western Cape. (www.wosa.co.za)

Wittwer, C.T., Reed, G.H., Gundry, C.N., Vandersteen, J.G., Pryor, R.J., 2003. High-resolution genotyping by amplicon melting analysis using LCGreen. Clinical Chemistry 49, 853-860.

Zhang, Y.P., Rowhani, A., 2000. A strategy for rapid cDNA cloning from double-stranded RNA templates isolated from plants infected with RNA viruses by using Taq DNA polymerase. Journal of Virological Methods 84, 59-63.

Zhang, Y.P., Uyemoto, J.K., Golino, D.A., Rowhani, A., 1998. Nucleotide sequence and RT-PCR detection of a virus associated with grapevine rupestris stem-pitting disease. Phytopathology 88, 1231-1237.